DIPLOMARBEIT

Titel der Diplomarbeit

Precision constraints and photonic Higgs decays in
the Two Higgs Doublet Model

angestrebter akademischer Grad

Magister/Magistra der Naturwissenschaften (Mag. rer.nat.)

Verfasserin / Verfasser:	Paul Posch
Matrikel-Nummer:	0202661
Studienrichtung (lt. Studienblatt):	411 Diplomstudium Physik
Betreuerin / Betreuer:	Gerhard Ecker

Wien, am 13. August 2009

Kurzfassung

In dieser Diplomarbeit wird eine mögliche Verstärkung der partiellen Zerfallsbreite von $h \to \gamma\gamma$ im Zwei-Higgs-Dublett Modell Typ I für 3 verschiedene Potentiale diskutiert. Um den erlaubten Parameterbereich einzuschränken, werden perturbative Unitaritätsschranken, Vakuumstabilitätsschranken und elektroschwache Präzisionstests verwendet. Im Gegensatz zum Zwei-Higgs-Dublett Modell Typ II sind für Typ I leichte geladene skalare Teilchen mit $M_{H^\pm} \approx 100$ GeV noch nicht ausgeschlossen. Die mögliche Verstärkung der partiellen Zerfallsbreite ist für den Typ I im Parameterbereich, in dem leichte Skalare erlaubt sind, stärker als für Typ II. Nach der Einführung der verschiedenen Higgs-Potentiale werden der elektroschwache Präzisionstest und theoretische Schranken vorgestellt. Eine Diskussion über $b \to s\gamma$ zeigt, warum für Typ I - im Gegensatz zu Typ II - keine leichten Skalare ausgeschlossen werden können. Für jedes Potential wird dann unter Berücksichtigung der eingeführten Schranken als Nebenbedingungen der Parameterbereich gesucht, für den $\Gamma(h \to \gamma\gamma)$ besonders groß wird. Die Ergebnisse unterscheiden sich entsprechend für jedes Potential.

Abstract

The purpose of this thesis is to investigate possible enhancement of the partial decay width of $h \to \gamma\gamma$ in the THDM (Two Higgs Doublet Model) Type I arising from the Higgs sector for three different Higgs potentials. To find the parameter region where this is possible, constraints from tree level perturbative unitarity, tree level vacuum stability, electroweak precision constraints on the W boson mass and the Z boson decays into bottom quarks are employed. Unlike the THDM Type II, there is no constraint which excludes light charged scalars $M_{H^\pm} \approx 100$ GeV for the Type I model. A possible enhancement is then found to be substantially larger in Type I than in Type II models, in the parameter region where light charged Higgs are still allowed.

After reviewing the Higgs potential, the electroweak precision and theory constraints are introduced. A discussion of the difference between Type I and Type II in $b \to s\gamma$ shows why no light charged scalars can be excluded for Type I with this decay. The parameter space and maximal enhancement region of $\Gamma(h \to \gamma\gamma)$ is then discussed for these three Higgs potentials.

Acknowledgement

It is a great pleasure to thank those who made this thesis possible. My utmost gratitude goes to my supervisor Gerhard Ecker, for his trust in me, his readiness on helping me with any questions I should have, and his enduring patience. He has made available his support in a number of ways, not only by sharing his great expertise in particle physics, but also by considerably improving my spoken and written English.

I would like to thank Walter Grimus and Helmut Neufeld for their great support, valuable discussions, and feedback when I presented parts of this thesis in our seminar.

It is also an honor to thank Gerhard Ecker, Helmut Neufeld, and Helmuth Hüffel for making it possible that I could go to various schools on particle physics, which tremendously helped me to broaden my general knowledge and understanding of particle physics.

I am indebted to many of my colleagues for numerous discussions about physics and their emotional support, especially Andreas Kastner, Julian Schmid and Christian Thomay.

Last but not least I want to thank my parents, without whose financial support and care this thesis could never have been written.

Contents

List of acronyms

ATLAS A Toroidal LHC ApparatuS

BSM Beyond the Standard Model

CMS Compact Muon Solenoid

CP Charge Parity

DM Dark Matter

FCNC Flavour Changing Neutral Currents

IDM Inert Doublet Model

ILC International Linear Collider

KamLAND Kamioka Liquid Scintillator Antineutrino Detector

LEP Large Electron Positron Collider

LHC Large Hadron Collider

LO Leading Order

MSSM Minimal Supersymmetric Standard Model

NLO Next to Leading Order

NNLO Next to Next to Leading Order

PDF Parton Distribution Function

QCD Quantum chromodynamics

QED Quantum electrodynamics

SLC Stanford Linear Collider

SM Standard Model

SNO Sudbury Neutrino Observatory

THDM Two Higgs Doublet Model

vev vacuum expectation value

1 Introduction

The Standard Model (SM) has been well established as the model of the electroweak interactions by various experiments at the Large Electron Positron Collider (LEP), Stanford Linear Collider (SLC) and Tevatron. Precise measurements of various electroweak observables have shown that electroweak interactions are well described by a $SU(2)\times U(1)$ gauge symmetry, which is spontaneously broken. However, experimental information about the mechanism which actually breaks this symmetry is yet to be obtained. In the SM, this mechanism is the Higgs mechanism, which uses the vacuum expectation value (vev) of a scalar doublet to break the $SU(2)\times U(1)$ symmetry and generate the masses of fermions, Z and W bosons. If the Higgs mechanism is realized in this simple form of the SM, it leads to one Charge Parity (CP) even elementary scalar particle. In the SM the mass range of its neutral scalar can be narrowed down to 90 GeV $\leq M_h \leq$ 200 GeV by fitting SM predictions to electroweak observables [1]. In general, if symmetry breaking is realized via the Higgs mechanism in a certain model, it will typically lead to at least one scalar particle with a mass below 1 TeV. One is therefore optimistic that these scalars will be seen at the Large Hadron Collider (LHC), which runs at a center of mass energy of 14 TeV.

As production and decay of the Higgs particles are obviously model dependent, one has to study several scenarios for electroweak symmetry breaking via the Higgs mechanism carefully, and calculate production and decay rates of the Higgs bosons at the LHC.

As the SM accomplishes electroweak symmetry breaking with only a single doublet, it is self-suggesting and also consistent with experimental data to consider the next-to-simplest model by enlarging the Higgs sector of the SM with an additional Higgs doublet. Once introduced, this not only leads to 4 additional Higgs particles, but also to several features the SM does not have. The Two Higgs Doublet Model (THDM) may be used to implement a Dark Matter (DM) candidate in a very simple way in the Inert Doublet Model (IDM) [2]. Also an enlarged Higgs sector provides possibilities for CP violation in the Higgs sector to successfully accomplish electroweak baryogenesis. Electroweak baryogenesis refers to the process of getting from a matter and anti-matter symmetric early universe to the observed universe, where only small amounts of anti-matter remain. Sakharov found the conditions [3], which need to be satisfied to accomplish such a transition. One of the conditions is CP violation. While the SM implements CP violation via the CKM matrix [4], it is not enough to successfully accomplish electroweak baryogenesis. Additional CP violation can be provided via the Higgs sector of the THDM via CP violating vevs, or a nontrivial complex phase in the mixing matrix of the neutral Higgs bosons [5]. Yet another reason to consider the THDM is that a lot of Beyond the Standard Model (BSM) models have an additional doublet. The most popular of these is the Minimal Supersymmetric Standard Model (MSSM).

Yet another physics the SM misses to explain are massive neutrinos[1]. There exist various BSM models to generate neutrino masses, which include additional doublets and one or more scalar singlets [6, 7, 8].

Therefore, the THDM should provide a good starting point to study BSM models at

[1] In contrast to DM and electroweak baryogenesis, this is a well established experimental fact, shown in experiments at Sudbury Neutrino Observatory (SNO), Kamioka Liquid Scintillator Antineutrino Detector (KamLAND) and Super-Kamiokande

the LHC. The THDM Type II, which has the Yukawa structure needed for the MSSM, has been studied extensively in the literature. The THDM Type I, where all fermions couple to only one Higgs doublet has not been studied as much, despite the fact that it may lead to interesting phenomenology [2, 9, 10, 11, 12, 13]. Furthermore, light charged scalars (95 GeV $\leq M_{H^\pm} \leq$ 200 GeV) are not yet excluded in the Type I model. While it is certainly possible to produce such light charged scalars directly at LHC, we will focus on their influence in loops. We will investigate, if large enhancement due to the charged Higgs in the partial decay width of $h \to \gamma\gamma$ is possible. Electroweak precision tests and unitarity constraints are then used to narrow down the parameter space where this might be realized.

In Sec. 2 we will discuss various choices for Higgs potentials. Sec. 3 then briefly discusses the gauge fixing in the THDM. In Sec. 4 we discuss various possibilities of Yukawa couplings to the Higgs bosons, by defining the Z_2 symmetry for the left-handed doublets and right-handed singlets. Electroweak precision tests are then used in Sec. 5 to constrain the parameter space of the THDM through the W boson mass m_W. Fermionic Z decays into bottom quarks and hadrons are then used to get lower bounds for $\tan\beta$. In Sec. 6 phenomenological differences between THDM Type I and Type II are discussed for inclusive decays of the bottom into strange quarks and photons. In Sec. 7, we use unitarity constraints to generally constrain the parameter region and to get upper bounds for $\tan\beta$. Sec. 8 investigates possible enhancement of the decay channel $h \to \gamma\gamma$, which is considered to be a discovery channel at LHC for a light SM Higgs, and applies the constraints obtained in Secs. 5 and 7 to the parameter region considered. In Sec. 9 we briefly discuss how deviations from these deviations of $h \to \gamma\gamma$ from the SM could be seen at LHC. Finally in the appendix we discuss conventions and give the couplings for the various potentials considered.

2 The potentials

2.1 Constructing the potential

We construct the most general Higgs potential under the assumptions of hermiticity, SU(2)×U(1) gauge symmetry and renormalizability. With these assumptions we get:

$$
\begin{aligned}
V =& m_{11}^2\Phi_1^\dagger\Phi_1 + m_{22}^2\Phi_2^\dagger\Phi_2 - \left[m_{12}^2\Phi_1^\dagger\Phi_2 + h.c.\right] \\
&+ \frac{1}{2}\lambda_1\left(\Phi_1^\dagger\Phi_1\right)^2 + \frac{1}{2}\lambda_2\left(\Phi_2^\dagger\Phi_2\right)^2 + \lambda_3\left(\Phi_1^\dagger\Phi_1\right)\left(\Phi_2^\dagger\Phi_2\right) + \lambda_4\left(\Phi_1^\dagger\Phi_2\right)\left(\Phi_2^\dagger\Phi_1\right) \\
&+ \left\{\frac{1}{2}\lambda_5\left(\Phi_1^\dagger\Phi_2\right)^2 + \left[\lambda_6\left(\Phi_1^\dagger\Phi_1\right) + \lambda_7\left(\Phi_2^\dagger\Phi_2\right)\right]\Phi_1^\dagger\Phi_2 + h.c.\right\} \qquad (1)
\end{aligned}
$$

where

$$
\begin{aligned}
\Phi_1 &= \begin{pmatrix} \varphi_1^+ \\ \dfrac{\varphi_1 + i\chi_1}{\sqrt{2}} \end{pmatrix} = \frac{1}{\sqrt{2}}\begin{pmatrix} \psi_2 + i\psi_1 \\ \psi_4 + i\psi_3 \end{pmatrix} \\
\Phi_2 &= \begin{pmatrix} \varphi_2^+ \\ \dfrac{\varphi_2 + i\chi_2}{\sqrt{2}} \end{pmatrix} = \frac{1}{\sqrt{2}}\begin{pmatrix} \psi_6 + i\psi_5 \\ \psi_8 + i\psi_7 \end{pmatrix} . \qquad (2)
\end{aligned}
$$

This is the most general potential with explicit CP violation. A potential will be CP-conserving if there exists a basis, in which all the parameters are real [14]. Without enforcing a particular symmetry, Higgs couplings will lead to Flavour Changing Neutral Currents (FCNC) in the Yukawa sector. As FCNC are strongly constrained by precision experiments, one either has to avoid a vast region of parameter space or enforce a discrete symmetry. One way to do this is to enforce the Z_2 symmetry

$$
\Phi_1 \to \Phi_1, \quad \Phi_2 \to -\Phi_2 . \qquad (3)
$$

The potential then simplifies to:

$$
\begin{aligned}
V_A =& \; m_{11}^2\Phi_1^\dagger\Phi_1 + m_{22}^2\Phi_2^\dagger\Phi_2 \\
&+ \frac{1}{2}\lambda_1\left(\Phi_1^\dagger\Phi_1\right)^2 + \frac{1}{2}\lambda_2\left(\Phi_2^\dagger\Phi_2\right)^2 + \lambda_3\left(\Phi_1^\dagger\Phi_1\right)\left(\Phi_2^\dagger\Phi_2\right) + \lambda_4\left(\Phi_1^\dagger\Phi_2\right)\left(\Phi_2^\dagger\Phi_1\right) \\
&+ \left[\frac{1}{2}\lambda_5\left(\Phi_1^\dagger\Phi_2\right)^2 + h.c.\right] . \qquad (4)
\end{aligned}
$$

After enforcing Z_2 symmetry, the only remaining complex parameter is λ_5. In this case we can simply rephase the fields to make the potential real. This means that one cannot have CP violation and Z_2 conservation at the same time. One way to keep a CP violating phase in the parameters is to consider a potential where Z_2 is only softly violated. This forbids Z_2 violating operators higher than mass dimension 2, while still allowing operators with mass dimension 2. Thus we can keep $m_{12}^2 \neq 0$. Keeping $\lambda_5 \neq 0$ as well, we get a non-trivial CP violating phase, while still getting rid of FCNC. In this work, we will only deal with CP conserving models. Therefore we will always work in a basis where all parameters are real. There are at present 3 popular potentials of this kind studied in the literature. In the following we will specify these potentials in their particular parametrization and give the couplings of their potentials. We will first discuss the more general case and then specialize to the other cases.

2.2 The potential V_λ with soft Z_2 violation

The potential V_λ is the Z_2 symmetric potential (4) with an additional term of operator mass dimension 2 breaking the Z_2 symmetry softly. It corresponds to (1) with $\lambda_6 = \lambda_7 = 0$ and all parameters being real:

$$\begin{aligned} V_\lambda = & m_{11}^2 \Phi_1^\dagger \Phi_1 + m_{22}^2 \Phi_2^\dagger \Phi_2 - \left[m_{12}^2 \Phi_1^\dagger \Phi_2 + h.c. \right] \\ & + \frac{1}{2}\lambda_1 \left(\Phi_1^\dagger \Phi_1 \right)^2 + \frac{1}{2}\lambda_2 \left(\Phi_2^\dagger \Phi_2 \right)^2 + \lambda_3 \left(\Phi_1^\dagger \Phi_1 \right) \left(\Phi_2^\dagger \Phi_2 \right) + \lambda_4 \left(\Phi_1^\dagger \Phi_2 \right) \left(\Phi_2^\dagger \Phi_1 \right) \\ & \left\{ + \frac{1}{2}\lambda_5 \left(\Phi_1^\dagger \Phi_2 \right)^2 + h.c. \right\} \end{aligned} \tag{5}$$

An alternative parametrization is often used in the literature [15], [16]:

$$\begin{aligned} V = & \Lambda_1(|\Phi_1|^2 - V_1^2)^2 + \Lambda_2(|\Phi_2|^2 - V_2^2)^2 + \Lambda_3[(|\Phi_1|^2 + |\Phi_2| - (V_1^2 + V_2^2)]^2 \\ & + \Lambda_4 \left[|\Phi_1|^2 |\Phi_2|^2 - |\Phi_1^\dagger \Phi_2|^2 \right] + \Lambda_5(\Re \Phi_1^\dagger \Phi_2 - V_1 V_2)^2 + \Lambda_6(\Im \Phi_1^\dagger \Phi_2)^2 \end{aligned} \tag{6}$$

where $V_{1,2} = v_{1,2}/\sqrt{2}$. The potential (6) can be translated into the generic basis (5) with substitutions given in [17]. This model has been implemented in FeynArts by Arhrib [16] and will be used in this work. Note that one can easily obtain the potentials V_A defined in (4) by setting $m_{12} = 0$ and V_B defined in (31) by setting $\lambda_5 = 0$.

2.2.1 Conditions for a realistic vacuum

To get stable and realistic vevs, the following conditions need to be satisfied:

- The potential must admit a non-trivial stationary point away from the origin ($v_1 = v_2 = 0$).
- The Hessian matrix of the potential must be positive semidefinite at the desired vacuum. This condition is equivalent to all Higgs masses being positive. As we have the massless pseudo-Goldstone bosons, this condition does not yet guarantee that this vacuum is a minimum.
- The potential must be bounded from below ($V > -\infty$).

The potential always admits a trivial stationary point at the origin, which is zero. To break the gauge symmetry $SU(2) \times U(1)$ one needs a nonzero minimum, which is lower than the trivial one ($v_1 = 0, v_2 = 0$).

2.2.2 Conditions for the vacuum to be bounded from below

As mentioned before, it is essential to ensure the potential to be bounded from below by deriving necessary and sufficient conditions where this is satisfied. We will derive these conditions for the potential V_λ (5), which is the most general of the potentials used in this work. It has 8 real arguments (8 fields involved). We use the real parametrization of Ref. [18]:

$$\begin{aligned}
V &= a_1 x_1 + a_2 x_2 + a_3 x_3 + b_{11} x_1^2 + b_{22} x_2^2 + b_{33} x_3^2 + b_{44} x_4^2 + b_{12} x_1 x_2 \\
x_1 &= |\Phi_1|^2 = \frac{1}{2}\left(\psi_1^2 + \psi_2^2 + \psi_3^2 + \psi_4^2\right) \\
x_2 &= |\Phi_2|^2 = \frac{1}{2}\left(\psi_5^2 + \psi_6^2 + \psi_7^2 + \psi_8^2\right) \\
x_3 &= \Re\Phi_1^\dagger\Phi_2 = \frac{1}{2}\left(\psi_1\psi_5 + \psi_2\psi_6 + \psi_3\psi_7 + \psi_4\psi_8\right) \\
x_4 &= \Im\Phi_1^\dagger\Phi_2 = \frac{1}{2}\left(-\psi_1\psi_6 + \psi_2\psi_5 + \psi_4\psi_7 - \psi_3\psi_8\right)
\end{aligned} \tag{7}$$

where now

$$\begin{gathered}
a_1 = m_{11}^2, \quad a_2 = m_{22}^2, \quad a_3 = -2m_{12}^2 \\
b_{11} = \frac{\lambda_1}{2}, \quad b_{22} = \frac{\lambda_2}{2}, \quad b_{33} = \lambda_4 + \lambda_5, \quad b_{44} = \lambda_4 - \lambda_5, \quad b_{12} = \lambda_3 \ .
\end{gathered} \tag{8}$$

The asymptotic behavior of V as $|x_i| \to \infty$ is determined by the bilinear terms $x_i x_j$. Neglecting the terms linear in x_i, one finds necessary conditions for the potential to be bounded from below. As x_1 and x_2 are independent variables their quadratic coefficients must be positive: $b_{11}, b_{22} \geq 0$. To get further restrictions we pick several directions. At first we start with $x_1 \neq 0$, $x_2 \neq 0$, $x_3 = x_4 = 0$. As $x_1, x_2 \geq 0$, we can use the parametrization $x_1 = \rho\cos^2\theta$, $x_2 = \rho\sin^2\theta$. For large ρ we can neglect the linear terms and get the vacuum stability condition for the selected direction:

$$\begin{aligned}
\rho^2\left[b_{11}\cos^4\theta + b_{22}\sin^4\theta + b_{12}\sin\theta^2\cos\theta^2\right] &> -\infty \\
b_{11}\cos^4\theta + b_{22}\sin^4\theta + b_{12}\sin\theta^2\cos\theta^2 &\geq 0 \\
b_{11}\cot^2\theta + b_{22}\tan^2\theta + b_{12} &\geq 0 \ .
\end{aligned} \tag{9}$$

Our task then reduces to find the minimum of the function

$$f(\tan\theta) = b_{11}\cot^2\theta + b_{22}\tan^2\theta + b_{12} \ . \tag{10}$$

This minimum is found at

$$\tan^2\theta = \sqrt{\frac{b_{11}}{b_{22}}} \ . \tag{11}$$

Inserting this back into (9) we get for the minimum

$$2\sqrt{b_{11}b_{22}} \geq -b_{12} \ . \tag{12}$$

We can use other directions to get further constraints: $x_1 \neq 0$, $x_2 \neq 0$, $x_3^2 = x_1 x_2$ with $x_4^2 = 0$, and $x_1 \neq 0$, $x_2 \neq 0$, $x_4^2 = x_1 x_2$ with $x_3^2 = 0$. Using similar arguments as before, going back to the parametrization of (5) we get the constraints

$$\begin{aligned}
\lambda_1,\ \lambda_2 \geq 0 \text{ and } -(\lambda_1\lambda_2)^{1/2} &< \lambda_3 \\
-(\lambda_1\lambda_2)^{1/2} &< \lambda_3 + \lambda_4 + \lambda_5 \\
-(\lambda_1\lambda_2)^{1/2} &< \lambda_3 + \lambda_4 - \lambda_5 \ .
\end{aligned} \tag{13}$$

Note that this is equivalent to the set of conditions

$$\begin{aligned} &\lambda_1,\, \lambda_2 \geq 0 \text{ and } -(\lambda_1\lambda_2)^{1/2} < \lambda_3 \\ &-(\lambda_1\lambda_2)^{1/2} < \lambda_3 + \lambda_4 - |\lambda_5|\;, \end{aligned} \tag{14}$$

which usually appears in the literature [2]. These are necessary and sufficient conditions to keep the vacuum stable at the tree level. These conditions are very powerful when it comes to constraining the parameter space of the Higgs sector, and they will be employed in Sec. 8.

2.2.3 The potential in the mass eigenbasis

To break the electroweak symmetry, the scalar potential has to have a global minimum with at least one nonzero vev. Despite the fact that this potential also has the possibility of spontaneous CP-violation, we will consider only CP-conserving minima in the following. We can then parametrize the two Higgs doublets as

$$\Phi_1 = \begin{pmatrix} \varphi_1^+ \\ \dfrac{v_1 + \varphi_1 + i\chi_1}{\sqrt{2}} \end{pmatrix} \quad , \quad \Phi_2 = \begin{pmatrix} \varphi_2^+ \\ \dfrac{v_2 + \varphi_2 + i\chi_2}{\sqrt{2}} \end{pmatrix} . \tag{15}$$

After inserting (15) into (5), we diagonalize the quadratic couplings to get the mass eigenstates

$$\begin{aligned} H^- &= \frac{1}{\sqrt{v_1^2+v_2^2}}\left(-v_2\varphi_1^- + v_1\varphi_2^-\right) \;, & G^- &= \frac{1}{\sqrt{v_1^2+v_2^2}}\left(v_1\varphi_1^- + v_2\varphi_2^-\right) \\ A &= \frac{1}{\sqrt{v_1^2+v_2^2}}\left(-v_2\chi_1 + v_1\chi_2\right) \;, & G^0 &= \frac{1}{\sqrt{v_1^2+v_2^2}}\left(v_1\chi_1 + v_2\chi_2\right) \end{aligned} \tag{16}$$

and the masses

$$M_{H^-}^2 = \frac{v_1^2+v_2^2}{2v_1v_2}\left[2m_{12}^2 - v_1v_2(\lambda_4+\lambda_5)\right] \;, \qquad M_A^2 = \frac{v_1^2+v_2^2}{v_1v_2}\left(m_{12}^2 - v_1v_2\lambda_5\right) \;. \tag{17}$$

The only non-trivial diagonalization is the one of the CP even scalars. Any real symmetric 2×2 matrix can be diagonalized with a matrix depending only on one angle:

$$\mathcal{L}_{M_{h,H}} = -\frac{1}{2}(\varphi_1,\varphi_2)\begin{pmatrix} a & c \\ c & d \end{pmatrix}\begin{pmatrix} \varphi_1 \\ \varphi_2 \end{pmatrix} = -\frac{1}{2}(H,h)\begin{pmatrix} M_H^2 & 0 \\ 0 & M_h^2 \end{pmatrix}\begin{pmatrix} H \\ h \end{pmatrix} \;, \tag{18}$$

with the masses

$$M_{H,h}^2 = \frac{1}{2}\left[a + d \pm \sqrt{(a-d)^2 + 4c^2}\right] \tag{19}$$

and the values

$$a = \frac{1}{v_1}(m_{12}^2 v_2 + v_1^3\lambda_1) \;, \quad c = \left[-m_{12}^2 + v_1v_2(\lambda_3+\lambda_4+\lambda_5)\right] \;, \quad d = \frac{1}{v_2}(m_{12}^2 v_1 + v_2^3\lambda_2)$$

$$H = c_\alpha\varphi_1 + s_\alpha\varphi_2 \;, \qquad h = -s_\alpha\varphi_1 + c_\alpha\varphi_2 \tag{20}$$

where

$$c_\alpha = \cos\alpha\ , \qquad s_\alpha = \sin\alpha\ . \tag{21}$$

G^0 and $G^\pm$ are the would-be Goldstone bosons, which stay massless and will become the longitudinal components of the W and Z bosons (See Sec. 3). For both masses M_H, M_h being nonzero, we can use the projection theorem to express the original mass matrix with its eigenvalues and eigenvectors. We then get:

$$a = M_H^2 c_\alpha^2 + M_h^2 s_\alpha^2\ , \qquad c = c_\alpha s_\alpha (M_H^2 - M_h^2)\ , \qquad d = M_H^2 s_\alpha^2 + M_h^2 c_\alpha^2\ . \tag{22}$$

To compare our parametrization with others more easily, we express all of the couplings with

$$M_H, \quad M_h, \quad M_A, \quad M_{H^\pm}, \quad \tan\beta, \quad \sin\alpha, \quad m_{12}^2, \tag{23}$$

where

$$\tan\beta \equiv \frac{v_2}{v_1}\ . \tag{24}$$

One usually further introduces the abbreviations

$$v \equiv \sqrt{v_1^2 + v_2^2}, \qquad v_2 = v\sin\beta, \qquad v_1 = v\cos\beta\ . \tag{25}$$

After this re-parametrization, one can simply go to the basis used in [16] by using $m_{12}^2 = \frac{v^2}{2}\sin\beta\cos\beta\Lambda_5$. The Feynman rules of the potential used in FeynArts [16] have been checked for this general case. The couplings of the potential will be given in Sec. 11.3, in the basis (23).

2.2.4 Tunneling to different minima

In some cases the parameter space of the potential admits two non-degenerate minima (v_1, v_2) and (v_1', v_2'). In this case, the vacuum may tunnel from the higher minimum to the lower one. If this happens, the masses of the Higgs bosons will also change! This was studied in Ref. [18]. Barroso et al. however concluded in a numerical analysis that this case is rather rare (out of 15 million examined points 37000 had this feature). We will not study this tunneling effects and try to avoid this parameter region.

2.3 The Z_2-symmetric potential

This is the version of the potential (5) without soft breaking ($m_{12}^2 = 0$). It corresponds to the model called V_A in [18]:

$$\begin{aligned} V_A = {} & m_{11}^2 \Phi_1^\dagger\Phi_1 + m_{22}^2 \Phi_2^\dagger\Phi_2 \\ & + \frac{1}{2}\lambda_1 \left(\Phi_1^\dagger\Phi_1\right)^2 + \frac{1}{2}\lambda_2 \left(\Phi_2^\dagger\Phi_2\right)^2 + \lambda_3 \left(\Phi_1^\dagger\Phi_1\right)\left(\Phi_2^\dagger\Phi_2\right) + \lambda_4 \left(\Phi_1^\dagger\Phi_2\right)\left(\Phi_2^\dagger\Phi_1\right) \\ & + \left[\frac{1}{2}\lambda_5 \left(\Phi_1^\dagger\Phi_2\right)^2 + h.c.\right]\ . \end{aligned} \tag{26}$$

2.3.1 Possible minima

The possible minima of this potential were studied in Ref. [18]. It provides 3 non-degenerate non-trivial solutions for possible stationary points. The first one amounts to

$$v_1 = 0, \qquad v_2^2 = -\frac{m_{22}^2}{\lambda_2}, \qquad V_I = -\frac{m_{22}^4}{2\lambda_2}. \tag{27}$$

As $\lambda_2 > 0$ because of (13) and $v_2 > 0$ the mass parameter m_{22}^2 must be negative: $m_{22}^2 < 0$. As the sign of v_2 is not fixed in (27), we have 2 possibilities $v_2 = \pm\sqrt{v_2^2}$. As $v_1 = 0$ the stationary point V_I has degeneracy 2 as $(0, +\sqrt{v_2^2})$ and $(0, -\sqrt{v_2^2})$ yield the same V_I. An analogous second stationary point exists at

$$v_2 = 0, \qquad v_1^2 = -\frac{m_{11}^2}{\lambda_1}, \qquad V_{II} = -\frac{m_{11}^4}{2\lambda_1}\ , \tag{28}$$

which in turn demands $m_{11}^2 < 0$. The degeneracy of V_{II} is also 2. If both (27) and (28) are allowed minima, tunneling may occur between these minima. We can avoid tunneling by simply enforcing $m_{22}^2 < 0\ , m_{11}^2 > 0$ for (27) and vice versa for these kind of models. If one of the above cases is realized, the model is referred to as the IDM [2]. For the third stationary point we get:

$$v_1^2 = \frac{\lambda_2 m_{11}^2 - (\lambda_3 + \lambda_4 + \lambda_5)m_{22}^2}{(\lambda_3 + \lambda_4 + \lambda_5)^2 - \lambda_1\lambda_2}, \qquad v_2^2 = \frac{\lambda_1 m_{22}^2 - (\lambda_3 + \lambda_4 + \lambda_5)m_{11}^2}{(\lambda_3 + \lambda_4 + \lambda_5)^2 - \lambda_1\lambda_2},$$
$$V_{III} = \frac{m_{11}^2 m_{22}^2(\lambda_3 + \lambda_4 + \lambda_5) - 1/2(m_{22}^4\lambda_1 + m_{11}^4\lambda_2)}{\lambda_1\lambda_2 - (\lambda_3 + \lambda_4 + \lambda_5)^2}\ . \tag{29}$$

V_{III} is always negative, which can be seen using the vacuum stability conditions (13). As we have 4 ways to choose the sign of v_1 and v_2 all yielding the same stationary point V_{III}, its degeneracy is 4. Including the stationary point at the origin, we therefore have 9 different stationary points in total. It was shown in [18] that if V_{III} is a minimum, V_I and V_{II} cannot be minima. One can also have V_{II} as the only minima, if one avoids tunneling ($m_{11}^2 < 0$, $m_{22}^2 > 0$). In the following, when referring to the IDM, we will always mean the vevs of (27) where $v_1 = 0$.

2.3.2 The potential in the mass eigenbasis

For the realization (29) where $v_1, v_2 \neq 0$ we can use the results of the discussion in Sec. 2.2.3 and set $m_{12} = 0$. This brings the potential into a physical basis where all the parameters of the potential are now expressed with $\tan\beta$, $\sin\alpha$ and the Higgs masses.
For the IDM however, there is no mixing angle and no dependence on $\tan\beta$. Hence 2 variables of the original parametrization will remain unexpressed. We will choose the vevs of (27) and insert them into (4). This gives us the Higgs masses:

$$M_h^2 = v_2^2\lambda_2 \qquad\qquad M_H^2 = m_{11}^2 + \frac{v_2^2}{2}(\lambda_3 + \lambda_4 + \lambda_5)$$
$$M_{H^\pm}^2 = m_{11}^2 + \frac{v_2^2}{2}\lambda_3 \qquad\qquad M_A^2 = m_{11}^2 + \frac{v_2^2}{2}(\lambda_3 + \lambda_4 - \lambda_5)\ . \tag{30}$$

Using (30), we can now express λ_2, λ_3, λ_4, λ_5 and calculate the couplings in the mass eigenbasis. As the Z_2-symmetry is unbroken in the IDM, the second doublet Φ_1 is inert. This means that the S-matrix is invariant under Z_2, and therefore particles of the inert doublet Φ_1 can only be pair-produced. Furthermore, the lightest particle of the inert doublet cannot decay and will contribute to Dark Matter.

2.4 The potential V_B with soft U(1) violation

Another alternative to define a potential is to enforce a U(1)-symmetry. To avoid a massless scalar appearing in the theory, one breaks it softly with $m_{12}^2 \neq 0$. This corresponds to the potential V_λ (5) with $\lambda_5 = 0$. In [18] this potential is called V_B:

$$\begin{aligned} V_B = & m_{11}^2 \Phi_1^\dagger \Phi_1 + m_{22}^2 \Phi_2^\dagger \Phi_2 - \left[m_{12}^2 \Phi_1^\dagger \Phi_2 + h.c. \right] \\ & + \frac{1}{2}\lambda_1 \left(\Phi_1^\dagger \Phi_1 \right)^2 + \frac{1}{2}\lambda_2 \left(\Phi_2^\dagger \Phi_2 \right)^2 + \lambda_3 \left(\Phi_1^\dagger \Phi_1 \right) \left(\Phi_2^\dagger \Phi_2 \right) + \lambda_4 \left(\Phi_1^\dagger \Phi_2 \right) \left(\Phi_2^\dagger \Phi_1 \right) \end{aligned} \tag{31}$$

Also in this case one can have 2 different non-trivial minima. This was discussed in [18]. We will again avoid the parameter space where this is possible. For the eigenbasis we can use the discussion of Sec. 2.2.3 setting $\lambda_5 = 0$. The couplings of V_B can be found in Sec. 11.3.

3 Scalar kinetic terms

After discussing the various possible choices for the potential, we will now study the interaction of the Higgs sector with the gauge bosons. This is given as

$$\mathcal{L}_{\text{kin}} = |D\phi_1|^2 + |D\phi_2|^2 \tag{32}$$

where D is the covariant derivative of $SU(2) \times U(1)^2$:

$$D_\mu \equiv \partial_\mu + ig\tilde{A}^a_\mu t^a + ig' Y B_\mu = \partial_\mu + ig^a A^a_\mu t^a \ . \tag{33}$$

Y is the $U(1)$ hypercharge and t^a are the normalized Pauli matrices $t^a = \sigma^a/2$. Please note that in principle there could also be a mixed term $D\phi_1 D\phi_2$ in (32), but this is eliminated by the Z_2-symmetry defined in (3). For the following discussion it is convenient to change into the real basis (2). We then have 8 real-valued scalar fields ψ_i. We can rewrite the infinitesimal gauge transformation of the fields with antisymmetric real matrices T^a:

$$\psi_i \to (1 + i\alpha^a t^a)_{ij}\psi_j = (1 - \alpha^a T^a)_{ij}\psi_j \tag{34}$$

and in turn also the covariant derivative to $D_\mu = \partial_\mu - g^a A^a_\mu T^a$. Expanding about the vevs $\psi_i \to \psi^0_i + \psi_i$, we get the following terms:

$$\begin{aligned}\mathcal{L}_{\text{kin}} =& \frac{1}{2}(\partial_\mu \psi_i)^2 - g^a A^a_\mu (\partial_\mu \psi_i T^a_{ij} \psi_j) + \frac{1}{2} g^a g^b A^a_\mu A^{b\mu} (T^a \psi)_i (T^b \psi)_i \\ & - g^a A^a_\mu (\partial_\mu \psi_i T^a_{ij} \psi^0_j) + g^a g^b A^a_\mu A^{b\mu} (T^a \psi^0)_i (T^b \psi)_i \\ & + \frac{1}{2} g^a g^b A^a_\mu A^{b\mu} (T^a \psi^0)_i (T^b \psi^0)_i \end{aligned} \tag{35}$$

where $\psi^0_i = \delta_{4i} v_1 + \delta_{8i} v_2$. We now define

$$F^a_i = g^a T^a_{ij} \psi^0_j \ . \tag{36}$$

To get F^a_i we just have to calculate the matrices T^a. Doing so we get

$$F^a_i = (G v_1, G v_2) \qquad \text{where} \quad G = \frac{1}{2}\begin{pmatrix} g & 0 & 0 & 0 \\ 0 & g & 0 & 0 \\ 0 & 0 & g & 0 \\ 0 & 0 & -g' & 0 \end{pmatrix}, \tag{37}$$

where F^a_i has 4 rows for the 4 gauge bosons and 8 columns for the 8 real scalar fields.

We first calculate the mass matrix of the gauge bosons. The terms bilinear in the gauge fields A^a are

$$\frac{1}{2} A^a_\mu A^{b\mu} F^a_i F^b_i = \frac{1}{2} A^a_\mu A^{b\mu} (m^2_{\text{gauge}})_{ab} \tag{38}$$

[2]This convention is called the Haber-Kane convention. Other conventions are the Denner convention $D_\mu = \partial_\mu - ig\tilde{A}^a_\mu t^a + ig' Y B_\mu$ and the Peskin-Schroeder convention $D_\mu = \partial_\mu - ig\tilde{A}^a_\mu t^a - ig' Y B_\mu$.

where

$$(m^2_{\text{gauge}})_{ab} = (FF^T)_{ab} = GG^T(v_1^2+v_2^2) = \frac{v_1^2+v_2^2}{4}\begin{pmatrix} g^2 & 0 & 0 & 0 \\ 0 & g^2 & 0 & 0 \\ 0 & 0 & g^2 & -gg' \\ 0 & 0 & -gg' & g'^2 \end{pmatrix} . \tag{39}$$

We diagonalize (39) in the usual way:

$$A^1 = \frac{1}{\sqrt{2}}\left(W^+ + W^-\right) , \qquad A^2 = \frac{1}{i\sqrt{2}}\left(W^- - W^+\right) \tag{40}$$

$$A^3 = \frac{1}{\sqrt{g^2+g'^2}}\left(g'A + gZ\right) , \qquad A^4 = B = \frac{1}{\sqrt{g^2+g'^2}}\left(gA - g'Z\right) \tag{41}$$

with A^a expressed in the mass eigenbasis as $W^\pm$, Z bosons and the massless photon A. This leads to the masses of the gauge bosons:

$$\mathcal{L}_{\text{g-mass}} = m_W^2 W^{+\mu}W^-_\mu + \frac{m_Z^2}{2}Z^2 \tag{42}$$

where

$$m_W = \frac{g\sqrt{v_1^2+v_2^2}}{2} , \qquad m_Z = \frac{\sqrt{v_1^2+v_2^2}\sqrt{g^2+g'^2}}{2}. \tag{43}$$

One then introduces the weak mixing angle

$$\cos\theta_W \equiv c_W \equiv \frac{m_W}{m_Z}. \tag{44}$$

As in the SM, we have the relation

$$e = \frac{gg'}{\sqrt{g^2+g'^2}}. \tag{45}$$

As e can be calculated from the fine structure constant, and m_W and m_Z were measured by precision experiments at LEP, one gets the following condition for the vevs:

$$v = \sqrt{v_1^2+v_2^2} \approx 246 \text{ GeV} . \tag{46}$$

We now use the Faddeev-Popov method to fix the gauge. We get for the generating functional:

$$Z = C' \int \mathcal{D}A\mathcal{D}\psi \;\exp\left[i\int d^4x \left(\mathcal{L}[A,\psi] - \frac{1}{2}(G)^2\right)\right] \det\left(\frac{\delta G}{\delta\alpha}\right) \tag{47}$$

where C' is just a normalization constant. The gauge fixing term is chosen to cancel the term $g^a A^a_\mu(\partial_\mu\psi_i T^a_{ij}\psi^0_j)$ in the Lagrangian (35). This can be done by choosing

$$G^a = \frac{1}{\sqrt{\xi}}\left(\partial_\mu A^{a\mu} + \xi F^a_i\psi_i\right) . \tag{48}$$

Note that only Goldstone bosons contribute to G^a. We therefore have:

$$-\frac{1}{2}G^2 = \frac{1}{2}A^a_\mu \left(\frac{1}{\xi}\partial^\mu\partial^\nu\right) A^a_\nu + A^{a\mu} F^a_i \partial_\mu \psi_i - \frac{1}{2}\xi \left[F^a_i \psi_i\right]^2 . \tag{49}$$

The last term gives the Goldstone bosons their masses:

$$(m^2_{\text{Gold}})_{ij} = \xi F^a_i F^a_j = \xi (F^T F)_{ij} = \xi \begin{pmatrix} G^T G v_1^2 & G^T G v_1 v_2 \\ G^T G v_1 v_2 & G^T G v_2^2 \end{pmatrix} = \xi V \otimes D \tag{50}$$

with matrices

$$V = \begin{pmatrix} v_1^2 & v_1 v_2 \\ v_1 v_2 & v_2^2 \end{pmatrix}, \quad D = G^T G = \frac{1}{4}\begin{pmatrix} g^2 & 0 & 0 & 0 \\ 0 & g^2 & 0 & 0 \\ 0 & 0 & g^2 + g'^2 & 0 \\ 0 & 0 & 0 & 0 \end{pmatrix}. \tag{51}$$

$D = G^T G$ is diagonal, but V is not. We can however easily diagonalize V. We then get for the mass matrix:

$$V \otimes D = (V_b \otimes 1)(D^V \otimes D)(V_b \otimes 1) \tag{52}$$

where

$$V_b = \frac{1}{\sqrt{v_1^2 + v_2^2}} \begin{pmatrix} v_1 & v_2 \\ v_2 & -v_1 \end{pmatrix}, \qquad D^V = \begin{pmatrix} v_1^2 + v_2^2 & 0 \\ 0 & 0 \end{pmatrix}. \tag{53}$$

Let us now see what the basis change does with the scalars:

$$\psi' = (V_b \otimes 1)\psi = \frac{1}{\sqrt{v_1^2 + v_2^2}} \begin{pmatrix} v_1 \tilde{\phi}_1 + v_2 \tilde{\phi}_2 \\ v_2 \tilde{\phi}_1 - v_1 \tilde{\phi}_2 \end{pmatrix} \tag{54}$$

where

$$\tilde{\phi}_1 \equiv (\psi_1, \psi_2, \psi_3, \psi_4), \quad \tilde{\phi}_2 \equiv (\psi_5, \psi_6, \psi_7, \psi_8). \tag{55}$$

Using this basis, we get the mass eigenstates

$$[F^a_i \psi_i]^2 = (v_1^2 + v_2^2)\psi'^T \begin{pmatrix} D & 0 \\ 0 & 0 \end{pmatrix} \psi' = (v_1 \tilde{\phi}_1 + v_2 \tilde{\phi}_2) D (v_1 \tilde{\phi}_1 + v_2 \tilde{\phi}_2). \tag{56}$$

Expanding this further, we get:

$$\frac{\xi}{2}\left[F^a_i \psi_i\right]^2 = \xi \frac{1}{8}\left[g^2 (v_1 \psi_1 + v_2 \psi_5)^2 + g^2 (v_1 \psi_2 + v_2 \psi_6)^2 + (g^2 + g'^2)(v_1 \psi_3 + v_2 \psi_7)^2\right] . \tag{57}$$

Using the mass eigenbasis of the scalars (16) one finds that (57) are the mass terms of the Goldstone bosons:

$$\frac{\xi}{2}\left[g^a F^a_i \psi_i\right]^2 = \frac{\xi}{4} g^2 (v_1^2 + v_2^2)(G^+ G^-) + \frac{\xi}{8}(g^2 + g'^2)(v_1^2 + v_2^2)(G^0)^2 . \tag{58}$$

The masses of the Goldstone bosons are proportional to the masses of their gauge boson counterparts:

$$m_{G^\pm} = \sqrt{\xi} m_W , \qquad m_{G^0} = \sqrt{\xi} m_Z \ . \tag{59}$$

In the Feynman-'t Hooft gauge ($\xi = 1$), these are exactly the masses of the gauge bosons. In the generating functional (47) we have a factor with a determinant, which depends on the gauge and Higgs fields. Using the Faddeev-Popov method (See e.g. Ref. [19]), we can easily write it as a Lagrangian:

$$\mathcal{L}_{\text{ghost}} = \overline{c}^a \left[-(\partial^\mu (\partial_\mu \delta^{ab} + \tilde{\epsilon}^{arb} A^r_\mu) - \xi g^a g^b (T^a \psi_0) T^b (\psi_0 + \psi) \right] c^b \tag{60}$$

$$g^a = \begin{cases} g & a \in \{1,2,3\} \\ g' & a = 4 \end{cases} , \qquad \tilde{\epsilon}^{arb} = \begin{cases} \epsilon^{arb} & a,r,b \in \{1,2,3\} \\ 0 & \text{else} \end{cases} . \tag{61}$$

The fields c in (60) are the anti-commuting ghost fields, arising solely from gauge fixing. We see that for the ghosts their mass matrix is proportional to the mass matrix of the gauge bosons, with the additional factor ξ:

$$m^2_{\text{ghosts}} = \xi m^2_{\text{gauge}} \ . \tag{62}$$

Therefore, we can use the basis of the gauge bosons to diagonalize the ghosts. After doing so, one can easily write down the Lagrangian in the mass eigenbasis of ghosts, gauge bosons, Goldstone bosons and Higgs particles.
We will now derive the propagators of these particles:

$$D^{\mu\nu}(k) = \frac{-i}{k^2 - m^2} \big[g^{\mu\nu} - \frac{k^\mu k^\nu}{k^2 - \xi m^2} (1 - \xi) \big], \quad G(k) = Y(k) = \frac{-i}{k^2 - \xi m^2}, \tag{63}$$

where D is the propagator of the gauge bosons with masses $m = m_W$ for the $W^\pm$, $m = m_Z$ for the Z boson and $m = 0$ for the photon in the mass eigenbasis. G is the propagator of the Goldstone bosons $G^\pm$ and G^0, while Y is the propagator of the ghosts, where we have one ghost field for each gauge boson (including the photon). The mass m appearing in the propagators G and Y therefore always is the mass of its corresponding gauge boson. It is apparent from this discussion that Goldstone bosons and ghosts are unphysical particles, as their masses depend on ξ, which is the arbitrarily chosen gauge fixing. ξ must cancel in physical observables like cross sections, decay rates and the like. If one wants to eliminate the unphysical degrees of freedom from the very beginning, one employs the unitary gauge $\xi \to \infty$. The propagators then simplify to:

$$D^{\mu\nu}(k) = \frac{-i}{k^2 - m^2} \big[g^{\mu\nu} - \frac{k^\mu k^\nu}{m^2} \big], \quad G(k) = Y(k) = 0. \tag{64}$$

In this case we can completely forget about the ghosts and Goldstone bosons and drop all their terms in the Lagrangian. The other possible choice already mentioned is the Feynman-'t Hooft gauge where $\xi = 1$. In this case we have

$$D^{\mu\nu}(k) = \frac{-i g^{\mu\nu}}{k^2 - m^2}, \quad G(k) = Y(k) = \frac{-i}{k^2 - m^2}, \tag{65}$$

where now the tensor structure of the propagator of the gauge bosons gets particularly simplified. This is the preferred choice when using the Passarino-Veltman reduction [20] to reduce tensor integrals. The Feynman-'t Hooft gauge will be used throughout this work.

4 Yukawa sector

We will now derive the Yukawa sector of the THDM. We first start with the most general Yukawa sector, which means we write down all gauge invariant terms that do not spoil renormalizability. This very general version of the THDM is called Type III in the literature and has FCNC. As these currents are quite suppressed in the SM, one needs to fine-tune the couplings or find a special Ansatz for the FCNC matrices. A simpler but quite effective approach is to introduce a symmetry to restrict FCNC. This is what is done in the cases known as Type I and Type II, which use a Z_2 symmetry to restrict FCNC. Throughout this chapter we will stick to the notation of [5].

4.1 Type III

To give mass to the fermions, we have to consider the most general Yukawa couplings invariant under $SU(2)_L \times U(1)$. Due to the chiral nature of the weak interaction, left-handed fermions are contained in weak isodoublets $(p,n)_L$, $(\nu_l, l^-)_L$, while the right-handed fermions are contained in weak isosinglets p_R, n_R, l_R^-. The weak hypercharge can be calculated with the formula $Q = I_3 + Y$. In the following we write down the hypercharge of fermion singlets and doublets, denoting p_i (n_i) as up-type (down-type) quarks with generation index i:

- Quark doublets $(p_i, n_i)_L$ must have $Y = 1/6$
- Quark singlets
  - p_{iR} have $Y = 2/3$
  - n_{iR} have $Y = -1/3$
- Lepton doublets $(\nu_l, l^-)_L$ must have $Y = -1/2$
- Lepton singlets
  - l_R^- have $Y = -1$
- both Higgs doublets: $Y = 1/2$

Note that there are no right-handed neutrinos ν_R in the standard version of the THDM[1]. Finding combinations of the above and their charge conjugates with hypercharge $Y = 0$ we obtain the most general renormalizable Yukawa couplings for the quarks:

$$\begin{aligned} -\mathcal{L}_{\mathrm{Y}} =& \overline{(p_i, n_i)}_L \Delta_{1,ij} \Phi_1 n_{jR} + \overline{(p_i, n_i)}_L \widetilde{\Phi}_1 \Gamma_{1,ij} p_{jR} \\ &+ \overline{(p_i, n_i)}_L \Delta_{2,ij} \Phi_2 n_{jR} + \overline{(p_i, n_i)}_L \widetilde{\Phi}_2 \Gamma_{2,ij} p_{jR} + h.c. \end{aligned} \tag{66}$$

[1]BSM models where mass generation mechanisms for neutrinos are considered are e.g. the Zee model [6] or the model of Aoki et al. [8] where the THDM is enriched with a charged scalar singlet and in the latter case with a charged and a neutral scalar singlet.

where $\widetilde{\Phi}_i = i\sigma_2 \Phi_i^*$. We get the mass terms and matrices:

$$\begin{aligned}
\mathcal{L}_{\text{q-mass}} &= -\overline{n}_{iL} M_{n,ij} n_{jR} - \overline{p}_{iL} M_{p,ij} p_{jR} + h.c. \\
M_p &= \frac{v}{\sqrt{2}} \left(\Gamma_1 \cos\beta + \Gamma_2 \sin\beta\right), \qquad M_n = \frac{v}{\sqrt{2}} \left(\Delta_1 \cos\beta + \Delta_2 \sin\beta\right) \ .
\end{aligned} \tag{67}$$

As before, we use $v_2 = v\sin\beta$, $v_1 = v\cos\beta$. To get real masses, we bi-diagonalize the matrices M_p and M_n using $p_L = U_L^p u_L$, $p_R = U_R^p u_R$, $n_L = U_L^n d_L$, $n_R = U_R^n d_R$ and get

$$\begin{aligned}
L_{q-mass} &= -\overline{d}_L U_L^{n\dagger} M_n U_R^n d_R - \overline{u}_L U_L^{p\dagger} M_p U_R^p u_R + h.c. \\
&= -\overline{d}_L \hat{M}_n d_R - \overline{u}_L \hat{M}_p u_R + h.c. = -\,-\,\overline{d}\hat{M}_n d - \overline{u}\hat{M}_p u
\end{aligned} \tag{68}$$

with diagonal, positive-definite mass matrices $\hat{M}_n$ for the down-type quarks and $\hat{M}_p$ for the up-type quarks. The u in (68) is a 3-vector containing the up-type quarks u, c and t, while d is a 3-vector containing d, s and b quarks. We can further identify $V_{CKM} = U_L^{p\dagger} U_L^n$ as the CKM-Matrix. We then define the matrices

$$\begin{aligned}
\rho^p &= U_L^{p\dagger} \left(-\Gamma_1 \sin\beta + \Gamma_2 \cos\beta\right) U_R^p \\
\rho^n &= U_L^{n\dagger} \left(-\Delta_1 \sin\beta + \Delta_2 \cos\beta\right) U_R^n \ ,
\end{aligned} \tag{69}$$

which are in general non-diagonal. Changing into the mass eigenstates we get

$$\begin{aligned}
-L_Y =& \frac{1}{v}\overline{d}\left[\hat{M}_n s_{\beta-\alpha} + \frac{v}{\sqrt{2}}\left(\rho^n P_R + \rho^{n\dagger} P_L\right) c_{\beta-\alpha}\right] dh \\
&+ \frac{1}{v}\overline{d}\left[\hat{M}_n c_{\beta-\alpha} - \frac{v}{\sqrt{2}}\left(\rho^n P_R + \rho^{n\dagger} P_L\right) s_{\beta-\alpha}\right] dH \\
&+ \frac{1}{v}\overline{u}\left[\hat{M}_p s_{\beta-\alpha} + \frac{v}{\sqrt{2}}\left(\rho^p P_R + \rho^{p\dagger} P_L\right) c_{\beta-\alpha}\right] uh \\
&+ \frac{1}{v}\overline{u}\left[\hat{M}_p c_{\beta-\alpha} - \frac{v}{\sqrt{2}}\left(\rho^p P_R + \rho^{p\dagger} P_L\right) s_{\beta-\alpha}\right] uH \\
&+ \frac{i}{\sqrt{2}}\overline{d}\left(\rho^n P_R - \rho^{n\dagger} P_L\right) dA - \frac{i}{\sqrt{2}}\overline{u}\left(\rho^p P_R - \rho^{p\dagger} P_L\right) uA \\
&+ \frac{i}{v}\overline{d}\hat{M}_n \gamma_5 d G^0 - \frac{i}{v}\overline{u}\hat{M}_p \gamma_5 u G^0 \\
&+ \left(\overline{u}\left[V_{CKM}\rho^n P_R - \rho^p V_{CKM} P_L\right] dH^+ \quad + h.c.\right) \\
&+ \left(\frac{\sqrt{2}}{v}\overline{u}\left[V_{CKM}\hat{M}_n P_R - \hat{M}_p V_{CKM} P_L\right] dG^+ + h.c.\right) \ .
\end{aligned} \tag{70}$$

As one in general cannot bi-diagonalize two matrices with the same unitary matrices, ρ^p and ρ^n will be complex and non-diagonal. Therefore, we get FCNC at the tree level as expected. One can get the leptonic couplings by substituting $(p,n)_L \rightarrow (\nu_l, l^-)_L$ and $n_R \rightarrow l_R^-$, which gives us FCNC for the leptons as well. Flavour physics tells us that these currents are strongly suppressed. In the SM this suppression is natural, as FCNC do not appear at tree level. To make the same true for the THDM, one uses the Z_2 symmetry.

Once specified for the potential (3) it must be extended to the Yukawa sector. This is done by specifying it for the fermion doublets and singlets of SU(2):

$$\begin{aligned} (p,n)_L \to \epsilon_L (p,n)_L, \quad n_R \to \eta_n n_R, \quad p_R \to \eta_p p_R \\ (\nu_l, l^-)_L \to \kappa_L (\nu_l, l^-)_L, \quad l_R^- \to \eta_l l_R \ . \end{aligned} \tag{71}$$

Together with the definition (3) this leads to 4 distinct versions of the Yukawa interactions [21, 22]. The different Yukawa sectors displayed in Tab. 1 obviously lead to different

Type	ϵ_L	η_n	η_p	κ_L	η_l
I	-1	+1	+1	-1	+1
X	-1	+1	-1	-1	-1
II	-1	-1	+1	-1	-1
Y	-1	-1	+1	-1	+1

Table 1: Z_2 symmetry leads to 4 Types of Yukawa interaction: Type I, X, II and Y.

phenomenology. Type II is the case of the MSSM where one Higgs doublet couples to up-type and the other to down-type quarks and leptons. Type Y is just the same as Type II, but with the leptons coupling to up-type instead of down-type quarks. In Type I all fermions couple to the same Higgs doublet, while in Type X quarks couple to one Higgs doublet and only leptons to the other doublet. Various studies were conducted on the phenomenology of Type II, but considerably less studies exist on the other Types[1]. As the couplings of Type Y and X can easily be derived once found for Type II and I, we will only study I and II and then concentrate our efforts on Type I for the rest of the work.

[1]Recently the phenomenology of Type X was studied in [13]

4.2 Type I

As mentioned before, in a Type I model the Z_2 symmetry is defined as $\epsilon_L = \kappa_L = -1$, $\eta_n = \eta_p = \eta_l = 1$. Applying it to (66), we conclude that $\Gamma_1 = \Delta_1 = 0$[1]. This simplifies the sector drastically:

$$\hat{M}_p = \frac{v}{\sqrt{2}} \sin\beta U_L^{p\dagger} \Gamma_2 U_R^p, \qquad \hat{M}_n = \frac{v}{\sqrt{2}} \sin\beta U_L^{n\dagger} \Delta_2 U_R^n$$
$$\rho^p = \cos\beta U_L^{p\dagger} \Gamma_2 U_R^p, \qquad \rho^n = \cos\beta U_L^{n\dagger} \Delta_2 U_R^n \; . \tag{72}$$

Now all of the above matrices are diagonal and FCNC eliminated. The Yukawa couplings simplify to

$$\begin{aligned} L_Y = \frac{1}{v}\Bigg[& -\frac{\cos\alpha}{\sin\beta}\overline{d}\hat{M}_n dh - \frac{\sin\alpha}{\sin\beta}\overline{d}\hat{M}_n dH \\ & -\frac{\cos\alpha}{\sin\beta}\overline{u}\hat{M}_p uh - \frac{\sin\alpha}{\sin\beta}\overline{u}\hat{M}_p uH \Bigg] \\ & -\frac{i}{v}\overline{d}\hat{M}_n\gamma_5 dG^0 + \frac{i}{v}\overline{u}\hat{M}_p\gamma_5 uG^0 \\ & -\frac{i}{v}\cot\beta\overline{d}\hat{M}_n\gamma^5 dA + \frac{i}{v}\cot\beta\overline{u}\hat{M}_p\gamma^5 uA \\ & -\frac{\sqrt{2}}{v}\cot\beta\left(\overline{u}\left[V_{CKM}\hat{M}_n P_R - \hat{M}_p V_{CKM} P_L\right] dH^+ \quad + h.c.\right) \\ & -\left(\frac{\sqrt{2}}{v}\overline{u}\left[V_{CKM}\hat{M}_n P_R - \hat{M}_p V_{CKM} P_L\right] dG^+ + h.c.\right) \; . \end{aligned} \tag{73}$$

The couplings are exactly those used in the FeynArts THDM. For CP-even scalars L_Y is symmetric under $u \leftrightarrow d$, while for CP-odd scalars the couplings have a relative minus sign. These Yukawa couplings allow for several features, which may quite differ from the SM Higgs couplings to the fermions. One interesting case is the fermiophobic limit for which $\cos\alpha = 0$, which was studied in [10, 11, 9, 12]. In this case the lightest Higgs h gets fermiophobic, which means that it will not decay to fermions at tree level (it may still decay to heavy fermions like $b\bar{b}$ at the 1-loop level [12, 23]). In this case the other CP even scalar H will be fermiophilic, as $\sin\alpha = 1$.
The IDM discussed in Sec. (2.3) is just a special case of (73), which one can get by $\sin\alpha = 0$ and $\sin\beta = \pi/2$. One can further derive a lower limit on $\tan\beta$ using perturbativity of the top-quark coupling. After diagonalization,

$$m_t = \frac{v\sin\beta}{\sqrt{2}}\lambda_t \; . \tag{74}$$

To preserve perturbativity at tree level, $|\lambda_t| \leq 4\pi$. As the vacuum expectation value is fixed at $v \approx 246$ GeV, this yields the lower limit:

$$0.1 \leq \tan\beta \; . \tag{75}$$

[1] This is equivalent to $\epsilon_L = \kappa_L = \eta_n = \eta_p = \eta_l = 1$, which results in $\Gamma_2 = \Delta_2 = 0$. As we want to check the FeynArts implementation of the THDM, we will use the convention $\Gamma_1 = \Delta_1 = 0$.

4.3 Type II

As seen in Tab. 1, in Type II the Z_2 symmetry of the Yukawa sector is defined as $\epsilon_L = \kappa_R = \eta_P = -1$ and $\eta_n = \eta_l = 1$. Then $\Gamma_1 = \Delta_2 = 0$, which again follows the convention of the FeynArts implementation of the THDM. This yields:

$$\hat{M}_p = \frac{v}{\sqrt{2}} \sin\beta U_L^{p\dagger} \Gamma_2 U_R^p, \qquad \hat{M}_n = \frac{v}{\sqrt{2}} \cos\beta U_L^{n\dagger} \Delta_1 U_R^n \tag{76}$$

$$\rho^p = \cos\beta U_L^{p\dagger} \Gamma_2 U_R^p, \qquad \rho^n = -\sin\beta U_L^{n\dagger} \Delta_1 U_R^n \ . \tag{77}$$

Again FCNC do not appear at tree level. The Yukawa couplings simplify to

$$\begin{aligned}
L_Y = \frac{1}{v}\Bigg[& \frac{\sin\alpha}{\cos\beta}\overline{d}\hat{M}_n dh - \frac{\cos\alpha}{\cos\beta}\overline{d}\hat{M}_n dH \\
& - \frac{\cos\alpha}{\sin\beta}\overline{u}\hat{M}_p uh - \frac{\sin\alpha}{\sin\beta}\overline{u}\hat{M}_p uH\Bigg] \\
& - \frac{i}{v}\overline{d}\hat{M}_n\gamma_5 dG^0 + \frac{i}{v}\overline{u}\hat{M}_p\gamma_5 uG^0 \\
& + \frac{i}{v}\tan\beta\overline{d}\hat{M}_n\gamma^5 dA + \frac{i}{v}\cot\beta\overline{u}\hat{M}_p\gamma^5 uA \\
& + \frac{\sqrt{2}}{v}\left(\overline{u}\left[\tan\beta V_{CKM}\hat{M}_n P_R + \cot\beta\hat{M}_p V_{CKM} P_L\right] dH^+ \quad + h.c.\right) \\
& - \frac{\sqrt{2}}{v}\left(\overline{u}\left[V_{CKM}\hat{M}_n P_R - \hat{M}_p V_{CKM} P_L\right] dG^+ + h.c.\right) \ .
\end{aligned} \tag{78}$$

This is the case needed for the MSSM. These are the couplings used in the FeynArts implementation of Type II.

As we now have not only $m_t \propto v_2$ but also $m_b \propto v_1$, we can use the previous lower limit for Type I and calculate an upper limit for $\tan\beta$. Following similar arguments as before, we conclude

$$0.1 \leq \tan\beta \leq 550 \ . \tag{79}$$

Due to the couplings of (78), a fermiophobic limit is not possible for Type II.

5 Electroweak precision tests

Electroweak precision tests are the decisive tests of the SM and any other electroweak theory. The nice feature of electroweak symmetry breaking is that one can define zeroth order natural relations. While being valid for all values of the couplings at tree level, going to higher orders these relations will receive corrections from particles contributing in loops. Therefore comparing precision measurements to a calculated natural relation with quantum corrections will yield a consistency test for a certain region of parameter space. In the case of the SM we get indirect constraints on the Higgs or the top mass. If we take the most precisely determined parameters as input parameters, we will in return get precise predictions from our theory as output. As of 2008, the most precise parameters are [24]:

$$\begin{aligned}
\alpha(0) &= 1/137.03599976(50) \\
m_Z &= 91.1876(21)\ \mathrm{GeV} \\
G_F &= 1.16637(1) \times 10^{-5}\mathrm{GeV}^{-2}\ . \qquad (80)
\end{aligned}$$

We will now use these values to calculate constraints on the THDM. The notation and conventions follow Ref. [25].

5.1 Constraints from m_W in the SM

The idea to use the correlation of the gauge boson masses as a test of the SM goes back to 1980 [26]. Fermi's constant G_F is determined via the lifetime of the muon, an experimental quantity, which has been determined to high accuracy. Almost 100 % of all muon decays are $\mu \to e\nu_\mu\overline{\nu}_e + (\gamma)$. Ignoring the other decay channels, one defines G_F via the following relation:

$$\Gamma_\mu = \frac{G_F^2 m_\mu^5}{192\pi^3} F\left(\frac{m_e^2}{m_\mu^2}\right)\left(1 + \frac{3}{5}\frac{m_\mu^2}{m_W^2}\right)(1 + \Delta_{\mathrm{QED}}) \qquad (81)$$

where Γ_μ is the total decay width of the muon and $F(x) = 1 - 8x - 12x^2 \log x + 8x^3 - x^4$. The QED corrections in the effective theory Δ_{QED} have been included in the definition. Calculating the corrections Δ_{QED} and inserting the muon lifetime one obtains the value for G_F as given in (80). On the other hand, one can calculate Γ_μ in the SM, which then only depends on SM parameters. Doing so, one finds the famous equation relating the SM parameters and Fermi's constant G_F [27]:

$$\frac{G_F}{\sqrt{2}} = \frac{\alpha\ \pi}{2 s_W^2 m_W^2}(1 + \Delta r)\ . \qquad (82)$$

Here s_W is the sine of the weak mixing angle $s_W = \sin\theta_W$ with

$$\sin^2\theta_W = 1 - \frac{m_W^2}{m_Z^2}\ . \qquad (83)$$

The quantity Δr is

$$\begin{aligned}\Delta r = \Pi^{AA}(0) - \frac{c_W^2}{s_W^2}\left(\frac{Re\Sigma^{ZZ}(m_Z^2)}{m_Z^2} - \frac{Re\Sigma^{WW}(m_W^2)}{m_W^2}\right) + 2\frac{c_W}{s_W}\frac{\Sigma^{AZ}(0)}{m_Z^2} \\ + \frac{\Sigma^{WW}(0) - Re\Sigma^{WW}(m_W^2)}{m_W^2} + \frac{\alpha}{4\pi s_W^2}\left(6 + \frac{7-4s_W^2}{2s_W^2}\log c_W^2\right) \ .\end{aligned} \tag{84}$$

Here Σ^{WW}, Σ^{ZZ}, Σ^{AZ} denote the transversal part of the self-energies of the W and Z boson. Π^{AA} is defined as

$$\Pi^{AA}(k^2) \equiv \frac{\partial \Sigma^{AA}(k^2)}{\partial\ k^2} \tag{85}$$

where again Σ^{AA} is the transversal self-energy of the photon.

Δr is then separated into finite quantities

$$\Delta r = \Delta\alpha - \frac{c_W^2}{s_W^2}\Delta\rho + \Delta r_{\text{rem}} \tag{86}$$

where

$$\Delta\rho \equiv \frac{\Sigma^{ZZ}(0)}{m_Z^2} - \frac{\Sigma^{WW}(0)}{m_W^2} - 2\frac{s_W}{c_W}\frac{\Sigma^{AZ}(0)}{m_Z^2}, \qquad \Delta\alpha \equiv -Re\Pi^{AA}(m_Z^2) + \Pi^{AA}(0) \tag{87}$$

$$\begin{aligned}\Delta r_{\text{rem}} \equiv \left(1 - \frac{c_W^2}{s_W^2}\right)\frac{\Sigma^{WW}(0) - Re\Sigma^{WW}(m_W^2)}{m_W^2} + Re\Pi^{AA}(m_Z^2) \\ + \frac{c_W^2}{s_W^2}\frac{\Sigma^{ZZ}(0) - Re\Sigma^{ZZ}(m_Z^2)}{m_Z^2} + \frac{\alpha}{4\pi s_W^2}\left(6 + \frac{7-4s_W^2}{2s_W^2}\log c_W^2\right) \ .\end{aligned} \tag{88}$$

Note that our definition of $\Delta\rho$ differs from the usual one by the additional Σ^{AZ}-term which was added in the above definition to get a UV finite quantity. If one considers the fermionic contribution only, this term vanishes.

For $\Delta\alpha$, all heavy particles decouple due to the Appelquist and Carazzone theorem [28]. It is reasonable to separate $\Delta\alpha$ into a hadronic and a leptonic component:

$$\Delta\alpha(m_Z^2) = \Delta\alpha^{\text{had}}(m_Z^2) + \Delta\alpha^{\text{lept}}(m_Z^2) \ . \tag{89}$$

The hadronic part cannot be calculated in perturbation theory, due to the nature of the strong interaction and its non-perturbative effects. It is calculated instead indirectly, with a dispersion integral over the normalized cross section of $\sigma(e^+e^- \rightarrow \text{hadrons})$:

$$\begin{aligned}\Delta\alpha^{\text{had}}(m_Z^2) &= -\frac{\alpha m_Z^2}{3\pi}\text{Re}\left(\int_{4m_\pi^2}^{\infty} \text{d}s' \frac{R_{\gamma\gamma}(s')}{s'(s'-m_Z^2)}\right) \\ R_{\gamma\gamma}(s) &= \frac{\sigma(e^+e^- \rightarrow \gamma^* \rightarrow \text{hadrons})}{\sigma(e^+e^- \rightarrow \gamma^* \rightarrow \mu^+\mu^-)}\end{aligned} \tag{90}$$

where $R_{\gamma\gamma}(s)$ is calculated over the problematic range using experimental data and using perturbative QCD for the high energy range (For more details see [29]). The top-contribution to (89) is very small, being around $\Delta\alpha_{top} \approx -10^{-4}$ and can be neglected.

The leptonic contribution $\alpha^{\rm lept}(m_Z^2)$ is calculated perturbatively and one usually includes the 3-loop level. For the total value of $\Delta\alpha(m_Z^2)$ we thus get

$$\Delta\alpha(m_Z^2) = 0.0594 \pm 0.0005, \tag{91}$$

where most of the error originates from the hadronic contribution.

Next we will deal with the other two observables $\Delta\rho$ and $\Delta r_{\rm rem}$ and discuss QCD corrections. QCD corrections appear as virtual corrections to the top. The observable $\Delta\rho$ depends stronger on the top, because $\Delta\rho^{\rm top} \propto m_t^2$ while $\Delta r_{\rm rem}^{\rm top} \propto \log(m_t^2/m_W^2)$. Therefore, we will only include QCD-corrections to $\Delta\rho$. These were already calculated up to the 4-loop level [30]. As the 4-loop corrections are small (shifting m_W around by about 2 MeV), we will only include the 3-loop level [31] which is more than accurate enough for our purpose. While the two-loop self-energy corrections are rather small, the two-loop fermionic contributions [32] are approximately the same size as the QCD corrections.

To sum up the irreducible W self-energy to all orders, the following approximation is often used [27]:

$$1 + \Delta r \to 1/(1-\Delta r), \tag{92}$$

which is valid for $\Delta\rho$ being not too big (for a more exact treatment see [33]). Using this relation, we get the following formula:

$$m_W^2 = \frac{1}{2}\left(m_Z^2 + \sqrt{m_Z^4 - \frac{4\alpha\pi}{\sqrt{2}G_F}\frac{m_Z^2}{1-\Delta r}}\right) . \tag{93}$$

Therefore one could use this formula to calculate m_W using the data (80). For our analysis it is practical to use a direct approach similar to [34]. Using (80) and $m_W = 80.398 \pm 0.025$ GeV [24] as experimental input values, one can calculate Δr from precision data:

$$\Delta r_{exp} = 0.0343 \pm 0.0020, \tag{94}$$

which is the experimental value of Δr with uncertainties resulting mostly from the uncertainty of m_W. We may now calculate Δr and compare the calculated value with (94).

5.2 Constraints from m_W in the THDM

The charged scalar in the THDM contributes to the muon decay already at tree level, so one would expect that not only the gauge self-energies of Δr in (84) but also the relation (82) must be changed. The tree level contribution is however suppressed by its couplings to the leptons $g_{H^+l^-\bar\nu}$ which is proportional to the lepton mass m_l while $g_{W^+l^-\bar\nu}$ is not:

$$g_{H^+l^-\bar\nu} \propto \frac{e m_l \tan^2\beta}{\sqrt{2}s_W m_W}, \qquad g_{W^+l^-\bar\nu} \propto \frac{e}{\sqrt{2}s_W} . \tag{95}$$

This implies suppression by a factor

$$\frac{m_e m_\mu}{m_W^2} \approx 10^{-8} - 10^{-6} \tag{96}$$

for $\tan\beta \leq 10$. As light charged scalars with $M_{H^\pm} \leq 78$ GeV were excluded by precision experiments at LEP [35], the propagator of the charged scalar cannot grow larger than the W boson propagator. Therefore, the contribution of the THDM to the muon decay at tree level can safely be neglected.

At the one-loop level, triangle diagrams with only one virtual Higgs coupling to the muon are the most dominant contributions of the THDM Higgs sector. Nonetheless, they are still not large enough to affect (82), because they are suppressed by a factor

$$\frac{m_\mu}{m_W} \approx 10^{-3} \; . \tag{97}$$

Hence the only sizeable contribution comes from the self-energy of vector bosons which are contained in Δr. The vertex corrections are the same as in the SM, and we can use the formula (84) for Δr and just insert the self-energies of the THDM.

We now separately reconsider the quantities of Δr in the THDM, $\Delta\alpha$, $\Delta\rho$ and Δr_{rem}. The charged Higgs contributes to $\Delta\alpha$, but again due to the Appelquist and Carazzone theorem this is only around

$$\Delta\alpha_{H^+} \approx 10^{-4} \tag{98}$$

and can be neglected. Hence for $\Delta\alpha$ we use the SM value. One of the parameters of Δr where the additional scalars of the THDM do contribute is $\Delta\rho$. For the $\Delta\rho$ parameter one also has to include the QCD corrections to the top quark, as it was done in the SM in Sec. 5.1. The Δr_{rem} QCD corrections will be ignored as before.

The biggest higher-order corrections we will ignore is the fermionic two-loop contribution (These include two-loop diagrams with Higgs bosons). In the SM, these are around

$$\Delta r_{f-2loop} \approx +0.004 \; . \tag{99}$$

Together with two-loop self-energy corrections of the gauge bosons and the Higgs sector [32], which we are neglecting too, this gives us an estimate of the uncertainty of our prediction

$$\Delta r^{th}_{\text{err}} \approx \pm 0.005 \; . \tag{100}$$

Adding this error linearly to the experimental error (94) at 2 σ, we can exclude $\Delta r < 0.0253$ and $\Delta r > 0.0343$ at 2 σ. At the one-loop level Δr is directly sensitive only to the gauge sector of the THDM, and not to the potential or the Yukawa couplings. It depends on only 5 unknown parameters, $\sin(\alpha-\beta)$, $M_{H^\pm}$, M_A, M_h, M_H. The additional contributions of the THDM to Δr are present only in the self energies of the W and the Z bosons. Calculating these and inserting them into (84) we get the one-loop result in the THDM with QCD corrections for the $\Delta\rho$ parameter. FeynArts was then employed to calculate Δr for various regions of parameter space. While in the SM the value of Δr was always around $\Delta r \approx 0.034$, in the THDM for certain parameter regions it can even be negative.

5.2.1 IDM

After implementing the described functions in a FeynArts program, we evaluated Δr for the IDM. In the IDM the scalar h couples to the gauge bosons like the SM Higgs. Therefore, we have $\alpha = 0$, $\beta = \pi/2$ and hence $\cos(\beta - \alpha) = 0$. Δr then depends only on the 4 Higgs masses. The decay signature $h \to \gamma\gamma$ in the SM, which we will study in Sec. 8, is only visible at the LHC if the Higgs is rather light ($M_h \approx 130$ GeV). We therefore evaluate Δr at $M_h = 130$ GeV. In Fig. 1, Δr is plotted for the IDM in the (M_A, M_H) plane for various charged Higgs masses. Regions, which are incompatible with the precision constraints (parameters for which $\Delta r < 0.0253$ or $\Delta r > 0.0433$) are shown in yellow.

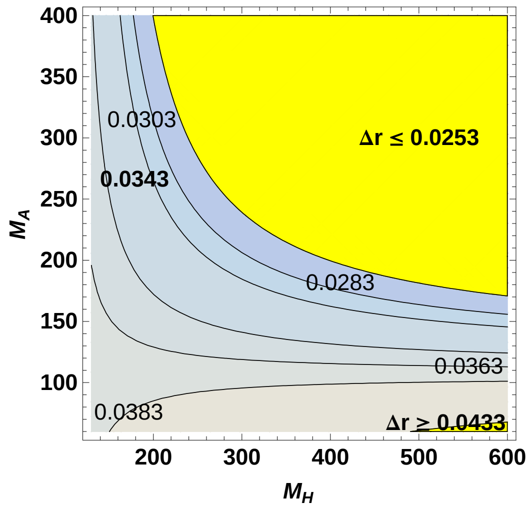

(a) Δr for a very light charged scalar $M_{H^\pm} =$ 100 GeV

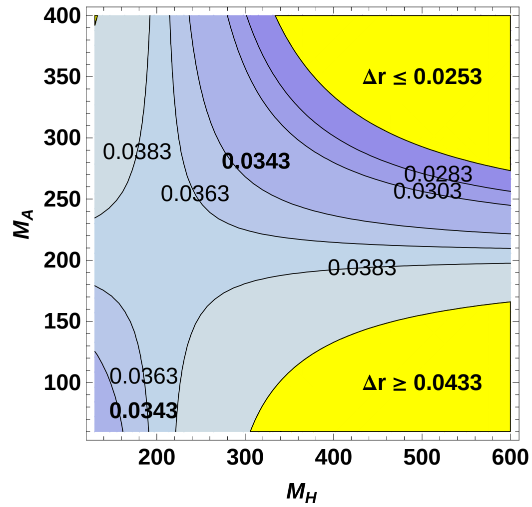

(b) Δr for a medium charged scalar $M_{H^\pm} =$ 200 GeV

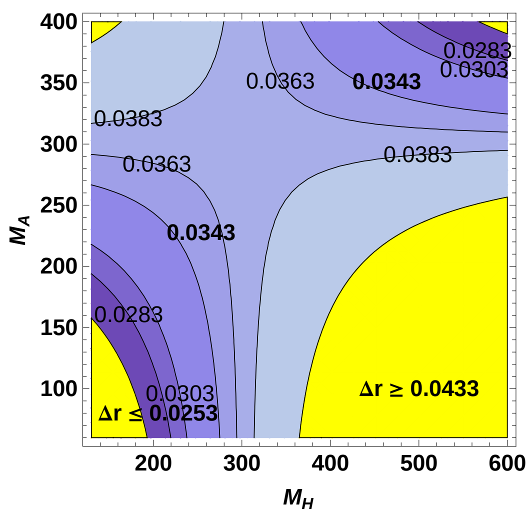

(c) Δr for a medium charged scalar $M_{H^\pm} =$ 300 GeV

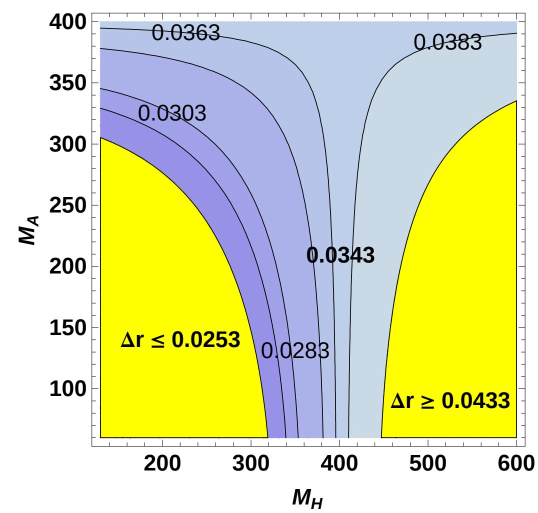

(d) Δr for a heavy charged scalar $M_{H^\pm} =$ 400 GeV.

Figure 1: Δr is displayed in the (M_H, M_A) plane for $M_h = 130$ GeV and $\cos(\beta - \alpha) = 0$. The excluded regions are marked in yellow.

In Fig. 1(a) we can see that for a light charged scalar ($M_{H^\pm} = 100$ GeV), either M_H or M_A must be small. On the other hand, as of Fig. 1(d), for a rather heavy charged scalar ($M_{H^\pm} = 400$ GeV), H must be rather heavy, or $M_A \approx 400$ GeV. We hence see that by setting $M_A \approx M_{H^\pm}$ or $M_H \approx M_{H^\pm}$ one can always render Δr compatible with the experimental value.

5.2.2 Other potentials

For the more general cases V_A, V_B, V_λ, the angle $\cos(\beta - \alpha)$ is a free parameter. Anticipating the discussion in Sec. 8.3 of the enhancement for the potential V_B we plot the value of Δr in the same regions as in Sec. 8.3. We see that for Fig. 2(a) nothing can be

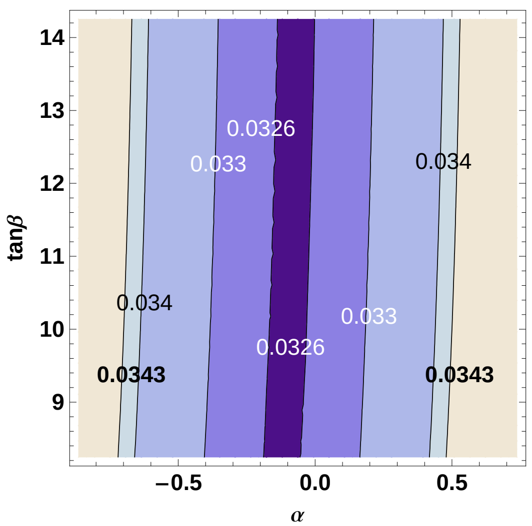

(a) Δr for $M_A = 200$ GeV and $M_H = 211$ GeV. No exclusion possible.

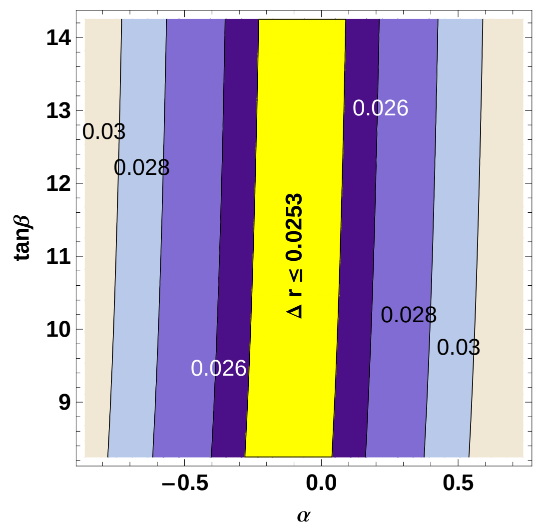

(b) Δr displayed for $M_A = 265$ GeV and $M_H = 272$ GeV.

Figure 2: Δr is displayed in the $(\tan\beta, \alpha)$ plane for $M_h = 130$ GeV, $M_{H^\pm} = 100$ GeV for several values of M_H, and M_A. The excluded regions are marked in yellow. We see that increasing both masses M_A and M_H, the value of Δr drops leading to a 2 σ excluded region.

excluded, while there is a certain exclusion region in Fig. 2(b) from $\alpha \approx (-0.4) - (0.0)$.

We show similar plots for the region we will examine for V_λ (Sec. 8.4). While we cannot see any exclusion in the region of Fig. 3(a), in Fig. 3(b) the values of Δr are very close to the 2 σ bound 0.0253. Parts of Fig. 3(b) region may therefore be excluded, if we could provide a better precision for Δr (for example by calculating the two-loop contributions in the THDM).

5.3 Z decays

The partial decay widths of the Z boson have been determined at the permille level at LEP [36]. The results are in quite good agreement with the SM at 1.5σ. The only

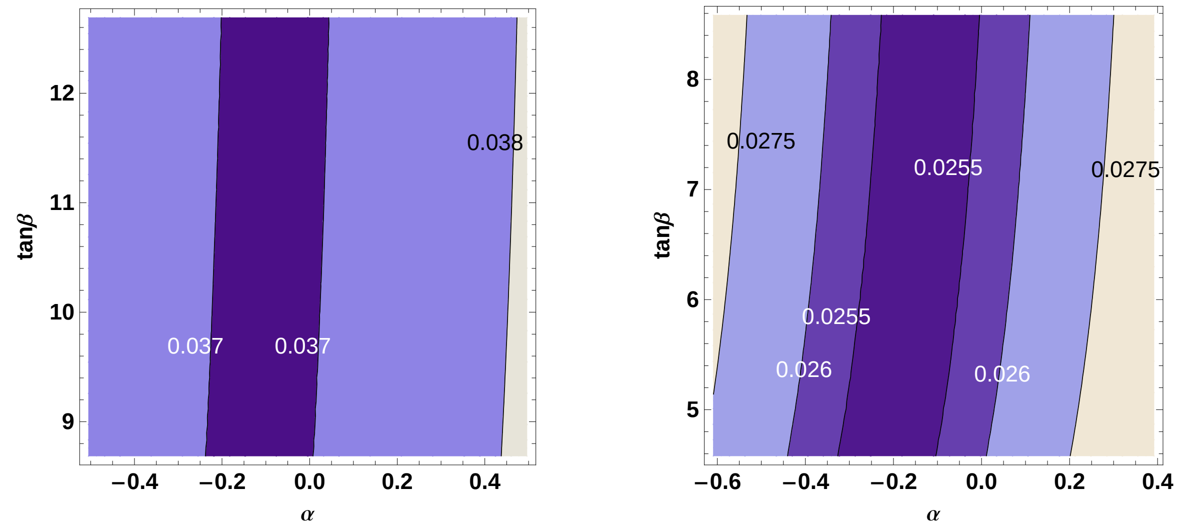

(a) Δr for $M_H = 333$ GeV, $M_A = 111$ GeV. No exclusion in the region displayed.

(b) Δr for $M_H = 279$ GeV and $M_A = 254$ GeV.

Figure 3: Δr is displayed in the $(\tan\beta,\, \alpha)$ plane for $M_h = 130$ GeV $M_{H^\pm} = 100$ GeV for two values of M_H and M_A. We see that there is no exclusion possible in both figures. In Fig. 3(b) one is close to the 2 σ exclusion region.

significant disagreement was found in the forward-backward asymmetry for $b\bar{b}$ production

$$A^b_{FB} \equiv \int_0^1 \frac{d\sigma(e^-e^+ \to b\bar{b})}{d\ \cos\theta}\, d\cos\theta - \int_{-1}^0 \frac{d\sigma(e^-e^+ \to b\bar{b})}{d\ \cos\theta}\, d\cos\theta\ , \tag{101}$$

which differs from its SM value by 2.5 σ. As the Z decays $Z \to f\bar{f}$ are all tree-level processes, we will get the strongest constraints for the Higgs sector by considering the final states with the largest radiative corrections. Any Higgs in a loop must couple to at least one of the outgoing fermions (f). The Higgs-fermion-fermion coupling is always proportional to the fermion mass

$$g_{hf\bar{f}} \propto \frac{m_f}{m_W} \tag{102}$$

and therefore suppressed when compared to the competing diagrams with the W and Z bosons. This means that the corrections due to the W and the Z will dominate, and that Higgs corrections are larger for heavier than for light final state fermions. We hence consider the heaviest kinematically allowed decay process $Z \to b\bar{b}$. As the self-energy of the Z-boson is already constrained by the previous discussion on Δr, we are now interested in observables where oblique corrections (corrections due to the self-energy of the gauge bosons) are small. This is the case for two prominent observables, R_b and A_b. R_b is the hadronic branching ratio of Z to b quarks:

$$R_b \equiv \frac{\Gamma(Z \to b\bar{b})}{\Gamma(Z \to \text{hadrons})}, \tag{103}$$

while A_b is the b-quark left-right asymmetry:

$$A_b \equiv \frac{\sigma(e^-_L \to b_F) - \sigma(e^-_L \to b_B) + \sigma(e^-_R \to b_B) - \sigma(e^-_R \to b_F)}{\sigma(e^-_L \to b_F) + \sigma(e^-_L \to b_B) + \sigma(e^-_R \to b_B) + \sigma(e^-_R \to b_F)} \tag{104}$$

where

$$\sigma(e^-_{L,R} \to b_F) = \int_0^1 \frac{d\sigma(e^-_{L,R}e^+ \to b\bar{b})}{d\ \cos\theta}\, d\cos\theta$$

$$\sigma(e^-_{L,R} \to b_B) = \int_{-1}^0 \frac{d\sigma(e^-_{L,R}e^+ \to b\bar{b})}{d\ \cos\theta}\, d\cos\theta\ . \tag{105}$$

The measurements were performed with a polarized beam at SLAC [37]. These cross sections are to be taken at the Z-resonance. We will now follow the discussions of Refs. [38, 39] to calculate R_b and A_b. In this approach, one defines effective $Zb\bar{b}$-couplings $\bar{g}_b^L$ and $\bar{g}_b^R$ to calculate these values. R_b and A_b then become

$$R_b = \left[1 + \frac{S_b}{\bar{s}_b C_b^{QCD} C_b^{QED}}\right]^{-1}, \qquad A_b = \frac{2\bar{r}_b(1-4\mu_b)^{1/2}}{1-4\mu_b+(1+2\mu_b)\bar{r}_b^2} \tag{106}$$

where

$$\bar{r}_b = \frac{\bar{v}_b}{\bar{a}_b}, \qquad \bar{s}_b = (\bar{a}_b)^2(1-6\mu_b) + (\bar{v}_b)^2 \tag{107}$$

$$\bar{v}_b = \bar{g}_b^L + \bar{g}_b^R, \qquad \bar{a}_b = \bar{g}_b^L - \bar{g}_b^R \tag{108}$$

$$S_b = \sum_{q\neq b,t} (\bar{a}_q)^2 + (\bar{v}_q)^2. \tag{109}$$

$\mu_b = (\bar{m}_b(m_Z)/m_Z)^2 \simeq 1.0 \times 10^{-3}$ is accounting for the effect of $m_b(m_Z) \neq 0$. $C_b^{QCD} = 0.9953$ and $C_b^{QED} = 0.99975$ are accounting for QCD and QED corrections, respectively (for an exact definition see [39]). S_b is the squared sum of the vector and axial-vector couplings over the first and second generation. In our approximation, contributions of the Higgs sector are neglected. From [39] we get $S_b = 1.3184$. The SM prediction with $m_t = 172$ GeV and $M_H = 149$ GeV then yields [39]

$$\bar{g}_b^L = -0.4208, \qquad \bar{g}_b^R = 0.0774\ , \tag{110}$$

with which one gets

$$R_b^{SM} = 0.21587\ , \qquad A_b^{SM} = 0.935\ . \tag{111}$$

The measured value of A_b has quite improved since 1996 and is now in agreement with the SM [37]:

$$R_b = 0.21629 \pm 0.00066, \qquad A_b = 0.923 \pm 0.020\ . \tag{112}$$

We will now consider corrections to these values due to the Higgs sector in THDM Type I to get further constraints on the parameter space of the model.

5.4 THDM corrections to R_b^{SM} and A_b^{SM}

Considering now contributions of the THDM, we write:

$$\bar{g}_b^{L,R} = \left(\bar{g}_b^{L,R}\right)_{SM} + \delta g_{\mathrm{T1}}^{L,R}\ . \tag{113}$$

In $(\bar{g}_b^{L,R})_{SM}$ we include the radiative corrections originating from the would-be Goldstone bosons, but not the neutral Higgs correction, which is contained in $\delta g_{\mathrm{T1}}^{L,R}$. In a first approximation in Type I, the neutral Higgs bosons can be ignored. One can see this by considering the couplings (73) of the Higgs bosons:

$$g_{(h,H)b\bar{b}} \propto \frac{m_b}{\sin\beta}, \qquad g_{Ab\bar{b}} \propto \frac{m_b}{\tan\beta} \tag{114}$$

$$g_{H^+b\bar{t}} \propto \frac{\cos\beta}{\sin\beta}\left(m_t P_L - m_b P_R\right) \ . \tag{115}$$

All the couplings are proportional to $1/\sin\beta$, therefore the neutral couplings cannot be enhanced compared to the charged Higgs. As the charged Higgs is the only Higgs coupling to the top at the one-loop level, it will always dominate the other scalar contributions. This is in contrast to the Type II model (78), where such an enhancement is possible:

$$g_{(h,H)b\bar{b}} \propto \frac{m_b}{\cos\beta}, \qquad g_{Ab\bar{b}} \propto m_b \tan\beta \tag{116}$$

$$g_{H^+b\bar{t}} \propto \frac{m_t}{\tan\beta} P_L + m_b \tan\beta P_R \ . \tag{117}$$

For $\cos\beta \ll 1$ the charged Higgs coupling proportional to m_t is reduced while all neutral couplings get enhanced.

As we are only interested in the Type I model we will ignore the neutral Higgs bosons. We will also ignore the oblique corrections to the processes, because their contribution to R_b and A_b is tiny, being in the percent range of the experimental error of R_b and A_b [38].

R_b and A_b can be expanded about their SM values, assuming corrections of the Higgs sector to be small [39]:

$$\delta R_b = -0.7785\ \delta g_{\mathrm{T1}}^L + 0.1409\ \delta g_{\mathrm{T1}}^R \tag{118}$$

$$\delta A_b = -0.2984\ \delta g_{\mathrm{T1}}^L - 1.623\ \delta g_{\mathrm{T1}}^R \ . \tag{119}$$

Using the calculated corrections of [38] one gets

$$\delta g_{\mathrm{T1}}^L = \frac{1}{16\pi^2}\left(\frac{e m_t}{\sqrt{2} m_W s_W}\cot\beta\right)^2 \frac{1}{2}\frac{e}{s_W c_W}\left[\frac{R}{R-1} - \frac{R\log R}{(R-1)^2}\right] \tag{120}$$

$$\delta g_{\mathrm{T1}}^R = -\frac{1}{16\pi^2}\left(\frac{e m_b}{\sqrt{2} m_W s_W}\cot\beta\right)^2 \frac{1}{2}\frac{e}{s_W c_W}\left[\frac{R}{R-1} - \frac{R\log R}{(R-1)^2}\right] \ . \tag{121}$$

Here R refers to the mass ratio $R \equiv m_t^2/M_{H^\pm}^2$. Note that the overall contribution of the charged Higgs bosons to R_b is always negative, since δg_{T1}^L (δg_{T1}^R) is always positive (negative). The same holds true for Type II. The correction δg_{T1}^R is much smaller than δg_{T1}^L. δA_b is typically $\delta A_b \approx 0.006$ and therefore too small compared to the experimental uncertainty. On the other hand, corrections to R_b are sizeable and can be used to exclude parameter space in the $(\tan\beta, M_{H^\pm})$-plane. We now calculate R_b with $m_b(m_Z) = 3$ GeV, $m_t = 171$ GeV. Due to the experimental error in (112), we get a 2 σ exclusion for $R_b < 0.215$.

Using the exclusion plot in Fig. (5), we get an exclusion at 2 σ:

$$\tan\beta \leq 3.3 \quad \text{excluded for} \quad M_{H^\pm} = 100 \text{ GeV}. \tag{122}$$

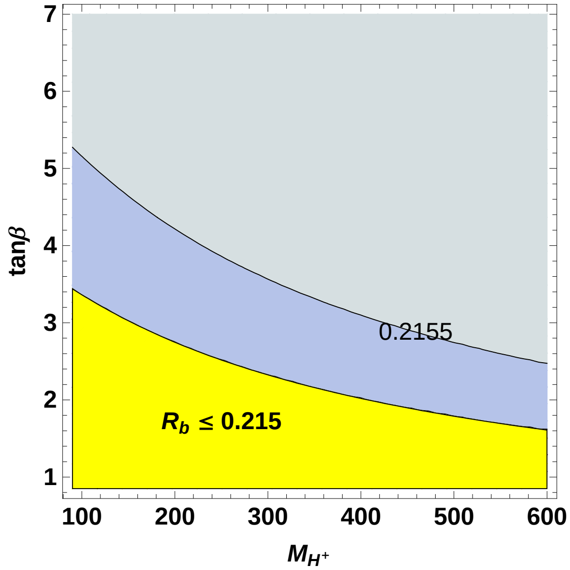

Figure 4: R_b is plotted against $(M_{H^\pm}, \tan\beta)$. Regions with $R_b \leq 0.215$ are excluded at $2\ \sigma$. One sees a behaviour similar to the $b \to s\gamma$ case shown in Fig. 6(b) of Sec. 6.

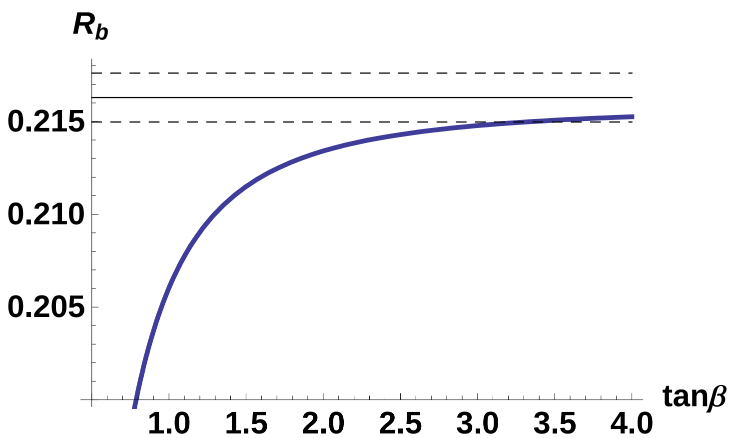

Figure 5: R_b in THDM Type I, with the charged Higgs at $M_{H^\pm} = 100$ GeV. The solid line indicates the experimental average, while the dashed lines indicate the $2\ \sigma$ bounds of the experimental value. Within the given error, we exclude all $\tan\beta \leq 3.3$.

6 Constraints from $b \to s\gamma$

Strong constraints on the parameter space of the THDM Type II also come from B-physics, especially from $b \to s\gamma$. In Type II one can exclude light charged Higgs bosons $M_{H^\pm} \leq 260$ GeV because of the indirect constraint from $b \to s\gamma$ [40]. We will now analyze why this is not possible for Type I. The experimental world average of the branching ratio of B mesons decaying into a photon and a Hadron containing a strange quark, is given in the 2006 analysis of Ref. [41]:

$$\mathcal{B}(\bar{B} \to X_s\gamma)_{exp} = (3.55 \pm 0.24^{+0.09}_{-0.10} \pm 0.03) \times 10^{-4} \ . \tag{123}$$

SM calculations were performed at Next to Next to Leading Order (NNLO) level [42] and gave the following result:

$$\mathcal{B}(\bar{B} \to X_s\gamma)^{\rm NNLO}_{\rm SM} = (3.15 \pm 0.23) \times 10^{-4} \ . \tag{124}$$

The SM value is about 1 σ smaller than the experimental value. For the THDM only calculations up to Next to Leading Order (NLO) exist [43, 44]. We will rederive the Leading Order (LO) result and then examine the theoretical properties of the THDM contribution. Then we will use the NLO result [43] to get a lower exlusion limit for $\tan\beta$ with $M_{H^\pm} \approx 100$ GeV.

6.1 1-loop contributions:

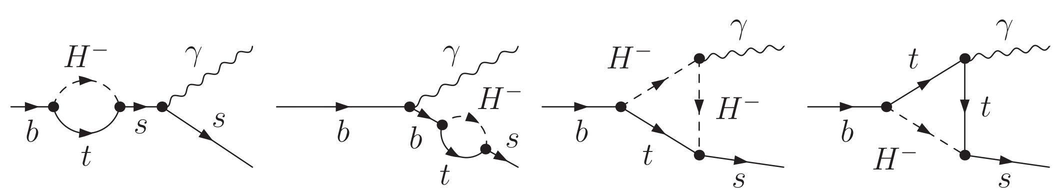

For the diagram M_a, we get the following amplitude:

$$\begin{aligned} iM_a =& \overline{u}(p_s)(-ie\gamma_\mu Q_d)\frac{i(\not{p}+m_s)}{p_b^2-m_s^2}(-i)\left[G_n^\dagger P_L + G_p^\dagger P_R\right]_{su} \\ &\times \int \frac{d^dk}{(2\pi)^d}\frac{i}{(p_b-k)^2-M_{H^\pm}^2}\frac{i(\not{k}+m_t)}{k^2-m_t^2}(-i)\left[G_nP_R+G_pP_L\right]_{ub}u(p_b)\epsilon^*_\mu(q) \ . \end{aligned} \tag{125}$$

Manipulating the denominator of the above and performing the integral, we get

$$\begin{aligned} iM_a =& \frac{ieQ_d\epsilon^*_\mu(q)}{m_b^2-m_s^2}\overline{u}(p_s)\gamma_\mu\left[m_tB(p_b^2,m_t^2,M_{H^\pm}^2)\left(m_sP_X+m_bP_X^{L\leftrightarrow R}\right)+\right. \\ &\left. +m_bB_{11}(p_b^2,m_t^2,M_{H^\pm}^2)\left(m_sP_Y+m_bP_Y^{L\leftrightarrow R}\right)\right]u(p_b) \end{aligned} \tag{126}$$

with

$$\begin{aligned} P_X &= \left[G_n^\dagger P_L + G_p^\dagger P_R\right]_{su}\left[G_nP_R+G_pP_L\right]_{ub} = (G_n^\dagger)_{su}(G_p)_{ub}P_L + (G_p^\dagger)_{su}(G_n)_{ub}P_R \\ P_Y &= \left[G_n^\dagger P_L + G_p^\dagger P_R\right]_{su}\left[G_nP_L+G_pP_R\right]_{ub} = (G_n^\dagger)_{su}(G_n)_{ub}P_L + (G_p^\dagger)_{su}(G_p)_{ub}P_R \ . \end{aligned} \tag{127}$$

For the initial state radiation diagram (M_b), we get:

$$iM_b = \overline{u}(p_s)(-i)\left[G_n^\dagger P_L + G_p^\dagger P_R\right]_{su}\int\frac{d^dk}{(2\pi)^d}\frac{i^2(\not{k}+m_t)}{(k^2-m_t^2)((p_s-k)^2-M_{H^\pm}^2)}$$
$$\times(-i)\left[G_nP_R+G_pP_L\right]_{ub}\frac{i(\not{p}_s+m_b)}{m_s^2-m_b^2}(-ieQ_d)\gamma_\mu u(p_b)\epsilon_\mu^*(q)\ . \quad (128)$$

Performing the integral and simplifying the denominator, we get:

$$iM_b = \frac{-ieQ_d\epsilon_\mu^*(q)}{m_b^2-m_s^2}\overline{u}(p_s)\gamma^\mu\left[m_tB(p_s^2,m_t^2,M_{H^\pm}^2)(m_sP_X+m_bP_X^{L\leftrightarrow R})+\right.$$
$$\left.+m_sB_{11}(p_s^2,m_t^2,M_{H^\pm}^2)(m_sP_Y^{L\leftrightarrow R}+m_bP_Y)\right]u(p_b)\ . \quad (129)$$

We calculate the diagram with 2 scalar propagators in the loop:

$$iM_c = \overline{u}(p_s)(-i)\left[G_n^\dagger P_L + G_p^\dagger P_R\right]_{su}\int\frac{d^dk}{(2\pi)^d}\frac{i(\not{k}+m_t)i^2ie(p_b+p_s-2k)^\mu}{(k^2-m_t^2)\left[(p_s-k)^2-M_{H^\pm}^2\right]\left[(p_b-k)^2-M_{H^\pm}^2\right]}$$
$$\times(-i)\left[G_nP_R+G_pP_L\right]_{ub}u(p_b)\epsilon_\mu^*(q) \quad (130)$$

$$iM_c = \overline{u}(p_s)(-ie)\Big\{\gamma^\mu P_Y^{L\leftrightarrow R}(-2C_{20}^H)+$$
$$+p_s^\mu\big[m_bP_Y(-2\tilde{C}_{22}^H+C_{11b}^H)+m_sP_Y^{L\leftrightarrow R}(-2C_{22a}^H+C_{11a}^H)+$$
$$+m_tP_X(-2C_{11a}^H+C^H)\big]+$$
$$+p_b^\mu\big[m_bP_Y(-2C_{22b}^H+C_{11b}^H)+m_sP_Y^{L\leftrightarrow R}(-2\tilde{C}_{22}^H+C_{11a}^H)+$$
$$+m_tP_X(-2C_{11b}^H+C^H)\big]\Big\}u(p_b)\epsilon_\mu^*(q)\ . \quad (131)$$

The photon is on-shell, therefore this simplifies to

$$iM_c = \overline{u}(p_s)(-ie)\Big\{\gamma^\mu P_Y^{L\leftrightarrow R}(-2C_{20}^H)+2p_b^\mu\Big[m_bP_Y(C_{11b}^H-\tilde{C}_{22}^H-C_{22b}^H)+$$
$$m_sP_Y^{L\leftrightarrow R}(C_{11a}^H-C_{22a}^H-C_{22}^H)+$$
$$m_tP_X(C^H-C_{11a}^H-C_{11b}^H)\Big]\Big\}u(p_b)\epsilon_\mu^*(q)\ , \quad (132)$$

where $C_{ija}^H = C_{ij}(p_s^2,p_b^2,(p_sp_b),m_t^2,M_{H^\pm}^2,M_{H^\pm}^2)$ and $C_{ijb}^H = C_{ij}(p_b^2,p_s^2,(p_sp_b),m_t^2,M_{H^\pm}^2,M_{H^\pm}^2)$. The next diagram ($M_d$) contains 2 fermion propagators in the loop:

$$iM_d = \overline{u}(p_s)(-i)\left[G_n^\dagger P_L + G_p^\dagger P_R\right]_{su}\int\frac{d^dk}{(2\pi)^d}\frac{i((\not{k}-\not{q})+m_t)(-ie)\gamma^\mu Q_u ii(\not{k}+m_t)}{(k^2-m_t^2)((k-q)^2-m_t^2)((p_b-k)^2-M_{H^\pm}^2)}$$
$$\times(-i)\left[G_nP_R+G_pP_L\right]_{ub}u(p_b)\epsilon_\mu^*(q)\ . \quad (133)$$

Evaluating the integral and simplifying the nominator we finally get:

$$
\begin{aligned}
iM_d = ieQ_u\overline{u}(p_s)\Bigg[\gamma^\mu\Bigg\{ & P_Y^{L\leftrightarrow R}\Big[(2-d)C_{20} + m_b^2(-C_{22b} - \tilde{C}_{22} + C_{11b}) + m_s^2\tilde{C}_{22} + m_t^2 C\Big] + \\
& + m_b m_s P_Y C_{11b} + m_b m_t P_X^{L\leftrightarrow R} C + m_t m_s P_X C\Bigg\} + \\
& +2q^\mu\Bigg\{ m_b P_Y(C_{22a} + \tilde{C}_{22} - (C_{11a} + C_{11b})) + m_s P_Y^{L\leftrightarrow R}(C_{11a} - C_{22a}) + \\
& m_t P_X(C_{11a} - C)\Bigg\} \\
& +2p_b^\mu\Big\{ m_b P_Y(C_{22b} + \tilde{C}_{22}) - m_s P_Y^{L\leftrightarrow R}\tilde{C}_{22} + m_t P_X C_{11b}\Big\} \\
& -2p_s^\mu\left\{m_b P_Y C_{11b} + m_t P_X C\right\}\Bigg] u(p_b)\ .
\end{aligned}
\tag{134}
$$

Further use of $\epsilon^\mu q_\mu = 0$ yields

$$
\begin{aligned}
iM_d = ieQ_u\overline{u}(p_s)\gamma^\mu\Bigg\{ & P_Y^{L\leftrightarrow R}\Big[(2-d)C_{20} + m_b^2(-C_{22b} - \tilde{C}_{22} + C_{11b}) + m_s^2\tilde{C}_{22} + m_t^2 C\Big] + \\
& + m_b m_s P_Y C_{11b} + m_b m_t P_X^{L\leftrightarrow R} C + m_t m_s P_X C\Bigg\} + \\
& +2p_b^\mu\Big\{ m_b P_Y(C_{22b} + \tilde{C}_{22} - C_{11b}) - m_s P_Y^{L\leftrightarrow R}\tilde{C}_{22} \\
& + m_t P_X(C_{11b} - C)\Big\} u(p_b)\ .
\end{aligned}
\tag{135}
$$

Let us now calculate P_X and P_Y in Type I and Type II for the charged Higgs bosons. Then

$$
P_X = \frac{e^2 V_{ts}^* V_{tb}}{2M_W^2 s_w^2} m_t g_n g_p \left[m_s P_L + m_b P_R\right] \approx \frac{e^2 V_{ts}^* V_{tb}}{2M_W^2 s_w^2} m_t g_n g_p m_b P_R \tag{136}
$$

$$
P_Y = \frac{e^2 V_{ts}^* V_{tb}}{2M_W^2 s_w^2}\left[g_n^2 m_s m_b P_L + m_t^2 g_p^2 P_R\right] \approx \frac{e^2 V_{ts}^* V_{tb}}{2M_W^2 s_w^2} m_t^2 g_p^2 P_R\ . \tag{137}
$$

6.1.1 Type I

For the Type I Yukawa couplings, $g_p = \cot\beta$ and $g_n = -\cot\beta$. P_X is negative for these couplings, and the $\cot\beta$ dependence factorizes, $M_{\mathrm{THDM}} \propto \cot^2\beta$. In this case P_X is negative, having opposite sign to the SM contribution. Depending on $\tan\beta$, the overall decay width will increase for $\tan\beta \ll 1$, as the contribution of the charged Higgs dominants the SM contribution, or decrease for $\tan\beta \approx 1$. For $\tan\beta \gg 1$ the THDM contribution vanishes and we have the SM case.

6.1.2 Type II

For Type II Yukawa couplings, $g_p = \cot\beta$ and $g_n = \tan\beta$. In this case P_X has the same sign as the SM contribution, therefore the THDM contribution always increases the decay width. Moreover, P_X does not depend on $\tan\beta$ at all. For $10 \leq \tan\beta \leq 10^3$ we have $P_Y \propto m_t^2 \cot^2\beta P_R$ and the dependence on $\tan\beta$ is strongly suppressed. For $\tan\beta \ll 1$ we receive additional large positive contributions from terms proportional to P_Y. As the SM value is in good agreement with experiment, and the THDM contribution is sizeable, one can derive an exclusion limit for $M_{H^\pm}$ independent of $\tan\beta$ (see Fig. 6(a) where the NLO result is plotted).

Evaluating the width numerically, in the SM we get at LO

$$\Gamma_{SM}(\bar{B} \to X_s\gamma) \approx 6.9 \times 10^{-17} \text{ GeV} . \tag{138}$$

We used the pole mass of the b-quark $m_b = 4.7$ GeV, $m_s = 0.15$ GeV and $\alpha^{-1} = 130$. Combining this with Γ_{SL} defined in (143) and $\mathcal{B}_{SL}$ defined in (141), we use (140) to get the branching ratio at LO:

$$\mathcal{B}(\bar{B} \to X_s\gamma)^{\text{LO}}_{\text{SM}} = 3.14 \times 10^{-4}. \tag{139}$$

We will now use a NLO discussion (which includes QCD corrections) to calculate exclusion regions for the THDM.

6.2 The NLO result in the THDM

In B physics, the framework of an effective low-energy theory with 5 quarks is often used. All particles with mass $m \gg m_b$ are integrated out. (For an excellent review of this approach see Ref. [45]). As a first approximation one uses the spectator quark model, in which only the heavy b-quark decays while the other sea quark (u or d) does not influence the decay products. One can then use Heavy Quark Effective Theory to calculate additional corrections of the order $1/m_b^2$ (See for example [46]). We will first introduce the formulas used in [43]. The inclusive branching ratio can be calculated as

$$\mathcal{B}(\bar{B} \to X_s\gamma) = \frac{\Gamma(\bar{B} \to X_s\gamma)}{\Gamma_{SL}} \mathcal{B}_{SL} \tag{140}$$

where $\mathcal{B}_{SL}$ refers to the semi-leptonic branching ratio $B \to Xl\nu$. A recent evaluation [24] of experiments at Belle, CLEO and Babar has shown that

$$\mathcal{B}_{SL} = (10.99 \pm 0.28) \times 10^{-2} . \tag{141}$$

The dominant contributions to these semi-leptonic decays are tree-level processes, with a virtual charged particle (W-boson and the $H^\pm$) mediating the decay. Even for a very light charged scalar $M_{H^\pm} \approx m_W$ the contribution of $H^\pm$ is suppressed by a factor

$$R_{H^\pm/W} \approx \frac{m_b m_l}{m_W^2} . \tag{142}$$

For the inclusive rate, the most dominant contribution comes from decays with final state electrons. As for these $R_{H^\pm/W} \approx 10^{-4}$, one can ignore the THDM contribution. With QCD corrections and non-perturbative corrections taken into account, one finds [43]

$$\Gamma_{SL} = \frac{G_F^2}{192\pi^2} |V_{cb}|^2 m_b^5 g(z) \left(1 - \frac{\alpha_s(\mu_b)}{3\pi} f(z) + \frac{\delta_{SL}^{NP}}{m_b^2}\right) \tag{143}$$

where

$$g(z) = 1 - 8z + 8z^3 - z^4 - 12z^2\log(z)\ , \quad f(z) = \left(\pi^2 - \frac{31}{4}\right)(1-\sqrt{z})^2 + \frac{3}{2}\ , \quad z = \frac{m_c^2}{m_b^2}\ ,$$

$$\delta_{SL}^{NP} = \frac{\lambda_1}{2} + \frac{3\lambda_2}{2}\left[1 - 4\frac{(1-z)^4}{g(z)}\right]\ , \quad \lambda_1 = -0.5\ \mathrm{GeV}^2\ , \quad \lambda_2 = -0.12\ \mathrm{GeV}^2\ . \tag{144}$$

The inclusive partial decay width is then found to be [43]

$$\begin{aligned}\Gamma(\bar{B}\to X_s\gamma) = &\frac{G_F^2}{32\pi^4}|V_{ts}^*V_{tb}|^2\alpha_{em}m_b^5\\ &\Bigg[|\bar{D}|^2 + A + \frac{\delta_\gamma^{NP}}{2m_b^2}|C_7^{0,eff}(\mu_b)|^2 + \\ &\frac{\delta_c^{NP}}{m_c^2}\Re\Big(C_7^{0,eff}(\mu_b)\Big)^*\left(C_2^{0,eff}(\mu_b) - \frac{1}{6}C_1^{0,eff}(\mu_b)\right)\Bigg]\ .\end{aligned} \tag{145}$$

Here $|\bar{D}|^2 \propto |M_{b\to\gamma s}|^2$ is proportional to the matrix element of $b\to\gamma s$, $A \propto |M_{b\to\gamma sg}|^2$ proportional to the gluon bremsstrahlung matrix element, and the terms proportional to $\delta_\gamma^{NP} = \lambda_1 - 9\lambda_2$ and $\delta_c^{NP} = -\lambda_2/9$ are corrections from Heavy Quark Effective Theory. The equation depends on two scales μ_b and μ_w because the Wilson coefficients are first calculated at a scale μ_w where QCD corrections are small, and then scaled down to $\mu_b \approx m_b$ by solving the appropriate renormalization group equation. In our calculation we used

$$\mu_w = m_W, \quad \mu_b = 4.8\ \mathrm{GeV}, \quad \alpha_s(M_Z) = 0.119, \quad \alpha_{em}^{-1} = 137.036, \quad M_t = 171.2\ \mathrm{GeV}\ . \tag{146}$$

By choosing $\alpha_{em}^{-1} = 137.036$ we take the recommendation of [47]. The residual scale dependence of $\mathcal{B}(\bar{B}\to X_s\gamma)$ introduces an error of $\pm^{0.01}_{0.20}$ [43]. Considering this and the errors of the input parameters, we get the SM prediction at NLO:

$$\begin{aligned}\mathcal{B}(\bar{B}\to X_s\gamma) = 3.54 \pm^{0.01}_{0.20}(\mu) \pm^{0.20}_{0.20}(\mathrm{param})\times 10^{-4} = \\ \approx 3.54\pm^{0.21}_{0.40}\times 10^{-4}\ .\end{aligned} \tag{147}$$

The SM contribution at NNLO decreases the NLO decay width by 10 percent. Hence the NLO SM result (147) is higher than the NNLO SM result (124). One can combine the NNLO SM result with the NLO result calculated in the THDM by considering the following: If we assume that contributions of diagrams arising at NNLO involving the additional particles of the THDM are rather small, it makes sense to consider $\mathcal{B}(\bar{B}\to X_s\gamma)$ for NNLO SM and NLO THDM contributions. In this case we write $\mathcal{B}(\bar{B}\to X_s\gamma)$ as

$$\mathcal{B}^{\mathrm{SM,\ THDM}}_{\mathrm{NNLO,\ NLO}}(\bar{B}\to X_s\gamma) \propto \left|A^{\mathrm{SM}}_{\mathrm{NLO}} + A^{\mathrm{SM}}_{\mathrm{NNLO}} + A^{\mathrm{THDM}}_{\mathrm{NLO}}\right|^2 \tag{148}$$

where $A^{\mathrm{SM}}_{\mathrm{NLO}}$ and $A^{\mathrm{SM}}_{\mathrm{NNLO}}$ refer to NLO and NNLO SM amplitudes respectively, and $A^{\mathrm{THDM}}_{\mathrm{NLO}}$ contains only the additional contributions of the THDM at NLO. If then $A^{\mathrm{THDM}}_{\mathrm{NLO}}A^{\mathrm{SM}}_{\mathrm{NNLO}} \ll 1$, we have

$$\begin{aligned}\mathcal{B}^{\mathrm{SM,\ THDM}}_{\mathrm{NNLO,\ NLO}}(\bar{B}\to X_s\gamma) &= \mathcal{B}^{\mathrm{THDM}}_{\mathrm{NLO}} + \mathcal{B}^{\mathrm{SM}}_{\mathrm{NNLO}} - \mathcal{B}^{\mathrm{SM}}_{\mathrm{NLO}} + \\ &= \mathcal{B}^{\mathrm{THDM}}_{\mathrm{NLO}} + (-0.39\pm^{0.23}_{0.40})\times 10^{-4}\ .\end{aligned} \tag{149}$$

Calculating $\mathcal{B}_{\rm NLO}^{\rm THDM}$ we can then employ (149) to get exclusion regions in the $(M_{H^\pm}, \tan\beta)$ plane.

To get an upper bound for $\mathcal{B}(\bar{B} \to X_s\gamma)$ we use the upper experimental error (123) at 2 σ, add the lower error from the theoretical prediction in (147), and the experimental value (123). Doing the same for the lower bound, we can then exclude at 95% C.L.

$$\mathcal{B}(\bar{B} \to X_s\gamma) \geq 4.67 \times 10^{-4} \quad \text{and} \quad \mathcal{B}(\bar{B} \to X_s\gamma) \leq 2.58 \times 10^{-4} \, . \tag{150}$$

As illustrated below in Fig. 6(a), in the Type II model for $M_{H^\pm} \leq 260$ GeV, the branching ratio $\mathcal{B}(\bar{B} \to X_s\gamma)$ exceeds the upper bound for all $\tan\beta$. Therefore the charged scalar must have a mass $M_{H^\pm} \geq 260$ GeV to still be compatible with B physics experiments. For smaller $\tan\beta$ values, the scalar must be even heavier to fulfill this constraint. In

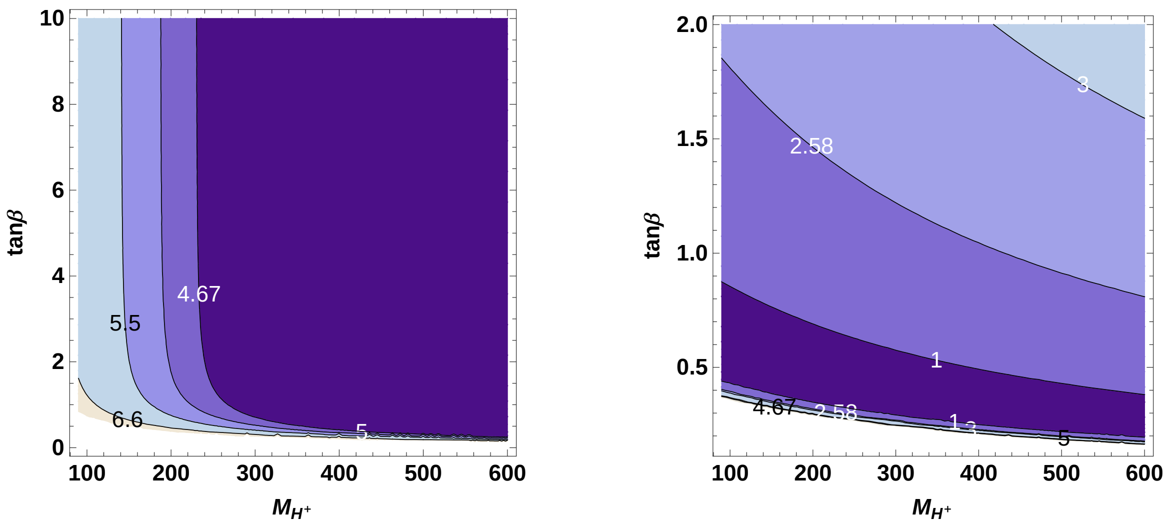

(a) The Type II model branching ratio is always greater than the SM value. As one can exclude all $\mathcal{B} \times 10^4 \geq 4.67$ at 2 σ, values of $M_{H^\pm} \leq 260$ GeV are excluded independent of $\tan\beta$.

(b) The Type I model branching ratio is always smaller than the SM value for $\tan\beta \geq 0.4$. For $\tan\beta \ll 1$ the branching ratio rises like $\mathcal{B} \propto \cot^4\beta$.

Figure 6: $\mathcal{B}(\bar{B} \to X_s\gamma) \times 10^4$ in Type II (Fig. 6(a)) and Type I (Fig. 6(b)) plotted against $\tan\beta$ and $M_{H^\pm}$.

Fig. 6 one can see the differences between the Type II and Type I THDM. While for Type II (Fig. 6(a)) one can easily exclude light scalars independent of $\tan\beta$, this is not possible for Type I (Fig. 6(b)). In the Type I model we can calculate a lower limit on $\tan\beta$ for a given mass of the charged Higgs $M_{H^\pm}$. Setting the mass of the charged scalar to $M_{H^\pm} = 100$ GeV we can exclude $\tan\beta \leq 1.9$, which is a much weaker bound than we previously calculated from fermionic Z decays (122). In Figs. 6(b) and 7 one sees yet another feature due to $M_{\rm THDM} \propto \cot^2\beta$: For low values of $\tan\beta$, the additional contributions of the THDM start to dominate the SM contributions, and therefore lead to very high values. This region is however already excluded due to the previous discussion in Sec. 5.3, as can be seen from Fig. 4. In Fig 7 we have plotted ($\tan\beta$, $\mathcal{B}(\bar{B} \to X_s\gamma) \times 10^4$) for $M_{H^\pm} = 100$ GeV in the Type I Model. Due to this plot, one can exclude $\tan\beta \leq 1.9$ for these light scalars, but this is a much weaker constraint than $\tan\beta \leq 3.3$ previously found in Sec. 5.4.

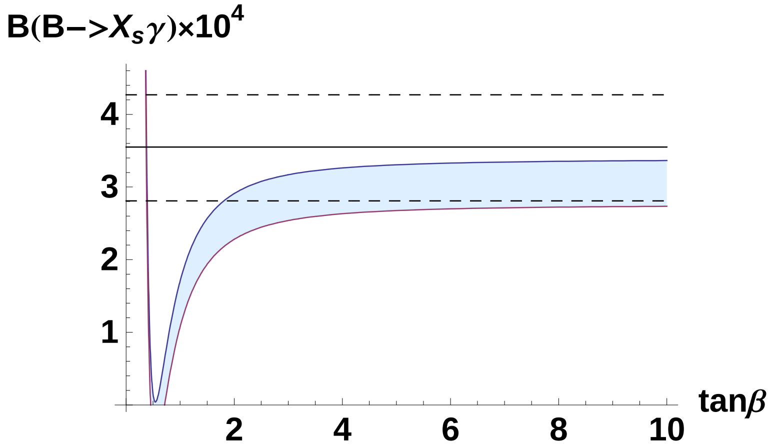

Figure 7: $\mathcal{B}(\bar{B} \to X_s\gamma) \times 10^4$ of Type I is plotted against $\tan\beta$. The scalar mass is fixed at $M_{H^\pm} = 100$ GeV. The solid line is the experimental average, while the dashed lines indicate the 2 σ bounds of the experimental values. We exclude $\tan\beta \leq 1.9$ for light charged scalars $H^\pm$ at $M_{H^\pm} = 100$ GeV, which is a much weaker bound than the one from Fig. 5, where we excluded $\tan\beta \leq 3.3$.

7 Unitarity constraints

Our motivation for considering unitarity constraints is to get theoretical constraints on the growth of the coupling $g_{hH^-H^+}$ which appears in the loop with the charged Higgs in the process $h \to \gamma\gamma$ discussed in Sec. 8. Unitarity constraints were first applied to the SM in [48]. Unitarity constraints in the THDM were considered in Refs. [49, 50, 51, 52]. We will apply the constraints derived in Ref. [52], as they provide the largest set of unitarity constraints, which are valid for the more general potential V_λ.

7.1 General analysis

A general investigation was done in [52], using the potential (5). For $m_{12}^2 = 0$ it was shown that constraints for the mass of the light CP even scalar M_h are strongly correlated with $\tan\beta$. For $M_h = 100$ GeV the corresponding constraint for $\tan\beta$ is

$$\tan\beta \leq 7. \tag{151}$$

This gets relaxed if we allow $m_{12}^2 \neq 0$. In this case, there is some parameter region compatible with unitarity constraints, for which

$$\tan\beta \leq 30 \tag{152}$$

may still be allowed. We will now analyze unitarity constraints for the parameter space, where a large enhancement of $\Gamma(h \to \gamma\gamma)$ as considered in Sec. 8 is possible.

7.2 IDM

In the IDM considering unitarity bounds is particularly simple, because for the couplings in Secs. 11.3.3 and 11.3.4 we find $m_W g_{hH^-H^+} \propto g_{h^2H^-H^+}$. We hence consider the process $\sigma(hH^+ \to hH^+)$ to get a unitarity constraint for the quartic coupling. For high energies $\sqrt{s} \gg M_h, M_{H^\pm}$ we can forget about everything but the quartic vertex coupling and get the typical constraint

$$|g_{h^2H^-H^+}| \leq 8\pi \tag{153}$$

or equivalently

$$|g_{hH^-H^+}| \leq \frac{16\pi m_W}{g} \quad \leftrightarrow \quad |m_{22}^2 - M_{H^\pm}^2| \leq \frac{4m_W^2 s_w}{\alpha}. \tag{154}$$

Inserting $\alpha^{-1} \approx 128$ we get a rather conservative bound:

$$\sqrt{|m_{22}^2 - M_{H^\pm}^2|} \leq 5m_W \tag{155}$$

7.3 The V_B case

For the potential V_B things look a bit more complicated. Various processes were used in Ref. [52] to constrain quartic couplings at high energies at the tree level. These lead to a set of unitarity constrained parameters $a_\pm, b_\pm, c_\pm, d_\pm, f_\pm, e_{1,2}, f_{1,2}, p_1$, for which the absolute values must be smaller than 8π. These parameters then depend on the parameters of the potential, which in the case of the potential V_B are the 4 Higgs masses and the two mixing angles $\tan\beta$ and $\cos\alpha$. We take the maximum of these parameters and normalize it to the violation bound 8π:

$$U_B(M_h, M_H, M_A, M_{H^\pm}, \beta, \alpha) = \frac{\mathrm{Max}(|a_\pm|, |b_\pm|, |c_\pm|, |d_\pm|, |f_\pm|, |e_{1,2}|, |f_{1,2}|, |p_1|)}{8\pi} . \quad (156)$$

Normalizing this way, the parameter region where $U_B \geq 1$ is excluded by unitarity. To get a feel for the unitarity constraints, we will study them for the case of a light charged scalar $H^\pm$ and a heavy A, in which case large enhancement of $\Gamma(h \to \gamma\gamma)$ is possible.

The region we will consider is $M_h = 130$ GeV, $M_{H^\pm} = 100$ GeV, $M_A = 500$ GeV. The remaining free parameters are M_H, $\tan\beta$ and $\sin\alpha$. U_B of (156) was then evaluated for various M_H and plotted in Fig. 8.

In Fig. 8 the region $U_B \geq 1$ is excluded by perturbative unitarity and marked in orange. The blue region with U_B smaller than 1 is not forbidden by the unitarity bounds (but obviously may be forbidden by other constraints). As can be seen in these plots, unitarity bounds constrain the high $\tan\beta$ region and are therefore complementary to the constraints from $Z \to b\bar{b}$, which restrict low values of $\tan\beta$ (for all plots displayed in Fig. 8, as $M_{H^\pm} = 100$ GeV, $\tan\beta \leq 3.3$ are excluded due to (122), independent of α). In Fig. 8 we see that if M_H gets smaller, the excluded region gets larger. Adding to these plots the constraint $\tan\beta \leq 3.3$ from $Z \to b\bar{b}$, one sees that the region displayed in Fig. 8(a) is completely excluded, while in Fig. 8(b) the allowed region is very small. Combining this even further with exclusion regions of Δr, one sees that all regions displayed in Fig. 8 are excluded. This still holds true, if we lower or raise M_H above the considered values. In this way, one can combine constraints to excluded a huge region of parameter space.

7.4 The V_λ case

Next we consider the potential V_λ[3]. The situation is very similar except that compared to V_B, we now have an additional parameter in the potential, m_{12}. We define the unitarity bound just the same way we did for V_B:

$$U_\lambda(M_h, M_H, M_A, M_{H^\pm}, \beta, \alpha, m_{12}) = \frac{\mathrm{Max}(|a_\pm|, |b_\pm|, |c_\pm|, |d_\pm|, |f_\pm|, |e_{1,2}|, |f_{1,2}|, |p_1|)}{8\pi} . \quad (157)$$

Now the unitarity constrained parameters $a_\pm, \ldots$ depend not only on the 4 Higgs masses and the 2 mixing angles, but also on the parameter m_{12}^2. We will not display any examples of the unitarity plots for V_λ here but use the constraint $U_\lambda \leq 1$ in the discussion of Sec. 8.4.

[3]Note that we do not discuss V_A here, because one can always get it from V_λ by setting $m_{12} = 0$.

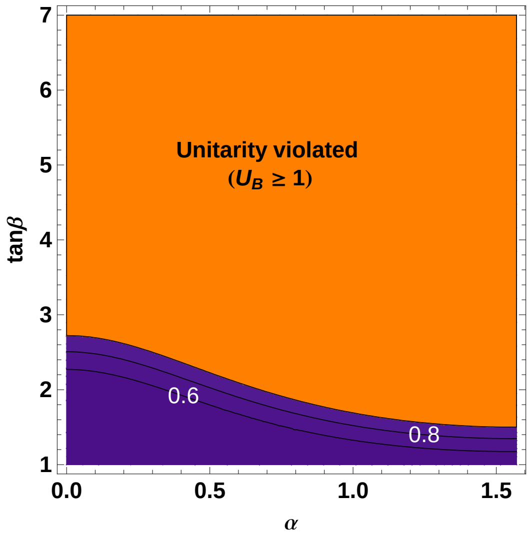

(a) U_B evaluated at $M_H = 400$ GeV.

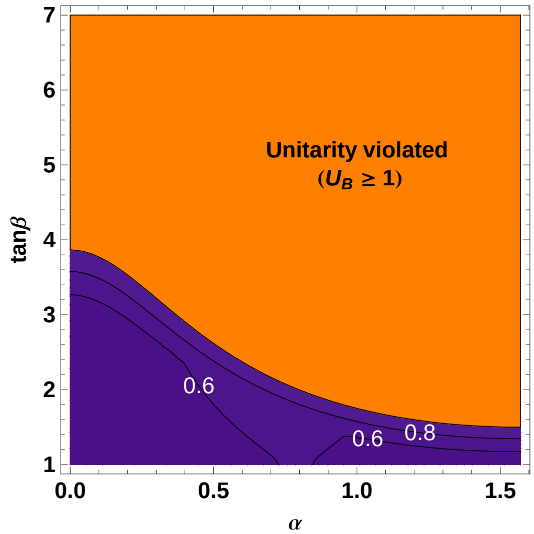

(b) U_B evaluated at $M_H = 450$ GeV

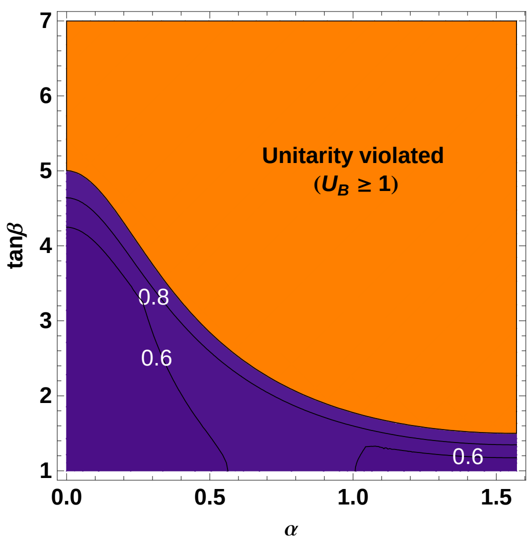

(c) U_B evaluated at $M_H = 470$ GeV

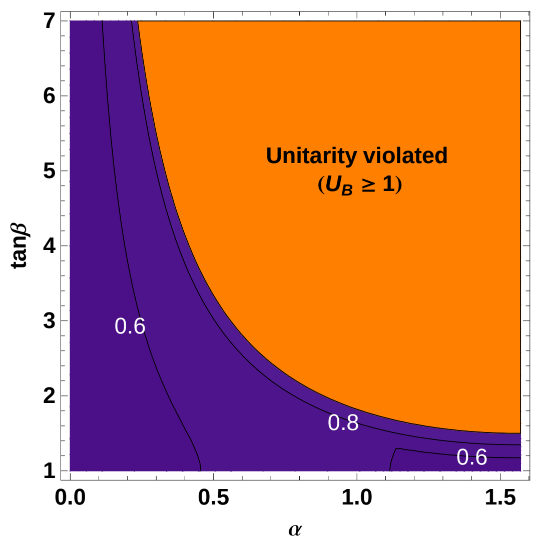

(d) U_B evaluated at $M_H = 500$ GeV

Figure 8: U_B plotted against $\tan\beta$ and α, and evaluated at $M_h = 130$ GeV, $M_{H^\pm} = 100$ GeV, $M_A = 500$ GeV for different values of M_H. The region in orange violates perturbative unitarity. Plots for even lighter values of H (i.e. $M_H = 100$ GeV) are similar to Fig. 8(a) and are not shown here.

8 $\mathbf{h} \to \gamma\gamma$

One decay channel of particular interest for Higgs searches in the SM at LHC is the decay of the Higgs particle to two photons. This is often referred to as the "silver" detection channel at LHC [1]. It is a rare event, but it has a particular clear signature against background for the mass range 100 GeV $< M_h <$ 150 GeV. As this is a loop mediated decay of the Higgs, one expects additional contributions arising from the enlarged Higgs sector in the THDM. It is hence interesting how large this partial decay width may get compared to the SM. While this decay has already been studied in Type II of the THDM [53, 54], in Type I it has only been studied in the fermiophobic limit [55, 9]. In Type II the partial decay width $\Gamma(h \to \gamma\gamma)$ can be enhanced only by around 25 % compared to the Standard Model due to the exclusion of light charged scalars with $M_{H^\pm} \leq 260$ GeV arising from B physics [53]. There is no such exclusion for the Type I case, in which charged Higgs bosons as light as $M_{H^\pm} \approx 100$ GeV are not yet excluded. We will therefore study if large enhancement comes about for such light charged Higgs bosons in Type I models.

The partial decay width $\Gamma(h \to \gamma\gamma)$ depends on the potential under consideration. We will therefore analyze it for the potentials considered in Sec. 2. For this calculation we again use the Haber-Kane sign convention as introduced in Sec. 3 in (33). Besides this sign convention, we stick to Ref. [19] for Feynman rules of vertices and propagators. The amplitude in the THDM is simply the SM amplitude (modulo the mixing of the vevs and Higgs bosons) and the contributions from the charged scalar of the Higgs sector. For the charged scalar contribution, only 3 diagrams have to be calculated:

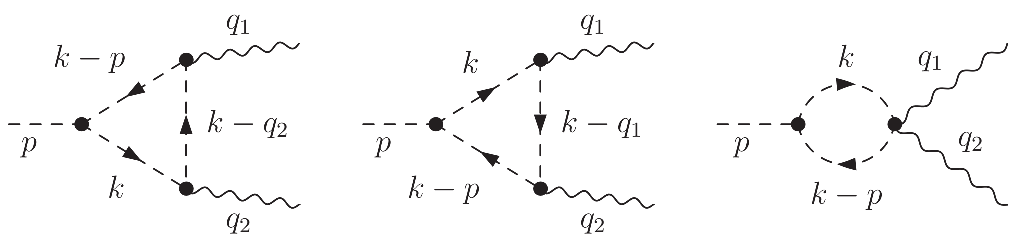

($\mathcal{A}_1$) ($\mathcal{A}_2$) ($\mathcal{A}_3$)

Using Feynman rules, we get

$$\mathcal{A}_1 = \epsilon^*(q_1)_\mu \epsilon^*(q_2)_\nu g_{hH^+H^-}(-e^2) \int \frac{d^dk}{(2\pi)^d} \frac{[2k-(p+q_2)]^\mu [2k-q_2]^\nu}{[k^2 - M_{H^\pm}^2][(k-q_2)^2 - M_{H^\pm}^2][(k-p)^2 - M_{H^\pm}^2]}$$

$$\mathcal{A}_2 = \epsilon^*(q_1)_\mu \epsilon^*(q_2)_\nu g_{hH^+H^-}(-e^2) \int \frac{d^dk}{(2\pi)^d} \frac{[2k-q_1]^\mu [2k-(p+q_1)]^\nu}{[(k-q_1)^2 - M_{H^\pm}^2][k^2 - M_{H^\pm}^2][(k-p)^2 - M_{H^\pm}^2]}$$

$$\mathcal{A}_3 = \epsilon^*(q_1)^\mu \epsilon^*(q_2)_\mu g_{hH^+H^-}(2e^2) \int \frac{d^dk}{(2\pi)^d} \frac{1}{[k^2 - M_{H^\pm}][(k-p)^2 - M_{H^\pm}^2]}. \tag{158}$$

Substituting $k' = p - k$ in $\mathcal{A}_1$ gives us $\mathcal{A}_1 = \mathcal{A}_2$. We perform the Passarino-Veltman reduction on $\mathcal{A}_1$. As on-shell photons are polarized orthogonal to their momentum, we have $\epsilon^*(q_1)_\mu q_1^\mu = 0$. We can rewrite $\mathcal{A}_1$ in the notation of Sec. 11.1:

$$\mathcal{A}_1 = \epsilon^*(q_1)^\mu \epsilon^*(q_2)^\nu g_{hH^+H^-}(-ie^2)[4\{\{k^\mu k^\nu\}\} - 4\{\{k^\mu\}\} q_1^\nu], \tag{159}$$

where $\{\{\}\}$ denotes the integral with three propagators in the loop. Applying Passarino-Veltman reduction, one finds:

$$\{\{k^\mu k^\nu\}\} = g^{\mu\nu} C_{20} + q_2^\mu q_1^\nu (C_{22b} + \tilde{C}_{22}) \ , \qquad \{\{k^\mu\}\} = q_2^\mu C_{11a}, \tag{160}$$

where the C-functions take the arguments $(p^2, q_1^2 = 0, pq_1, M_{H^\pm}^2, M_{H^\pm}^2, M_{H^\pm}^2)$[4].
Also calculating $\mathcal{A}_3$ we get the contribution of the Higgs sector in the THDM:

$$\mathcal{A}_{H^+} = \mathcal{A}_1 + \mathcal{A}_2 + \mathcal{A}_3 = \tag{161}$$

$$= \epsilon^*(q_1)_\mu \epsilon^*(q_2)_\nu g_{hH^+H^-}(-e^2)\left[g^{\mu\nu}(8C_{20} - 2B(p^2)) + 4q_2^\mu q_1^\nu \left(2C_{22b} + 2\tilde{C}_{22} - 2C_{11a}\right)\right] \tag{162}$$

Divergencies occur only in C_{20} and $B(p^2)$ and they cancel:

$$\mathrm{Div}(\mathcal{A}_{H^+}) = \epsilon^*(q_1)_\mu \epsilon^*(q_2)_\nu g_{hH^+H^-} 2(-e^2)\left[g^{\mu\nu}(4\frac{1}{4}B(0) - B(0))\right]. \tag{163}$$

The contribution of the charged Higgs must be finite because there is no tree-level coupling which could introduce a counterterm, nor could divergencies cancel with the fermionic or gauge boson contributions because these are never proportional to $g_{hH^+H^-}$. As the theory is renormalizable, the terms must be finite. The same holds separately for the contributions of the fermions and the gauge sector. It is now easy to insert the Passarino-Veltman functions and get an analytical expression:

$$\mathcal{A}_{H^+} = \epsilon^*(q_1)_\mu \epsilon^*(q_2)_\nu g_{hH^+H^-}(-e^2)\frac{2}{(4\pi)^2}\tau_{H^\pm} A_0(\tau_{H^\pm})\left[-g^{\mu\nu} + 2\frac{q_2^\mu q_1^\nu}{M_h^2}\right] \ , \tag{164}$$

where $\tau_i = \frac{M_h}{4m_i}$ with $i \in \{W, f\}$ and $\tau_{H^\pm} = \frac{M_h}{4M_{H^\pm}}$. Before we can calculate the squared matrix element, we also need the SM contributions. These contributions were calculated with FeynArts [56] and FormCalc [57] and expressed with the Passarino-Veltman functions. After a short calculation one gets the well-known expressions [58]:

$$\begin{aligned}
\mathcal{A}_{\mathrm{W}} &= \epsilon^*(q_1)_\mu \epsilon^*(q_2)_\nu g_{\mathrm{W}} \frac{e^3 M_h^2}{m_W s_W 2(4\pi)^2} A_1(\tau_W)\left[-g^{\mu\nu} + 2\frac{q_2^\mu q_1^\nu}{M_h^2}\right] \\
\mathcal{A}_{\mathrm{f}} &= \epsilon^*(q_1)_\mu \epsilon^*(q_2)_\nu g_f \frac{e^3 M_h^2}{m_W s_W 2(4\pi)^2} Q_f^2 N_c A_{1/2}(\tau_f)\left[-g^{\mu\nu} + 2\frac{q_2^\mu q_1^\nu}{M_h^2}\right].
\end{aligned} \tag{165}$$

The form factors A_i are:

$$\begin{aligned}
A_0(\tau) &= -[\tau - f(\tau)]\tau^{-2} \\
A_{1/2}(\tau) &= 2[\tau + (\tau - 1)f(\tau)]\tau^{-2} \\
A_1(\tau) &= -[2\tau^2 + 3\tau + 3(2\tau - 1)f(\tau)]\tau^{-2}
\end{aligned} \tag{166}$$

and

$$f(\tau) = \begin{cases} \arcsin^2\sqrt{\tau} & \tau \leq 1 \\ -\dfrac{1}{4}\left[\log\dfrac{1+\sqrt{1-\tau^{-1}}}{1-\sqrt{1-\tau^{-1}}} - i\pi\right]^2 & \tau > 1 \end{cases} . \tag{167}$$

[4] We use the A,B,C notation of [20]

The total amplitude $\mathcal{A}$ is then

$$\mathcal{A} = \mathcal{A}_{\rm W} + \mathcal{A}_{\rm f} + \mathcal{A}_{H^+}. \tag{168}$$

We can now calculate the matrix element squared for unpolarized photons

$$\sum_{\rm Pol} |\mathcal{A}|^2 = \sum_{\rm Pol} \epsilon^*_{1\mu}\epsilon^*_{2\nu}\hat{\mathcal{A}}^{\mu\nu}\epsilon_{1\mu'}\epsilon_{2\nu'}(\hat{\mathcal{A}}^{\mu'\nu'})^* = \hat{\mathcal{A}}_{\mu\nu}(\hat{\mathcal{A}}^{\mu\nu})^* \tag{169}$$

where $\sum_{\rm Pol}$ stands for the polarization sum of the photons. $\hat{\mathcal{A}}^{\mu\nu}$ is the total matrix element, without the polarization vectors $\epsilon^*(q_1)^\mu\epsilon^*(q_2)^\nu$. The final result is

$$\sum_{\rm Pol} |\mathcal{A}|^2 = 2\left(\frac{e^3 M_h^2}{m_W s_W 2(4\pi)^2}\right)^2 \Bigg| \sum_{f\in\{t,b\}} g_f Q_f^2 N_c A_{1/2}(\tau_f) + g_W A_1(\tau_W) + \frac{g_{hH^+H^-} m_W s_W}{e M_{H^\pm}^2} A_0(\tau_{H^\pm})\Bigg|^2 . \tag{170}$$

With the squared matrix element calculated, we just have to include the phase space factor to get the partial decay width:

$$\Gamma(h\to\gamma\gamma) = \frac{G_\mu \alpha^2 M_h^3}{128\sqrt{2}\pi^3}\Bigg| \sum_{f\in\{t,b\}} g_f Q_f^2 N_c A_{1/2}(\tau_f) + g_W A_1(\tau_W) + g_h A_0(\tau_{H^\pm})\Bigg|^2, \tag{171}$$

where

$$g_h \equiv \frac{g_{hH^+H^-} m_W s_W}{e M_{H^\pm}^2} \ . \tag{172}$$

Note that we get the SM case by setting $g_W = g_f = 1$ and $g_h = 0$. In a Type I THDM, g_f is identical for up-type and down-type quarks. For the CP-even Higgs h we get

$$g_W = \sin(\beta-\alpha)\ , \qquad g_f = \frac{\cos\alpha}{\sin\beta}. \tag{173}$$

The coupling g_W is generic for all Types of THDMs depending only indirectly on the potential or the Yukawa couplings. The coupling g_h obviously depends on the potential and has to be evaluated for each potential separately.

To look for large enhancement via the charged Higgs, one has to compare the form factors $A_i(\tau_i)$ for the parameter region of interest. We investigate large enhancement in the region 100 GeV $\leq M_h \leq$ 160 GeV and $M_{H^\pm} \geq$ 95 GeV. The form factors are plotted in Fig. 9. The region of interest is marked in red in the plots. One sees that A_1 is always negative, while $A_{1/2}$ and A_0 are both positive. Also A_1 is by far the dominant contribution, being around $A_1 \approx -12$, while $A_0 \approx 0.4$ and $A_{1/2} \approx 1.4$.

If we assume $g_W \geq 0$, g_h must be negative and $g_h \approx -10$ to get competitive to the W bosons. In this case the contribution of the charged Higgs bosons has the same sign and the same size as the one of the W bosons. Alternatively, the charged Higgs contribution may get larger than the W boson contribution while still having opposite sign, which happens if $g_h \approx 20$. In both of these cases, the couplings get very large, and therefore one

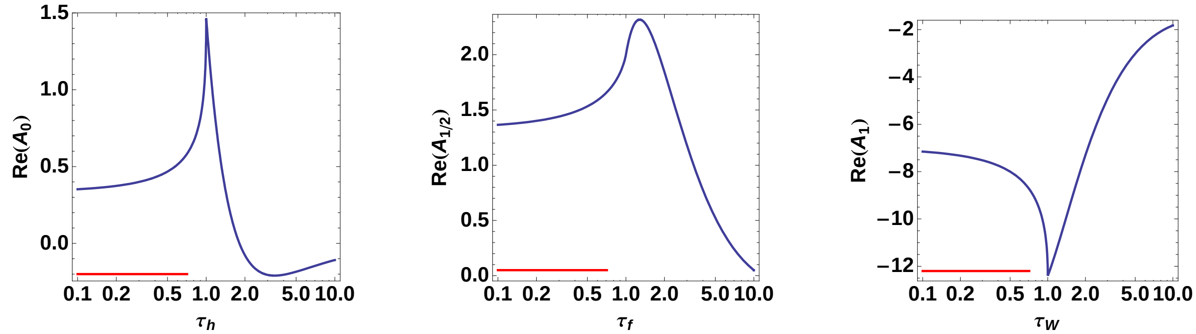

(a) The real part of the scalar form factor A_0 is plotted against τ_h.

(b) The real part of the fermionic form factor $A_{1/2}$ is plotted against τ_f.

(c) The real part of the bosonic form factor A_1 is plotted against τ_W.

Figure 9: The real parts of the scalar form factors A_0, $A_{1/2}$ and A_1 are plotted against τ_i. The region of interest for 100 GeV $\leq M_h \leq$ 160 GeV and $M_{H^\pm} \geq$ 95 GeV is marked in red.

should expect to get strong constraints from perturbative unitarity and vacuum stability. For a useful comparison we analyze the partial decay width normalized to its value in the SM:

$$R_{\gamma\gamma} = \frac{\Gamma(h \to \gamma\gamma)_{THDM}}{\Gamma(h \to \gamma\gamma)_{SM}}. \tag{174}$$

One then maximizes this rate, subject to the constraints from perturbative unitarity, vacuum stability, R_b and Δr. The first two constraints are particularly important since they depend directly on the potential. For the maximization procedure $M_h = 130$ GeV and $M_{H^\pm} = 100$ GeV unless stated otherwise. Also all particle masses are assumed to be lighter than 1 TeV. The maximization was done in Mathematica 6, using its three different maximization algorithms. While these algorithms do not prove that a certain point is a maximum for its region, they easily find the regions where the width is enhanced. One does so for each potential, discussing the differences.

8.1 IDM

As the lightest Higgs of the IDM behaves exactly like the SM Higgs when coupling to SM particles, we have $g_W = g_f = 1$ (which corresponds to $\alpha = 0$, $\beta = \pi/2$). Using the couplings of Sec. 11.3.3, we get

$$\Gamma(h \to \gamma\gamma) = \frac{G_\mu \alpha^2 M_h^3}{128\sqrt{2}\pi^3} \left| \sum_{f\in\{t,b\}} Q_f^2 N_c A_{1/2}(\tau_f) + A_1(\tau_W) + \frac{m_{11}^2 - M_{H^\pm}^2}{M_{H^\pm}^2} A_0(\tau_{H^\pm}) \right|^2. \tag{175}$$

We can have a negative or positive contribution of the IDM depending on the difference of $m_{11}^2 - M_{H^\pm}^2$. As $m_{11}^2 \geq 0$ (Sec. 2.3.1) and A_0 is negative, to get g_h negative we must have $m_{11} \ll M_{H^\pm}$. In this case however, $|g_h| \approx 1$, and therefore we get only a slight enhancement around 10% as shown in Fig. 10(a).

In the opposite case $m_{11} \gg M_{H^\pm}$ the partial width will decrease. The unitarity bound of

Sec. 7.2 tells us that in this case we have $m_{11} \leq 400$ GeV. In this case, the sign of g_h is positive, and decreases the partial width.

Furthermore, it is not possible that m_{11} gets too large if M_h is small because of the constraints from vacuum stability (14), which can be seen in Fig. 10(b).

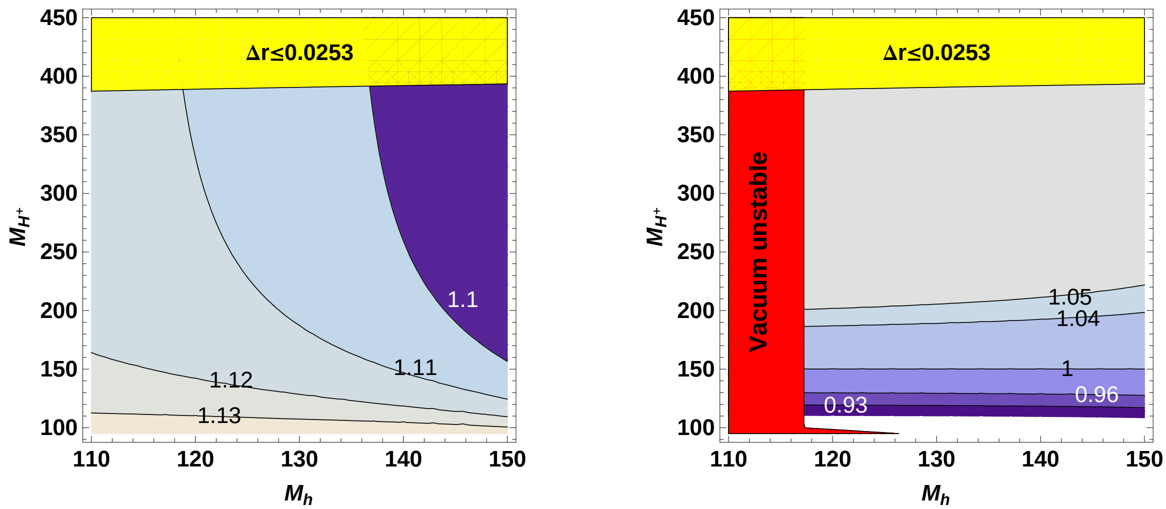

(a) $R_{\gamma\gamma}$ for $m_{11} = 0$. The enhancement is around 10%, increasing slightly for a light $M_{H^\pm}$.

(b) $R_{\gamma\gamma}$ for $m_{11} = 150$ GeV. We see that $R_{\gamma\gamma}$ decreases, if we rise m_{11}.

Figure 10: The partial decay width $\Gamma(h \to \gamma\gamma)$ of the IDM normalized to the SM value Γ_{IDM}/Γ_{SM}. The region for which the vacuum gets unstable at the tree-level is marked in red, while the region excluded by Δr is marked in yellow. The exclusion regions were calculated for $\lambda_1 = 0.75$, $M_H = 300$ GeV, $M_A = 100$ GeV. One sees that with rising m_{11}, the region excluded due to vacuum stability gets bigger as well.

8.2 Enhancement for V_A

Next we investigate the potential V_A defined in (4). Using the vertex coupling of Sec. 11.3, we then get for g_h

$$g_h = g_1 + g_2 \tag{176}$$

where

$$g_1 = s_{\beta-\alpha}\left(1 - \frac{M_h^2}{2M_{H^\pm}^2}\right) \tag{177}$$

$$g_2 = \frac{c_{\alpha+\beta}}{s_{2\beta}} \frac{M_h^2}{M_{H^\pm}^2}. \tag{178}$$

g_1 is positive except for a small charged scalar mass $M_{H^\pm}$. As due to LEP light charged scalars are excluded, we have $M_{H^\pm} \geq 95$ GeV, and therefore $|g_1| \lesssim 1$ for the considered range of M_h. Therefore we cannot expect large enhancement from g_1.

As g_2 is proportional to $M_h^2/M_{H^\pm}^2$, we should expect enhancement only for a light charged scalar $M_{H^\pm} \approx 100$ GeV. For this range, $\tan\beta \geq 3.3$ due to (122). Expanding the trigonometric functions, we see that

$$g_2 \propto \frac{1}{2}\left[\frac{c_\alpha}{s_\beta} - \frac{s_\alpha}{c_\beta}\right]. \tag{179}$$

Therefore only the term with $1/c_\beta$ may grow for large $\tan\beta$ values. The unitarity constraints of Sec. 7 tell us that in the case of V_A for light $M_h \approx 100$ GeV only $\tan\beta \leq 7$ are allowed. Then $g_2 \approx -4$ for $\tan\beta \approx 7$ and $\alpha = \pi/2$. Moreover, in this region the coupling to the gauge bosons gets small, $|\sin(\beta-\alpha)| \approx 0.1$, which results in $R_{\gamma\gamma}$ itself getting pretty small.

Employing the maximization procedure, we see that the partial decay width gets reduced compared to the SM, with typical maximal values $R_{\gamma\gamma} \approx 0.83$ for $M_h = 130$ GeV as shown in Figs. 11(a) and 11(b)[5].

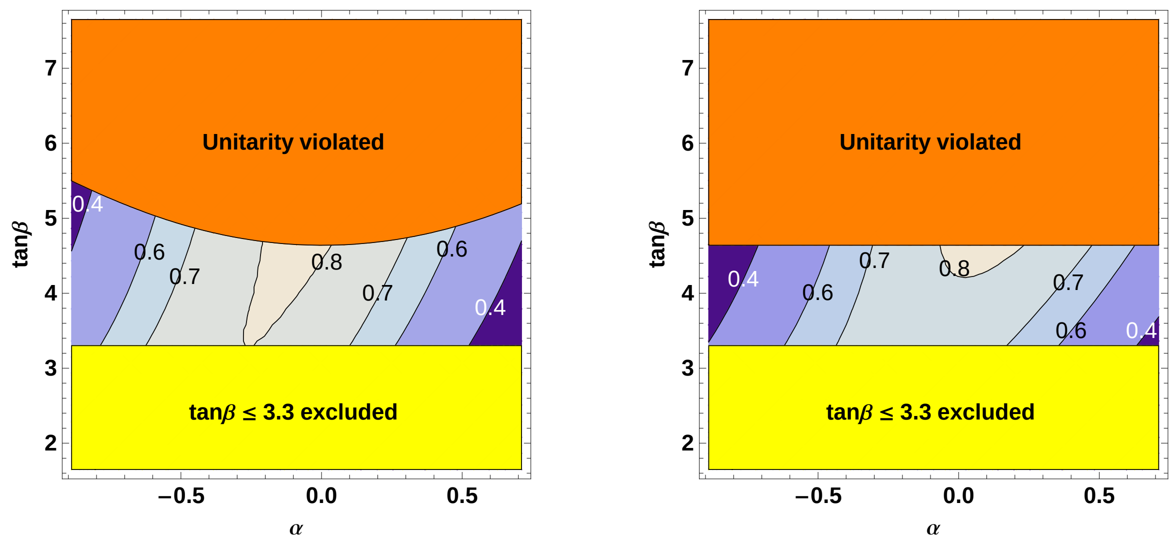

(a) $R_{\gamma\gamma}$ is shown for $M_h = 110$ GeV.

(b) $R_{\gamma\gamma}$ is shown for $M_h = 150$ GeV. Increasing M_h increases g_h and therefore reduces $R_{\gamma\gamma}$.

Figure 11: $R_{\gamma\gamma}$ analyzed for the V_A potential, for $M_{H^\pm} = 100$ GeV, $M_A = 100$ GeV, $M_H = 150$ GeV. We see that there is no enhancement, but a reduction compared to the SM. The region in orange is excluded due to perturbative unitarity, while the region in yellow is excluded due to the R_b constraint. The region is not forbidden by Δr or the vacuum stability conditions.

8.3 Enhancement for V_B

For the V_B potential we have

$$g_h = g_1 + g_2 + g_3 \tag{180}$$

[5]Note that even if one allows for heavy charged scalars with $M_{H^\pm} \approx 600$ GeV for V_A one still finds only $R_{\gamma\gamma} \approx 0.9$, and therefore the partial width is still smaller than the one of the SM

where g_1 and g_2 are as defined in (178) and the additional term g_3 which is

$$g_3 = -\frac{c_{\alpha+\beta}}{s_{2\beta}} \frac{M_A^2}{M_{H^\pm}^2}. \tag{181}$$

In this case, we can get large enhancement, provided $M_A \gg M_{H^\pm}$. g_3 has a very similar structure to g_2, except that now we have the opposite sign, and $M_h \to M_A$. This means we should expect large enhancement for small values of α. Unitarity and vacuum stability constraints are however quite restrictive for such large values of M_A and employing the maximization procedure, we may only get up to $R_{\gamma\gamma} \approx 1.6$ for a certain small region. This tiny region is shown in Fig. 12(a)

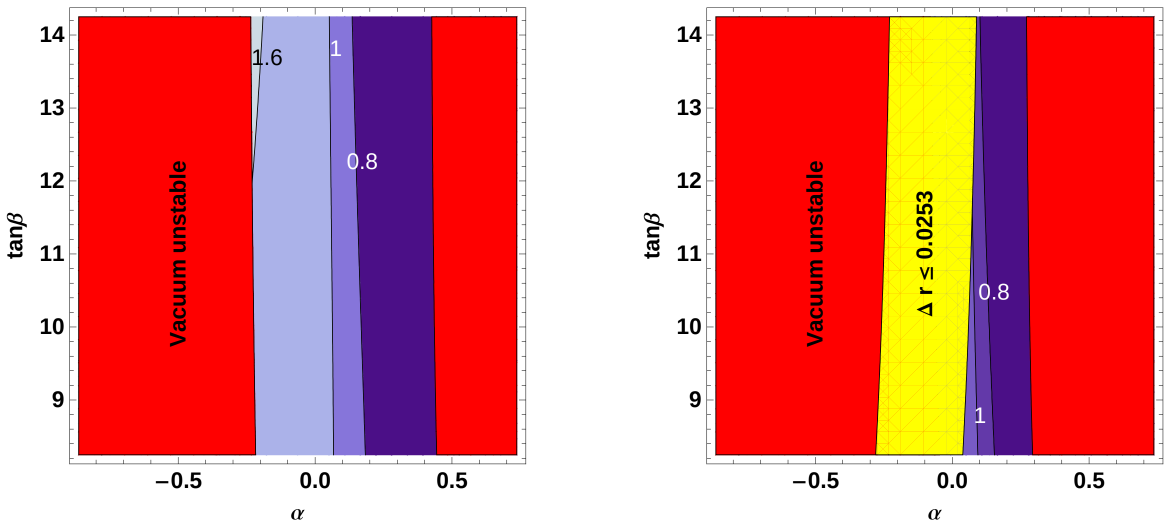

(a) $R_{\gamma\gamma}$ evaluated for $M_A = 200$ GeV and $M_H = 211$ GeV. The evaluation of Δr of this region can be seen in Fig. 2(a).

(b) $R_{\gamma\gamma}$ evaluated for $M_A = 265$ GeV and $M_H = 272$ GeV. The evaluation of Δr of this region can be seen in Fig. 2(b).

Figure 12: $R_{\gamma\gamma}$ analyzed for a V_B potential, for $M_h = 130$ GeV and $M_{H^\pm} = 100$ GeV. We see that $R_{\gamma\gamma} \approx 1.6$ is possible in the region displayed in Fig. 12(a). While increasing M_A does increase $R_{\gamma\gamma}$, it introduces a 2 σ forbidden region due to the electroweak precision test of Δr.

8.4 Enhancement for V_λ

At last we will study the V_λ potential, where m_{12}^2 is a free parameter. Again we have

$$g_h = g_1 + g_2 + g_3, \tag{182}$$

where g_1 and g_2 are again the parameters defined in (178). This time g_3 is not fixed via the masses, but is proportional to m_{12}^2:

$$g_3 = -\frac{c_{\alpha+\beta}}{2 s_\beta^2 c_\beta^2} \frac{m_{12}^2}{M_{H^\pm}^2}. \tag{183}$$

This means that the only difference to V_B is that we now have m_{12} instead of M_A. Therefore, compared to V_A one has one additional parameter in the potential. One might expect that due to the additional degree of freedom one should get a lot more space for fine-tuning and therefore a much stronger enhancement than in the V_B case. But as the constraints from unitarity, vacuum stability and Δr are quite restrictive the results are very similar to the V_B case. Typically one can find enhancement by around $R_{\gamma\gamma} \approx 1.6$ (Figs. 13(a), 13(b)), or $R_{\gamma\gamma} \approx 1.7$ in a much smaller region (Fig. 13(c)). Also note that the region displayed in Fig. 13(b) has rather low values of Δr, which are pretty close to the 2 σ exclusion limit.

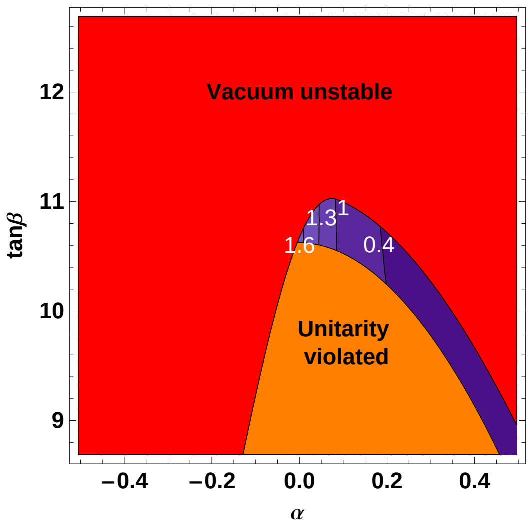

(a) $R_{\gamma\gamma}$ with $M_H = 111$ GeV, $M_A = 333$ GeV and $m_{12} = 100$ GeV. For the value of Δr in the displayed region see Fig. 3(a).

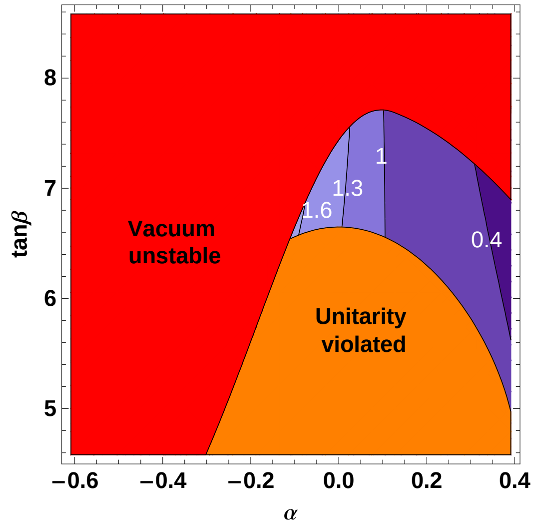

(b) $R_{\gamma\gamma}$ with $M_H = 279$ GeV and $M_A = 254$ GeV and $m_{12} = 100$ GeV. For the value of Δr in the displayed region see Fig. 3(b).

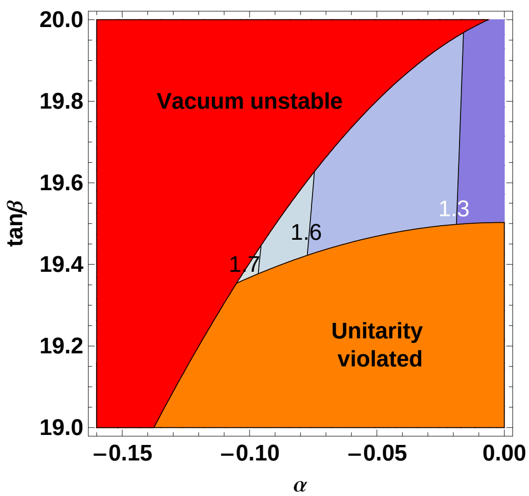

(c) $R_{\gamma\gamma}$ with $M_H = 224$ GeV, $M_A = 102$ GeV and $m_{12} = 50$ GeV. $\Delta r \approx 0.035$ in this region and therefore allowed.

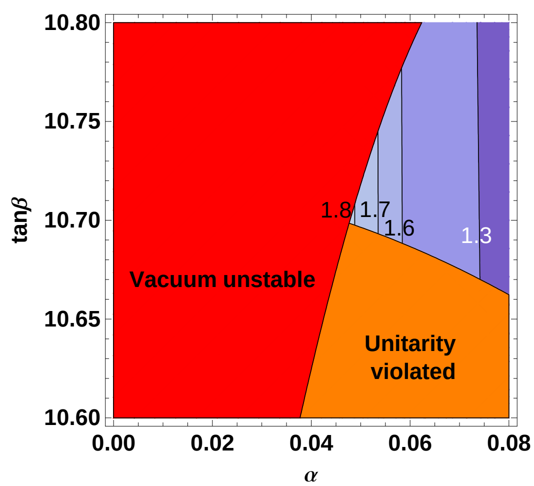

(d) $R_{\gamma\gamma}$ with $M_H = 496$ GeV, $M_A = 365$ GeV and $m_{12} = 150$ GeV. This region is completely excluded by Δr, which is approximately zero in this region.

Figure 13: $R_{\gamma\gamma}$ analyzed for the V_λ potential (5), for $M_h = 130$ GeV, $M_{H^\pm} = 100$ GeV. The region excluded by the unitarity bound is displayed in orange, the region excluded due to vacuum stability is displayed in red.

9 Analysis of the process at LHC

It is now reasonable to ask, whether deviations from the SM discussed in Sec. 8 could be studied at the LHC. At LHC the event rate for the process $h \to \gamma\gamma$ is

$$\frac{dN}{dt} = \mathcal{L}\sigma(pp \to h \to \gamma\gamma) \; , \tag{184}$$

where $\mathcal{L}$ is the collider luminosity. The LHC is designed to run at $\sqrt{s} \approx 14$ TeV with a luminosity of 100 fb^{-1} per year [1]. During its entire operation, one hopes to collect at least 300 fb^{-1} of data per experiment.

For 110 GeV $\leq M_h \leq$ 150 GeV in the SM, Higgs production is dominated by gluon fusion $\sigma(pp \to gg \to h)$, which is around $80 - 84\%$. The next important one is vector boson fusion, $\sigma(pp \to qqVV^\dagger \to qqh)$, which is around $10{-}12\%$ and associated production with W, Z bosons and $t\bar{t}$, which amount to another $6 - 8\%$ for this mass range. Ignoring interference effects, this adds up to

$$\frac{dN}{dt} = \mathcal{L}\left[\sigma(pp \to gg \to h \to \gamma\gamma) + \sigma(pp \to VV \to h \to \gamma\gamma) + \ldots\right] \; . \tag{185}$$

Integrating this over a certain time period, one gets the number of expected signal events of $h \to \gamma\gamma$. The number of events was studied in Ref. [59] for an integrated luminosity of 100 fb^{-1} and the combined statistical error given was 9.4% for a combined study at A Toroidal LHC ApparatuS (ATLAS) and Compact Muon Solenoid (CMS). Another more recent study finds 17% accuracy at CMS for only 30 fb^{-1} integrated luminosity [60]. This means that a deviation as described in Secs. 8.3 and 8.4 of the SM value of $\Gamma(h \to \gamma\gamma)$ can be measured at the LHC.

Let us first directly compare the event rate of the SM with the THDM. As a first approximation, we will only consider gluon gluon fusion at LO[6].

9.1 A LO comparison

At leading order, the cross section $\sigma_{LO}(pp \to h)$ in the narrow width approximation is particularly simple

$$\sigma_{LO}(pp \to h) = \sigma_0^h \tau_h \frac{d\mathcal{L}}{d\tau_h} \tag{186}$$

where for the THDM Type I σ_{LO} is just proportional to the squared coupling to fermions (as the couplings to the quarks are identical)

$$\sigma_0^h \propto g_{hff}^2 \tag{187}$$

and

$$\frac{d\mathcal{L}^{gg}}{d\tau} = \int_\tau^1 \frac{dx}{x} \; g(x, \mu_F^2) g(\tau/x, \mu_F^2) \tag{188}$$

[6] As the NLO contributions are around 40 % [1], this makes only sense for a qualitative discussion.

where $\tau_h = M_h^2/s$ and g are the parton densities, defined at the scale μ_F. Note that for the considered mass range

$$100 \text{ GeV} \leq M_h \leq 150 \text{ GeV} \tag{189}$$

the total width Γ_h is smaller than the Higgs boson mass M_h by 3 orders of magnitude. The Narrow Width Approximation is therefore reasonably satisfied. As the parton densities do not depend on the Higgs sector, the rate of the THDM compared to the rate of the SM is

$$Q_{THDM} = \frac{N_{THDM}}{N_{SM}} = g_{hff}^2 \frac{\Gamma^{THDM}(h \to \gamma\gamma)}{\Gamma^{SM}(h \to \gamma\gamma)} \frac{\Gamma^{SM}}{\Gamma^{THDM}} \ . \tag{190}$$

If we moreover have $g_{hff} \approx 1$ and $|\sin(\beta-\alpha)| \approx 1$, as the total decay width is dominated by decays into $b\bar{b}$ and WW^* in this region, we have $\Gamma^{SM} \approx \Gamma^{THDM}$, and therefore

$$Q_{THDM} = \frac{\Gamma^{THDM}(h \to \gamma\gamma)}{\Gamma^{SM}(h \to \gamma\gamma)} \ . \tag{191}$$

These assumptions are reasonably satisfied for the regions we plotted in the figures of Sec. 8. Another way is to consider a ratio of event numbers of two different decay channels.

9.2 A ratio of events

Another discovery channel for h in the mass range 120 GeV $\leq M_h \leq$ 150 GeV is the Higgs decay into one on-shell and one off-shell W boson $h \to WW^*$. While this might be suppressed in the THDM due to the couplings of Higgs to the W bosons $\sin(\beta - \alpha)$, it is not suppressed in our region of interest, where enhancement happens. Considering the event rate of $h \to \gamma\gamma$ and $h \to WW^*$ one gets

$$R_{\gamma/W} = \frac{N(h \to \gamma\gamma)}{N(h \to WW^*)} \approx \frac{\Gamma(h \to \gamma\gamma)}{\Gamma(h \to WW^*)} \ . \tag{192}$$

For this observable, there is no dependence on the production process, and therefore uncertainties arise solely from event statistics and detector efficiency. For this observable, one can get an accuracy of 11-16% in the mass range 120 GeV $\leq M_h \leq$ 150 GeV for an integrated luminosity of 200 fb^{-1}[59] [7]. While (192) does not depend on the branching ratios of these decays, the associated uncertainties due to statistics do. One therefore must again assume that the event rate of the THDM is not significantly smaller then in the SM by assuming $g_{hff} \approx 1$ and $\sin(\beta - \alpha) \approx 1$ to get the same accuracy as given in [59].

[7] Note that for smaller masses, the signal over background ratio gets much smaller resulting in a much larger uncertainty due to statistics.

10 Conclusion

We have discussed a possible enhancement of the partial decay width $\Gamma(h \to \gamma\gamma)$ in the THDM Type I for light charged scalars with $M_{H^\pm} \approx 100$ GeV. While for the Type II model light scalars can be excluded using the indirect constraint from $b \to s\gamma$, such a $\tan\beta$ independent exclusion is not possible in the Type I model due to the different Yukawa couplings. For this model $b \to s\gamma$ leads to a less powerful constraint, which excludes $\tan\beta \leq 1.9$ for $M_{H^\pm} = 100$ GeV (Sec. 6). Therefore, in the Type I model the most important constraint on the mass of the charged Higgs bosons comes from LEP, which is $M_{H^\pm} \geq 95$ GeV [24].

For light charged scalars one finds a much better constraint for $\tan\beta$ by considering the decays of the Z boson into hadrons: For $M_{H^\pm} \approx 100$ GeV, one finds that $\tan\beta \leq 3.3$ can be excluded (see Sec. 5.4).

The partial decay width $\Gamma(h \to \gamma\gamma)$ depends on the potential via the coupling of the neutral Higgs to the charged scalars. This means that a possible enhancement depends on the potential and its available parameter space. Therefore, restricting the parameter space of the THDM with constraints on the potential restricts a possible enhancement of $\Gamma(h \to \gamma\gamma)$. The most important direct constraints on the potential are perturbative unitarity (Sec. 7) and vacuum stability (Sec. 2). They are quite restrictive for large couplings and therefore were particularly important for our study. Other constraints considered were the aforementioned exclusion of $\tan\beta$ due to decays of the Z boson (Sec. 5.3), and constraints from Δr restricting the self energies of the vector bosons (Sec. 5.2). While these are not directly sensitive to the potential, they impose restrictions on the masses of the Higgs bosons and their couplings to the gauge bosons.

After introducing all these constraints we maximized $\Gamma(h \to \gamma\gamma)$ subject to them for light charged scalars $M_{H^\pm} \approx 100$ GeV in the $h \to \gamma\gamma$ discovery region of the LHC in the SM for 100 GeV $\leq M_h \leq$ 150 GeV (Sec. 8). The magnitude of possible enhancement was quite different for each potential considered. While for the IDM the maximal possible enhancement was found to be around 10% compared to the SM, for the potential V_A the partial width was at least 15% lower than the SM value. Results were rather similar for V_B and V_λ, where enhancement was around 60 % in the former case and around 70 % in the latter case. This is much larger than the 25 % found for V_λ for heavy charged scalars $M_{H^\pm} \approx 400$ GeV studied in Ref. [53]. As the accuracy of the LHC in determining $\sigma(pp \to h+X)\mathcal{B}(h \to \gamma\gamma)$ is around $10-20$%, one might be able to see a large enhancement, which we found to be possible for the potentials V_B and V_λ. Combining measurements at the photon collider option of the International Linear Collider (ILC) with the e^+e^- collider option, the accuracy of the partial width for a SM Higgs with $M_h = 120$ GeV can be determined with 3% accuracy [61]. This might enable one to distinguish even between the potentials V_B and V_λ.

11 Appendix

11.1 Conventions for the Passarino-Veltman functions

In our calculation of the amplitude for $b \to s\gamma$ we employed the analytic expressions of functions given in Ref. [62]. There the generic tensor integral is defined as:

$$\{\{\ldots\{k_\nu\ldots\}\ldots\}\} = \frac{1}{i}\int_{C_F}\frac{d^Dk}{(2\pi)^D}\frac{k_\nu\ldots}{[k^2-m_1^2][(k-p_a)^2-m_2^2][(k-p_b)^2-m_3^2]\ldots} \tag{193}$$

where each bracket $\{\}$ stands for one internal momentum and therefore

$$\text{number of brackets} = \text{number of propagators } -1 \; . \tag{194}$$

C_F stands for the Feynman prescription $m^2 \to m^2 - i\epsilon$. Using Passarino-Veltman reduction [20], one can reduce any one-loop tensor integral to one-loop scalar integrals. Employing the conventions of [62], we can reduce any expression like $\{\{k_\mu\ldots\}\}$ to scalar integrals. For integrals with 3 internal propagators we have

$$\begin{aligned}\{\{k_\mu\}\} &= p_{a\mu}\,C_{11a} + p_{b\mu}\,C_{11b}\\ \{\{k_\mu k_\nu\}\} &= g_{\mu\nu}\,C_{20} + p_{a\mu}p_{a\nu}\,C_{22a} + p_{b\mu}p_{b\nu}\,C_{22b} + (p_{a\mu}p_{b\nu}+p_{b\mu}p_{a\nu})\,\tilde{C}_{22}\end{aligned} \tag{195}$$

where C^U_{ij} takes the arguments $C^U_{ij}(p_a^2, p_b^2, (p_ap_b), m_1^2, m_2^2, m_3^2)$. One can find the exact analytical expressions in Ref. [62].
FeynArts uses a slightly different convention. It is therefore practical to know how to translate between these 2 conventions if one intends to compare analytic results with FeynArts. One finds the FeynArts convention in the LoopTools manual. There the generic tensor integral is defined as:

$$T^N_{\mu_1\ldots\mu_p} = \frac{(2\pi\mu)^{4-D}}{i\pi^2}\int_{C_F} d^Dq\frac{q_{\mu_1}\cdots q_{\mu_p}}{[q^2-m_1^2][(q+k_1)^2-m_2^2]\ldots[(q+k_{N-1})^2-m_N^2]} \tag{196}$$

where

$$k_j = \sum_{i=1}^{j} p_i \; . \tag{197}$$

The reduced scalar C functions are defined via the sums

$$\begin{aligned}(C^L)^\mu &= k_1^\mu C_1^L + k_2^\mu C_2^L\\ (C^L)^{\mu\nu} &= g^{\mu\nu}C^L_{00} + \sum_{i,j=1}^{2} k_i^\mu k_j^\nu C^L_{ij}\end{aligned} \tag{198}$$

where the functions take the arguments $C^L_n(p_1^2, p_2^2, (p_1+p_2)^2, m_1^2, m_2^2, m_3^2)$. If we want to translate this result into the convention of Ref. [62], we simply reparametrize (193) by setting $p_a = -p_1 = -k_1$, $p_b = -(p_1+p_2) = -k_2$ and $\mu = 1$ and get

$$C^L_\mu = (4\pi)^2 C^U_\mu$$

where C^L_μ takes the arguments $C^L_\mu(p_1^2, p_2^2, (p_1+p_2)^2, m_1^2, m_2^2, m_3^2)$ and C^U_μ takes $C^U_\mu(p_1^2, (p_1+p_2)^2, \frac{1}{2}[(p_1+p_2)^2+(p_1^2-p_2^2)], m_1^2, m_2^2, m_3^2)$. Using this together with (198) and (195) we get

$$k_1 C^L_1 + k_2 C^L_2 = (4\pi)^2 \left(-k_1 C^U_{11a} - k_2 C^U_{11b}\right) \ .$$

Equating the coefficients, we simply get

$$C^L_1 = -(4\pi)^2 C^U_{11a} \ , \qquad\qquad C^L_2 = -(4\pi)^2 C^U_{11b} \ , \tag{199}$$

where again $C^U(p_1^2, (p_1+p_2)^2, \frac{1}{2}[(p_1+p_2)^2+(p_1^2-p_2^2)], m_1^2, m_2^2, m_3^2)$. Analogous arguments can be applied for translating $C^L_{\mu\nu}$ into $C^U_{\mu\nu}$. In this case there is no relative minus and we simply get

$$C^L_{00} = (4\pi)^2 C^U_{20}, \quad C^L_{11} = (4\pi)^2 C^U_{22a}, \quad C^L_{22} = (4\pi)^2 C^U_{22b}, \quad C^L_{12} = (4\pi)^2 \tilde{C}^U_{22} \ . \tag{200}$$

In general there is a relative minus sign for tensor integrals with an odd number of momenta in the denominator, while there is a positive sign for an even number of momenta. The factor $(4\pi)^2$ is there in both cases. With the above, we can easily render a calculation of a matrix element M by FormCalc into an analytic result in the conventions of [62]. To give a particularly simple example of an analytical calculation of the functions in [20], we will calculate the B function for 2 equal masses.

11.2 1-loop integral with 2 propagators of equal mass M

When using dimensional regularization, we define the B function as follows:

$$B(p^2, M^2, M^2) = \frac{1}{i} \int \frac{d^dk}{(2\pi)^d} \frac{1}{(k^2 - M^2 + i\epsilon)[(k-p^2) - M^2 + i\epsilon]} \ . \tag{201}$$

Using Feynman parametrization, we get

$$\begin{aligned} B(p^2, M^2, M^2) &= \frac{1}{i} \int_0^1 dx \int \frac{d^dk}{(2\pi)^d} \frac{1}{\left[x(k^2 - M^2) + (1-x)((k-p)^2 - M^2) + i\epsilon\right]^2} = \\ &= \frac{1}{i} \int_0^1 dx \int \frac{d^dk}{(2\pi)^d} \frac{1}{(l^2 - \Delta)^2} \end{aligned} \tag{202}$$

with $l = k - (1-x)p$ and $\Delta = p^2(x^2 - x) + M^2 - i\epsilon$. After Wick rotation ($l^0 \to i l^0_E$) and expanding about $\epsilon = 4 - d$ we get:

$$\begin{aligned} B(p^2, M^2, M^2) &= \frac{1}{(4\pi)^2} \int_0^1 dx \left(\frac{2}{\epsilon} - \log\Delta - \gamma + \log(4\pi) \right) = \\ &= \frac{1}{(4\pi)^2} \int_0^1 dx \left(\frac{2}{\epsilon} - \left(\log\frac{\Delta}{\mu^2} + 1 \right) - 2\log\mu - \gamma + \log(4\pi) + 1 \right) \\ &= \frac{2}{(4\pi)^2} \int_0^1 (1 - \epsilon\log\mu) \left(\frac{1}{\epsilon} - \frac{1}{2}(\gamma - \log(4\pi) - 1) \right) \quad + \\ &\quad - \frac{1}{(4\pi)^2} \int_0^1 dx \left(1 + \log\frac{\Delta}{\mu^2} \right) \ . \end{aligned} \tag{203}$$

With partial integration, and writing $1 - \epsilon \log \mu = \mu^{-\epsilon}$ we get

$$B(p^2, M^2, M^2) = -2\Lambda(\mu) - \frac{1}{(4\pi)^2}\left(1 + \log\frac{M^2}{\mu^2}\right) + \frac{1}{(4\pi)^2}\int_0^1 \frac{2x^2 - x}{x^2 - x + \frac{M^2}{p^2} - i\epsilon}$$

$$\text{with } \Lambda(\mu) = \frac{1}{(4\pi)^2}\mu^{4-d}\left(\frac{1}{4-d} - \frac{1}{2}\left(\log 4\pi + 1 - \gamma\right)\right) \tag{204}$$

We now calculate the integral that gives the finite contributions.
If the denominator does not vanish (the roots of the polynomial in the denominator are complex) we can forget about the $i\epsilon$ term and calculate:

$$\overline{B}(p^2, M^2, M^2) = \frac{1}{(4\pi)^2}\int_0^1 \frac{2x^2 - x}{x^2 - x + r - i\epsilon} = \frac{1}{(4\pi)^2}\int_0^1 \frac{2x^2 - x}{(x-\lambda)(x-\overline{\lambda})} \tag{205}$$

where $r = \frac{M^2}{p^2}$ and $\lambda = 1/2(1 + \sqrt{1-4r}) = 1/2(1 + i\sqrt{4r-1})$. For $p^2 > 0$ the condition of having an imaginary denominator is equivalent to $p^2 < 4M^2$. In this case we have the roots λ and $\overline{\lambda}$ (complex conjugate). If $p^2 < 0$ then both roots will be real.

$$\begin{aligned}
\int \frac{x^2}{x^2 - x + r} &= \frac{1}{\lambda - \overline{\lambda}}\left(\lambda \int \frac{x}{x-\lambda} - \overline{\lambda}\int \frac{x}{x-\overline{\lambda}}\right) \\
&= \frac{1}{\lambda - \overline{\lambda}}\left(\lambda^2 \log(x-\lambda) - \overline{\lambda}^2 \log(x - \overline{\lambda})\right) + x \\
&= x + 2\Re(\lambda)\log|x-\lambda| + \frac{\Re(\lambda)^2 - \Im(\lambda)^2}{\Im(\lambda)}\arg(x-\lambda)
\end{aligned} \tag{206}$$

Note that this result is real again as it should be. As $\Im(x-\lambda) < 0$, the parameter of arg runs in the lower half of the complex plane. To get the values in a smooth way, we rotate the $(x-\lambda)$ by $\pi/2$ into the area of the complex plane, where $\arg(z) = \arctan(\Im(z)/\Re(z))$. Rotating the parameter we get $e^{i(\pi/2)}(x-\lambda) = \Im(\lambda) + i\Re(x-\lambda)$ and for our integral

$$\int \frac{x^2}{x^2 - x + r} = x + 2\Re(\lambda)\log|x-\lambda| + \frac{\Re(\lambda)^2 - \Im(\lambda)^2}{\Im(\lambda)}\left(\arctan\left(\frac{\Re(x-\lambda)}{\Im(\lambda)}\right) - \frac{\pi}{2}\right) . \tag{207}$$

With $w = \sqrt{|4r-1|}$ we therefore get

$$\begin{aligned}
\int_0^1 \frac{x^2}{x^2 - x + r} &= 1 + \frac{2-4r}{2w}\left(\arctan\left(\frac{1}{w}\right) - \arctan\left(\frac{-1}{w}\right)\right) \\
&= 1 + \frac{2-4r}{w}\arctan\left(\frac{1}{w}\right)
\end{aligned} \tag{208}$$

$$\begin{aligned}
\int_0^1 \frac{x}{x^2 - x + r} &= \frac{1}{\lambda - \overline{\lambda}}\left(\lambda\int\frac{1}{x-\lambda} - \overline{\lambda}\int\frac{1}{x-\overline{\lambda}}\right) \\
&= \log|x-\lambda| + \frac{\Re(\lambda)}{\Im(\lambda)}\left(\arctan\left(\frac{\Re(x-\lambda)}{\Im(\lambda)}\right) - \frac{\pi}{2}\right)
\end{aligned} \tag{209}$$

where we used the same rotation as before. Evaluating at our boundaries we get

$$\int_0^1 \frac{x}{x^2 - x + r} = \frac{2}{w} \arctan\left(\frac{1}{w}\right) \ . \tag{210}$$

Bringing both together yields

$$\int_0^1 \frac{2x^2 - x}{x^2 - x + r} = 2 - 2w \arctan\left(\frac{1}{w}\right) \ . \tag{211}$$

Let us now assume that the polynomial of the denominator has real roots. We again have two roots $r_1 = 1/2(1+\sqrt{1-4r})+i\epsilon = \lambda + i\epsilon$ and $r_2 = 1/2(1-\sqrt{1-4r})-i\epsilon = \lambda' - i\epsilon$. The propagators may now go on-shell. In this case, the $i\epsilon$ is not to be neglected. This is exactly the case if one of the roots is in the intervall $[0,1]$ which is equivalent to $w < 1 \leftrightarrow r > 0$. As this is not possible for $p^2 < 0$, we first assume $p^2 > 0$. To have real roots, we need $p^2 > 4M^2$. In this case we will always integrate over the range where $i\epsilon$ contributes. We can use the results we got before integration, with $\lambda \to r_1$ and $\overline{\lambda} \to r_2$. When doing the integration, we use the Sokhotsky-Weierstrass theorem $\frac{1}{x \pm i\epsilon} = P.V.\frac{1}{x} \mp i\pi\delta(x)$:

$$\begin{aligned}
\int_0^1 \frac{x}{x - r_1} = \int_0^1 \frac{x}{x - \lambda - i\epsilon} &= P.V. \int_0^1 \frac{x}{x-\lambda} + \int_0^1 x\delta(x-\lambda) \\
&= P.V. \int_0^1 \frac{x}{x-\lambda} + i\pi\lambda \ .
\end{aligned} \tag{212}$$

For the second root, we have the opposite sign of $i\epsilon$ and therefore we get:

$$\int_0^1 \frac{x}{x - r_2} = \int_0^1 \frac{x}{x - \lambda' + i\epsilon} = P.V. \int_0^1 \frac{x}{x - \lambda'} - i\pi\lambda' \ . \tag{213}$$

In the same way we calculate the other imaginary contribution

$$\Im\left(\int_0^1 \frac{x}{x^2 - x + r}\right) = \pi\frac{\lambda + \lambda'}{\lambda - \lambda'} \ . \tag{214}$$

In total we get

$$\Im\left(\int_0^1 \frac{2x^2 - x}{x^2 - x + r}\right) = \frac{\pi}{\lambda - \lambda'}\left(2(\lambda^2 + \lambda'^2) - (\lambda + \lambda')\right) = \pi w \ . \tag{215}$$

The calculation of the integrals for the real roots is very similar to the case with the complex poles. We finally get:

$$\begin{aligned}
\Re\left(\int_0^1 \frac{2x^2 - x}{x^2 - x + r}\right) &= 2 + \frac{2(\lambda^2 + \lambda'^2) - (\lambda + \lambda')}{\lambda - \lambda'} \log\frac{|\lambda'|}{|\lambda|} \\
&= 2 + \frac{2}{w}\log\frac{|1-w|}{|1+w|} \ .
\end{aligned} \tag{216}$$

As for $p^2 < 0$ we get the same result, just without the real part, we can write our result for the real roots in the following compact way:

$$\overline{B}(p^2, M^2, M^2) = \frac{1}{(4\pi)^2}\left(w \log\left|\frac{1-w}{1+w}\right| + 2 + i\pi w \Theta(p^2)\right) \tag{217}$$

and for the complex roots

$$\overline{B}(p^2, M^2, M^2) = \frac{1}{(4\pi)^2}\left(-2w \arctan\left(\frac{1}{w}\right) + 2\right) \tag{218}$$

with $w = \sqrt{|1-4r|}$. An interesting special case is $p^2 = 0$. We then have:

$$B(0, M^2, M^2) = -2\Lambda(\mu) - \frac{1}{(4\pi)^2}\left(1 + \log\frac{M^2}{\mu^2}\right) \ . \tag{219}$$

A further interesting special case to consider is $B(0, M_P^2, M_Q^2)$, for which we get:

$$B(0, M_P^2, M_Q^2) = -2\Lambda(\mu) + \frac{\bar{A}(M_P^2) - \bar{A}(M_Q^2)}{M_P^2 - M_Q^2} \ . \tag{220}$$

11.3 The couplings of the potentials

We list the vertex couplings of the Lagrangian of the Higgs sector for various potentials. We will only list the couplings of the most general CP-conserving case (5) and the IDM. One can get the potential V_A (4) by simply setting $m_{12}^2 = 0$, and V_B (31) by setting $m_{12}^2 = M_A^2 s_{2\beta}/2$. This obviously leads to different phenomenology. The most general CP-conserving potential (5) was implemented in FeynArts [16] and its Feynman rules were verified (A comparison with the FeynArts model file THDM.mod was done). To get the Feynman rules, as usual just multiply each coupling by the number of permutations of identical particles and the imaginary unit i.

11.3.1 Trilinear couplings - V_λ

We first give the trilinear couplings of the most general CP-conserving potential V_λ:

$$\begin{aligned}
g_{A^2h} &= \frac{g}{32M_W c_\beta^2 s_\beta^2}\left((2M_A^2-M_h^2)c_{\alpha-3\beta}s_{2\beta}+c_{\alpha+\beta}\left(8m_{12}^2-(2M_A^2+3M_h^2)s_{2\beta}\right)\right)\\
g_{AG^0h} &= \frac{g}{2M_W}(M_A^2-M_h^2)c_{\alpha-\beta}\\
g_{G^{02}h} &= \frac{g}{4M_W}M_h^2 s_{\alpha-\beta}\\
g_{G^-G^+h} &= \frac{g}{2M_W}M_h^2 s_{\alpha-\beta}\\
g_{h^3} &= \frac{g}{64M_W c_\beta^2 s_\beta^2}\left(16m_{12}^2 c_{\alpha+\beta}c_{\alpha-\beta}^2+M_h^2\left(3s_{\alpha-\beta}+s_{3(\alpha-\beta)}-s_{3\alpha+\beta}-3s_{\alpha+3\beta}\right)\right)\\
g_{A^2H} &= \frac{g}{32M_W c_\beta^2 s_\beta^2}\left((2M_A^2-M_H^2)s_{\alpha-3\beta}s_{2\beta}+\left(8m_{12}^2-(2M_A^2+3M_H^2)s_{2\beta}\right)s_{\alpha+\beta}\right)\\
g_{AG^0H} &= \frac{g}{2M_W}(M_A^2-M_H^2)s_{\alpha-\beta}\\
g_{G^{02}H} &= -\frac{g}{4M_W}M_H^2 c_{\alpha-\beta}\\
g_{G^-G^+H} &= -\frac{g}{2M_W}M_H^2 c_{\alpha-\beta}\\
g_{h^2H} &= \frac{g}{4M_W c_\beta s_\beta}c_{\alpha-\beta}\left(-m_{12}^2-c_\alpha s_\alpha\left(-\frac{3m_{12}^2}{c_\beta s_\beta}+2M_h^2+M_H^2\right)\right)\\
g_{hH^2} &= \frac{g}{4M_W s_{2\beta}}s_{\alpha-\beta}\left(2m_{12}^2-s_{2\alpha}\left(-\frac{3m_{12}^2}{c_\beta s_\beta}+M_h^2+2M_H^2\right)\right)\\
g_{H^3} &= \frac{g}{64M_W c_\beta^2 s_\beta^2}\left(16m_{12}^2 s_{\alpha+\beta}s_{\alpha-\beta}^2+M_H^2\left(-3c_{\alpha-\beta}+c_{3(\alpha-\beta)}-c_{3\alpha+\beta}+3c_{\alpha+3\beta}\right)\right)\\
g_{AG^+H^-} &= -\frac{ig}{2M_W}(M_A^2-M_{H^\pm}^2)\\
g_{G^+hH^-} &= -\frac{g}{2M_W}(M_h^2-M_{H^\pm}^2)c_{\alpha-\beta}\\
g_{G^+HH^-} &= -\frac{g}{2M_W}(M_H^2-M_{H^\pm}^2)s_{\alpha-\beta}\\
g_{AG^-H^+} &= -\frac{ig}{2M_W}(M_{H^\pm}^2-M_A^2)\\
g_{G^-hH^+} &= -\frac{g}{2M_W}(M_h^2-M_{H^\pm}^2)c_{\alpha-\beta}\\
g_{G^-HH^+} &= -\frac{g}{2M_W}(M_H^2-M_{H^\pm}^2)s_{\alpha-\beta}\\
g_{hH^-H^+} &= -\frac{g}{16M_W c_\beta^2 s_\beta^2}\left((M_h^2-2M_{H^\pm}^2)c_{\alpha-3\beta}s_{2\beta}+c_{\alpha+\beta}\left((3M_h^2+2M_{H^\pm}^2)s_{2\beta}-8m_{12}^2\right)\right)\\
g_{HH^-H^+} &= -\frac{g}{16M_W c_\beta^2 s_\beta^2}\left((M_H^2-2M_{H^\pm}^2)s_{\alpha-3\beta}s_{2\beta}+\left((3M_H^2+2M_{H^\pm}^2)s_{2\beta}-8m_{12}^2\right)s_{\alpha+\beta}\right)
\end{aligned}$$

11.3.2 Quartic couplings - V_λ

$$g_{A^4} = -\frac{g^2}{256M_W^2}\left(\frac{(M_h^2-M_H^2)c_{2\alpha}\left(15c_{2\beta}+c_{6\beta}\right)}{s_{2\beta}^2}+2\left(-\frac{32m_{12}^2\mathrm{ct}_{2\beta}^2}{s_{2\beta}}+\right.\right.$$
$$\left.\left.+2(M_H^2-M_h^2)s_{2\alpha}s_{2\beta}+\frac{(M_h^2+M_H^2)\left(3c_{4\beta}+5\right)}{s_{2\beta}^2}\right)\right)$$
$$g_{A^3G^0} = -\frac{g^2}{32M_W^2}\left(\frac{(M_h^2-M_H^2)\left(3c_{2\alpha}+c_{2(\alpha-2\beta)}\right)}{s_{2\beta}}+4\mathrm{ct}_{2\beta}\left(-\frac{4m_{12}^2}{s_{2\beta}}+M_h^2+M_H^2\right)\right)$$
$$g_{A^2G^{02}} = \frac{g^2}{128M_W^2c_\beta s_\beta}\left(16m_{12}^2+(M_h^2-M_H^2)\left(s_{2\alpha}+3s_{2(\alpha-2\beta)}\right)-6(M_h^2+M_H^2)s_{2\beta}\right)$$
$$g_{AG^{03}} = \frac{g^2}{16M_W^2}(M_h^2-M_H^2)s_{2(\alpha-\beta)}$$
$$g_{G^{04}} = -\frac{g^2}{64M_W^2}\left(M_h^2+M_H^2+(M_H^2-M_h^2)c_{2(\alpha-\beta)}\right)$$
$$g_{A^2G^-G^+} = \frac{g^2}{64M_W^2c_\beta s_\beta}\left(16m_{12}^2+(M_h^2-M_H^2)\left(3s_{2\alpha}+s_{2(\alpha-2\beta)}\right)+\right.$$
$$\left.-2(M_h^2+M_H^2+4M_{H^\pm}^2)s_{2\beta}\right)$$
$$g_{AG^-G^0G^+} = \frac{g^2}{8M_W^2}(M_h^2-M_H^2)s_{2(\alpha-\beta)}$$
$$g_{G^-G^{02}G^+} = -\frac{g^2}{16M_W^2}\left(M_h^2+M_H^2+(M_H^2-M_h^2)c_{2(\alpha-\beta)}\right)$$
$$g_{G^{-2}G^{+2}} = -\frac{g^2}{16M_W^2}\left(M_h^2+M_H^2+(M_H^2-M_h^2)c_{2(\alpha-\beta)}\right)$$
$$g_{A^2h^2} = -\frac{g^2}{16M_W^2}\left(M_h^2\mathrm{ct}_\beta^2c_\alpha^4+(M_H^2-M_h^2)s_\alpha t_\beta c_\alpha^3+\left(-m_{12}^2\mathrm{ct}_\beta^3+M_H^2s_\alpha^2\mathrm{ct}_\beta^2+\right.\right.$$
$$\left.+2M_A^2s_\beta^2+t_\beta\left(M_H^2s_\alpha^2t_\beta-m_{12}^2\right)\right)c_\alpha^2+$$
$$+s_\alpha\left((M_H^2-M_h^2)\mathrm{ct}_\beta s_\alpha^2+4\left(m_{12}^2-M_A^2c_\beta s_\beta\right)\right)c_\alpha+$$
$$\left.s_\alpha^2\left(2M_A^2c_\beta^2+M_h^2s_\alpha^2t_\beta^2-m_{12}^2\left(t_\beta^3+\mathrm{ct}_\beta\right)\right)\right)$$
$$g_{AG^0h^2} = \frac{g^2}{128M_W^2c_\beta^2s_\beta^2}c_{\alpha-\beta}\left(8m_{12}^2c_{\alpha-3\beta}+8m_{12}^2c_{\alpha+\beta}\right.$$
$$\left.-2\left(2M_A^2c_{\alpha-3\beta}+(M_h^2-M_H^2)c_{3\alpha-\beta}+(-2M_A^2+3M_h^2+M_H^2)c_{\alpha+\beta}\right)s_{2\beta}\right)$$
$$g_{G^{02}h^2} = \frac{g^2}{128M_W^2c_\beta s_\beta}\left(8c_{2(\alpha-\beta)}m_{12}^2+8m_{12}^2-2(M_A^2-M_h^2+M_H^2)s_{2\alpha}+2M_A^2s_{2(\alpha-2\beta)}+\right.$$
$$\left.+(M_h^2-M_H^2)s_{4\alpha-2\beta}-(4M_A^2+3M_h^2+M_H^2)s_{2\beta}\right)$$
$$g_{G^-G^+h^2} = \frac{g^2}{64M_W^2c_\beta s_\beta}\left(8c_{2(\alpha-\beta)}m_{12}^2+8m_{12}^2+2(M_h^2-M_H^2-M_{H^\pm}^2)s_{2\alpha}+2M_{H^\pm}^2s_{2(\alpha-2\beta)}+\right.$$
$$\left.+(M_h^2-M_H^2)s_{4\alpha-2\beta}-(3M_h^2+M_H^2+4M_{H^\pm}^2)s_{2\beta}\right)$$

$$g_{h^4} = -\frac{g^2}{32M_W^2}\left(\frac{M_h^2 c_\alpha^6}{s_\beta^2} + \frac{\left(M_H^2 s_\alpha^2 - m_{12}^2 \mathrm{ct}_\beta\right) c_\alpha^4}{s_\beta^2} + \frac{4(M_H^2 - M_h^2) s_\alpha^3 c_\alpha^3}{s_{2\beta}} + \right.$$
$$\left. + s_\alpha^2 \left(\frac{\frac{M_H^2 s_\alpha^2}{c_\beta} + \frac{4m_{12}^2}{s_\beta}}{c_\beta} - \frac{4m_{12}^2}{s_{2\beta}}\right) c_\alpha^2 + \frac{s_\alpha^4 \left(M_h^2 s_\alpha^2 - m_{12}^2 t_\beta\right)}{c_\beta^2}\right)$$

$$g_{A^2hH} = \frac{g^2}{64M_W^2}\left(-\frac{\left(M_h^2 - M_H^2\right)\left(c_{4\beta} + 3\right) s_{4\alpha}}{s_{2\beta}^2} + 8c_{2\alpha}\left(2m_{12}^2 - M_A^2 s_{2\beta}\right) + \right.$$
$$+ 2\mathrm{ct}_{2\beta}\Bigg(- M_h^2 + M_H^2 + (M_h^2 - M_H^2) c_{4\alpha} +$$
$$\left.\left. + \frac{s_{2\alpha}\left(3M_A^2 - 4(M_h^2 + M_H^2) + \frac{4m_{12}^2\left(c_{4\beta}+3\right) - M_A^2 s_{6\beta}}{s_{2\beta}}\right)}{s_{2\beta}}\right)\right)$$

$$g_{AG^0hH} = -\frac{g^2}{16M_W^2}\Bigg[M_h^2 - M_H^2 + (M_H^2 - M_h^2) c_{4\alpha} - 4c_{2\alpha}\left(M_A^2 c_{2\beta} - 2m_{12}^2 \mathrm{ct}_{2\beta}\right) +$$
$$+ (M_h^2 - M_H^2)\mathrm{ct}_{2\beta} s_{4\alpha} + 2s_{2\alpha}\left(\frac{c_{4\beta} M_A^2 - M_A^2 + M_h^2 + M_H^2}{s_{2\beta}} - 4m_{12}^2 \mathrm{ct}_{2\beta}^2\right)\Bigg]$$

$$g_{G^{02}hH} = \frac{g^2}{32M_W^2 c_\beta s_\beta} s_{2(\alpha-\beta)}\left(4m_{12}^2 + (M_h^2 - M_H^2) s_{2\alpha} - 2M_A^2 s_{2\beta}\right)$$

$$g_{G^-G^+hH} = \frac{g^2}{16M_W^2 c_\beta s_\beta} s_{2(\alpha-\beta)}\left(4m_{12}^2 + (M_h^2 - M_H^2) s_{2\alpha} - 2M_{H^\pm}^2 s_{2\beta}\right)$$

$$g_{h^3H} = -\frac{g^2}{16M_W^2 s_{2\beta}^2} c_{\alpha-\beta} s_{2\alpha}\left((M_h^2 - M_H^2) c_{3\alpha-\beta} + c_{\alpha+\beta}\left(-\frac{8m_{12}^2}{s_{2\beta}} + 3M_h^2 + M_H^2\right)\right)$$

$$g_{A^2H^2} = -\frac{g^2}{16M_W^2}\left(M_H^2 t_\beta^2 c_\alpha^4 + (M_H^2 - M_h^2)\mathrm{ct}_\beta s_\alpha c_\alpha^3 + \left(2M_A^2 c_\beta^2 + M_h^2 \mathrm{ct}_\beta^2 s_\alpha^2 - m_{12}^2 \mathrm{ct}_\beta + \right.\right.$$
$$\left. + t_\beta^2\left(M_h^2 s_\alpha^2 - m_{12}^2 t_\beta\right)\right) c_\alpha^2 + s_\alpha\left(\left(M_H^2 - M_h^2\right) s_\alpha^2 t_\beta - 4m_{12}^2\right) c_\alpha + M_A^2 s_{2\alpha} s_{2\beta}$$
$$\left. + s_\alpha^2\left(-m_{12}^2 \mathrm{ct}_\beta^3 + M_H^2 s_\alpha^2 \mathrm{ct}_\beta^2 + 2M_A^2 s_\beta^2 - m_{12}^2 t_\beta\right)\right)$$

$$g_{AG^0H^2} = -\frac{g^2}{16M_W^2 s_{2\beta}} s_{\alpha-\beta}\Bigg(2M_A^2 s_{\alpha-3\beta} - 8m_{12}^2 \mathrm{ct}_{2\beta} s_{\alpha-\beta} + (M_h^2 - M_H^2) s_{3\alpha-\beta} +$$
$$+ (-2M_A^2 + M_h^2 + 3M_H^2) s_{\alpha+\beta}\Bigg)$$

$$g_{G^{02}H^2} = -\frac{g^2}{128M_W^2 c_\beta s_\beta}\left(8c_{2(\alpha-\beta)} m_{12}^2 - 8m_{12}^2 - 2(M_A^2 + M_h^2 - M_H^2) s_{2\alpha} + 2M_A^2 s_{2(\alpha-2\beta)} + \right.$$
$$\left. + (M_h^2 - M_H^2) s_{4\alpha-2\beta} + (4M_A^2 + M_h^2 + 3M_H^2) s_{2\beta}\right)$$

$$g_{G^-G^+H^2} = -\frac{g^2}{64M_W^2 c_\beta s_\beta}\left(8c_{2(\alpha-\beta)} m_{12}^2 - 8m_{12}^2 - 2(M_h^2 - M_H^2 + M_{H^\pm}^2) s_{2\alpha} + 2M_{H^\pm}^2 s_{2(\alpha-2\beta)} + \right.$$
$$\left. + (M_h^2 - M_H^2) s_{4\alpha-2\beta} + (M_h^2 + 3M_H^2 + 4M_{H^\pm}^2) s_{2\beta}\right)$$

$$
\begin{aligned}
g_{h^2H^2} &= -\frac{g^2}{128M_W^2 s_{2\beta}}\left(2s_{2\alpha}\left(-M_h^2+M_H^2+\frac{3\left(2(M_h^2+M_H^2)s_{2\alpha}+(M_h^2-M_H^2)s_{4\alpha-2\beta}\right)}{s_{2\beta}}\right)+\right.\\
&\left.-\frac{8m_{12}^2\left(-3c_{4\alpha}+c_{4\beta}+2\right)}{s_{2\beta}^2}\right)\\
g_{hH^3} &= -\frac{g^2}{16M_W^2 s_{2\beta}^2}s_{2\alpha}s_{\alpha-\beta}\left((M_h^2-M_H^2)s_{3\alpha-\beta}+\left(-\frac{8m_{12}^2}{s_{2\beta}}+M_h^2+3M_H^2\right)s_{\alpha+\beta}\right)\\
g_{H^4} &= -\frac{g^2}{32M_W^2}\left(\frac{M_H^2c_\alpha^6}{c_\beta^2}+\frac{\left(M_h^2s_\alpha^2-m_{12}^2t_\beta\right)c_\alpha^4}{c_\beta^2}+\frac{4(M_H^2-M_h^2)s_\alpha^3c_\alpha^3}{s_{2\beta}}+\right.\\
&\left.+s_\alpha^2\left(\frac{\frac{M_h^2s_\alpha^2}{s_\beta}+\frac{4m_{12}^2}{c_\beta}}{s_\beta}-\frac{4m_{12}^2}{s_{2\beta}}\right)c_\alpha^2+\frac{s_\alpha^4\left(M_H^2s_\alpha^2-m_{12}^2\mathrm{ct}_\beta\right)}{s_\beta^2}\right)\\
g_{A^2G^+H^-} &= -\frac{g^2}{32M_W^2}\left(\frac{\left(M_h^2-M_H^2\right)\left(3c_{2\alpha}+c_{2(\alpha-2\beta)}\right)}{s_{2\beta}}+4\mathrm{ct}_{2\beta}\left(-\frac{4m_{12}^2}{s_{2\beta}}+M_h^2+M_H^2\right)\right)\\
g_{AG^0G^+H^-} &= -\frac{g^2}{8M_W^2}\left(M_h^2+M_H^2-2M_{H^\pm}^2+(M_h^2-M_H^2)c_{2(\alpha-\beta)}\right)\\
g_{G^{02}G^+H^-} &= \frac{g^2}{16M_W^2}(M_h^2-M_H^2)s_{2(\alpha-\beta)}\\
g_{G^-G^{+2}H^-} &= \frac{g^2}{8M_W^2}(M_h^2-M_H^2)s_{2(\alpha-\beta)}\\
g_{AG^+hH^-} &= -\frac{ig^2}{4M_W^2}(M_{H^\pm}^2-M_A^2)s_{\alpha-\beta}\\
g_{G^0G^+hH^-} &= -\frac{ig^2}{4M_W^2}(M_{H^\pm}^2-M_A^2)c_{\alpha-\beta}\\
g_{G^+h^2H^-} &= \frac{g^2}{64M_W^2c_\beta^2s_\beta^2}c_{\alpha-\beta}\left((M_H^2-M_h^2)c_{3\alpha-\beta}s_{2\beta}+c_{\alpha+\beta}\left(4m_{12}^2-(3M_h^2+M_H^2-2M_{H^\pm}^2)s_{2\beta}\right)+\right.\\
&\left.+\ c_{\alpha-3\beta}\left(4m_{12}^2-2M_{H^\pm}^2s_{2\beta}\right)\right)\\
g_{AG^+HH^-} &= -\frac{ig^2}{4M_W^2}(M_A^2-M_{H^\pm}^2)c_{\alpha-\beta}\\
g_{G^0G^+HH^-} &= -\frac{ig^2}{4M_W^2}(M_{H^\pm}^2-M_A^2)s_{\alpha-\beta}\\
g_{G^+hHH^-} &= -\frac{g^2}{16M_W^2}\left(M_h^2-M_H^2+(M_H^2-M_h^2)c_{4\alpha}-4c_{2\alpha}\left(M_{H^\pm}^2c_{2\beta}-2m_{12}^2\mathrm{ct}_{2\beta}\right)+\right.\\
&\left.+\ (M_h^2-M_H^2)\mathrm{ct}_{2\beta}s_{4\alpha}+2s_{2\alpha}\left(\frac{M_h^2+M_H^2-M_{H^\pm}^2+M_{H^\pm}^2c_{4\beta}}{s_{2\beta}}-4m_{12}^2\mathrm{ct}_{2\beta}^2\right)\right)
\end{aligned}
$$

$$g_{G^+H^2H^-} = \frac{g^2}{16M_W^2}s_{\alpha-\beta}\left(4M_{H^\pm}^2c_{\alpha-\beta} + \frac{8m_{12}^2\mathrm{ct}_{2\beta}s_{\alpha-\beta} + (M_H^2-M_h^2)s_{3\alpha-\beta} - (M_h^2+3M_H^2)s_{\alpha+\beta}}{s_{2\beta}}\right)$$

$$g_{G^{+2}H^{-2}} = -\frac{g^2}{16M_W^2}\left(-2M_A^2 + M_h^2 + M_H^2 + (M_h^2-M_H^2)c_{2(\alpha-\beta)}\right)$$

$$g_{A^2G^-H^+} = -\frac{g^2}{32M_W^2}\left(\frac{(M_h^2-M_H^2)\left(3c_{2\alpha}+c_{2(\alpha-2\beta)}\right)}{s_{2\beta}} + 4\mathrm{ct}_{2\beta}\left(-\frac{4m_{12}^2}{s_{2\beta}} + M_h^2 + M_H^2\right)\right)$$

$$g_{AG^-G^0H^+} = -\frac{g^2}{8M_W^2}\left(M_h^2 + M_H^2 - 2M_{H^\pm}^2 + (M_h^2-M_H^2)c_{2(\alpha-\beta)}\right)$$

$$g_{G^-G^{02}H^+} = \frac{g^2}{16M_W^2}(M_h^2-M_H^2)s_{2(\alpha-\beta)}$$

$$g_{G^{-2}G^+H^+} = \frac{g^2}{8M_W^2}(M_h^2-M_H^2)s_{2(\alpha-\beta)}$$

$$g_{AG^-hH^+} = -\frac{ig^2}{4M_W^2}(M_A^2-M_{H^\pm}^2)s_{\alpha-\beta}$$

$$g_{G^-G^0hH^+} = -\frac{ig^2}{4M_W^2}(M_A^2-M_{H^\pm}^2)c_{\alpha-\beta}$$

$$\begin{aligned} g_{G^-h^2H^+} = {} & \frac{g^2}{64M_W^2c_\beta^2s_\beta^2}c_{\alpha-\beta}\left((M_H^2-M_h^2)c_{3\alpha-\beta}s_{2\beta} + c_{\alpha+\beta}\left(4m_{12}^2 - (3M_h^2+M_H^2-2M_{H^\pm}^2)s_{2\beta}\right) + \right. \\ & \left. + \; c_{\alpha-3\beta}\left(4m_{12}^2 - 2M_{H^\pm}^2s_{2\beta}\right)\right) \end{aligned}$$

$$g_{AG^-HH^+} = -\frac{ig^2}{4M_W^2}(M_{H^\pm}^2-M_A^2)c_{\alpha-\beta}$$

$$g_{G^-G^0HH^+} = -\frac{ig^2}{4M_W^2}(M_A^2-M_{H^\pm}^2)s_{\alpha-\beta}$$

$$\begin{aligned} g_{G^-hHH^+} = {} & -\frac{g^2}{16M_W^2}\left(M_h^2 - M_H^2 + (M_H^2-M_h^2)c_{4\alpha} - 4c_{2\alpha}\left(M_{H^\pm}^2c_{2\beta} - 2m_{12}^2\mathrm{ct}_{2\beta}\right) + \right. \\ & \left. + \; (M_h^2-M_H^2)\mathrm{ct}_{2\beta}s_{4\alpha} + 2s_{2\alpha}\left(\frac{M_h^2+M_H^2-M_{H^\pm}^2+M_{H^\pm}^2c_{4\beta}}{s_{2\beta}} - 4m_{12}^2\mathrm{ct}_{2\beta}^2\right)\right) \end{aligned}$$

$$g_{G^-H^2H^+} = \frac{g^2}{16M_W^2}s_{\alpha-\beta}\left(4M_{H^\pm}^2c_{\alpha-\beta} + \frac{8m_{12}^2\mathrm{ct}_{2\beta}s_{\alpha-\beta} + (M_H^2-M_h^2)s_{3\alpha-\beta} - (M_h^2+3M_H^2)s_{\alpha+\beta}}{s_{2\beta}}\right)$$

$$\begin{aligned} g_{A^2H^-H^+} = {} & -\frac{g^2}{64M_W^2}\left(\frac{(M_h^2-M_H^2)c_{2\alpha}\left(15c_{2\beta}+c_{6\beta}\right)}{s_{2\beta}^2} + 2\left(-\frac{32m_{12}^2\mathrm{ct}_{2\beta}^2}{s_{2\beta}} + \right.\right. \\ & \left.\left. + \; 2(M_H^2-M_h^2)s_{2\alpha}s_{2\beta} + \frac{(M_h^2+M_H^2)\left(3c_{4\beta}+5\right)}{s_{2\beta}^2}\right)\right) \end{aligned}$$

$$g_{AG^0H^-H^+} = -\frac{g^2}{16M_W^2}\left(\frac{(M_h^2-M_H^2)\left(3c_{2\alpha}+c_{2(\alpha-2\beta)}\right)}{s_{2\beta}} + 4\mathrm{ct}_{2\beta}\left(-\frac{4m_{12}^2}{s_{2\beta}} + M_h^2 + M_H^2\right)\right)$$

$$g_{G^0{}^2 H^- H^+} = \frac{g^2}{64 M_W^2 c_\beta s_\beta}\left(16 m_{12}^2 + (M_h^2 - M_H^2)\left(3 s_{2\alpha} + s_{2(\alpha-2\beta)}\right) - 2(M_h^2 + M_H^2 + 4 M_{H^\pm}^2) s_{2\beta}\right)$$

$$g_{G^- G^+ H^- H^+} = \frac{g^2}{16 M_W^2 c_\beta s_\beta}\left(8 m_{12}^2 + (M_h^2 - M_H^2) s_{2\alpha} + (M_h^2 - M_H^2) s_{2(\alpha-2\beta)} - 2(M_A^2 + M_h^2 + M_H^2) s_{2\beta}\right)$$

$$\begin{aligned} g_{h^2 H^- H^+} = -\frac{g^2}{8 M_W^2}\Big(& M_h^2 \mathrm{ct}_\beta^2 c_\alpha^4 + (M_H^2 - M_h^2) s_\alpha t_\beta c_\alpha^3 + \big(-m_{12}^2 \mathrm{ct}_\beta^3 + M_H^2 s_\alpha^2 \mathrm{ct}_\beta^2 + 2 M_{H^\pm}^2 s_\beta^2 + \\ &+ t_\beta\left(M_H^2 s_\alpha^2 t_\beta - m_{12}^2\right)\big) c_\alpha^2 + s_\alpha\left((M_H^2 - M_h^2)\mathrm{ct}_\beta s_\alpha^2 + 4\left(m_{12}^2 - M_{H^\pm}^2 c_\beta s_\beta\right)\right) c_\alpha + \\ &+ s_\alpha^2\left(2 M_{H^\pm}^2 c_\beta^2 + M_h^2 s_\alpha^2 t_\beta^2 - m_{12}^2\left(t_\beta^3 + \mathrm{ct}_\beta\right)\right)\Big) \end{aligned}$$

$$\begin{aligned} g_{hHH^-H^+} = \frac{g^2}{32 M_W^2}\Bigg(& -\frac{(M_h^2 - M_H^2)(c_{4\beta}+3) s_{4\alpha}}{s_{2\beta}^2} + 8 c_{2\alpha}\left(2 m_{12}^2 - M_{H^\pm}^2 s_{2\beta}\right) + \\ &+ 2\mathrm{ct}_{2\beta}\Bigg(-M_h^2 + M_H^2 + (M_h^2 - M_H^2) c_{4\alpha} + \\ &\frac{s_{2\alpha}}{s_{2\beta}}\left(-4(M_h^2 + M_H^2) + 3 M_{H^\pm}^2 + \frac{4 m_{12}^2 (c_{4\beta}+3) - M_{H^\pm}^2 s_{6\beta}}{s_{2\beta}}\right)\Bigg)\Bigg) \end{aligned}$$

$$\begin{aligned} g_{H^2 H^- H^+} = -\frac{g^2}{8 M_W^2}\Bigg(& M_H^2 t_\beta^2 c_\alpha^4 + (M_H^2 - M_h^2)\mathrm{ct}_\beta s_\alpha c_\alpha^3 + \Bigg(2 M_{H^\pm}^2 c_\beta^2 + M_h^2 \mathrm{ct}_\beta^2 s_\alpha^2 - m_{12}^2 \mathrm{ct}_\beta + \\ &+ t_\beta^2\left(M_h^2 s_\alpha^2 - m_{12}^2 t_\beta\right)\Bigg) c_\alpha^2 + s_\alpha\left((M_H^2 - M_h^2) s_\alpha^2 t_\beta - 4 m_{12}^2\right) c_\alpha + M_{H^\pm}^2 s_{2\alpha} s_{2\beta} + \\ &+ s_\alpha^2\left(-m_{12}^2 \mathrm{ct}_\beta^3 + M_H^2 s_\alpha^2 \mathrm{ct}_\beta^2 + 2 M_{H^\pm}^2 s_\beta^2 - m_{12}^2 t_\beta\right)\Bigg) \end{aligned}$$

$$g_{G^+ H^{-2} H^+} = -\frac{g^2}{16 M_W^2}\left(\frac{(M_h^2 - M_H^2)\left(3 c_{2\alpha} + c_{2(\alpha-2\beta)}\right)}{s_{2\beta}} + 4\mathrm{ct}_{2\beta}\left(-\frac{4 m_{12}^2}{s_{2\beta}} + M_h^2 + M_H^2\right)\right)$$

$$g_{G^{-2} H^{+2}} = -\frac{g^2}{16 M_W^2}\left(-2 M_A^2 + M_h^2 + M_H^2 + (M_h^2 - M_H^2) c_{2(\alpha-\beta)}\right)$$

$$g_{G^- H^- H^{+2}} = -\frac{g^2}{16 M_W^2}\left(\frac{(M_h^2 - M_H^2)\left(3 c_{2\alpha} + c_{2(\alpha-2\beta)}\right)}{s_{2\beta}} + 4\mathrm{ct}_{2\beta}\left(-\frac{4 m_{12}^2}{s_{2\beta}} + M_h^2 + M_H^2\right)\right)$$

$$\begin{aligned} g_{H^{-2} H^{+2}} = -\frac{g^2}{64 M_W^2}\Bigg(& \frac{(M_h^2 - M_H^2) c_{2\alpha}(15 c_{2\beta} + c_{6\beta})}{s_{2\beta}^2} + 2\Bigg(-\frac{32 m_{12}^2 \mathrm{ct}_{2\beta}^2}{s_{2\beta}} + 2(M_H^2 - M_h^2) s_{2\alpha} s_{2\beta} + \\ &+ \frac{(M_h^2 + M_H^2)(3 c_{4\beta} + 5)}{s_{2\beta}^2}\Bigg)\Bigg) \end{aligned}$$

11.3.3 Trilinear couplings - V_{IDM}

In this section, we specify the couplings of the potential V_{IDM}. As the Z_2 symmetry is not broken by the second vacuum expectation value, all the couplings with an odd number of inert fields H, A, H^+ must vanish. Hence inert particles can only be produced pairwise and the lightest inert particle will be a candidate for dark matter. Also note that $M_h < M_H$ does not hold in the IDM.

$$
\begin{aligned}
g_{A^2h} &= \tfrac{g}{2M_W}(m_{11}^2 - M_A^2) & g_{G^{02}h} &= -\tfrac{g}{4M_W}M_h^2 \\
g_{G^-G^+h} &= -\tfrac{g}{2M_W}M_h^2 & g_{h^3} &= -\tfrac{g}{4M_W}M_h^2 \\
g_{AG^0H} &= -\tfrac{g}{2M_W}(M_A^2 - M_H^2) & g_{hH^2} &= \tfrac{g}{2M_W}(m_{11}^2 - M_H^2) \\
g_{AG^+H^-} &= -\tfrac{ig}{2M_W}(M_A^2 - M_{H^\pm}^2) & g_{G^+HH^-} &= \tfrac{g}{2M_W}(M_H^2 - M_{H^\pm}^2) \\
g_{AG^-H^+} &= -\tfrac{ig}{2M_W}(M_{H^\pm}^2 - M_A^2) & g_{G^-HH^+} &= \tfrac{g}{2M_W}(M_H^2 - M_{H^\pm}^2) \\
g_{hH^-H^+} &= \tfrac{g}{M_W}(m_{11}^2 - M_{H^\pm}^2) & &
\end{aligned}
$$

11.3.4 Quartic couplings - V_{IDM}

$$
\begin{aligned}
g_{A^4} &= -\tfrac{1}{8}\lambda_1 & g_{A^2G^{02}} &= \tfrac{g^2}{8M_W^2}(m_{11}^2 - M_H^2) \\
g_{G^{04}} &= -\tfrac{g^2}{32M_W^2}M_h^2 & g_{A^2G^-G^+} &= \tfrac{g^2}{4M_W^2}(m_{11}^2 - M_{H^\pm}^2) \\
g_{G^-G^{02}G^+} &= -\tfrac{g^2}{8M_W^2}M_h^2 & g_{G^{-2}G^{+2}} &= -\tfrac{g^2}{8M_W^2}M_h^2 \\
g_{A^2h^2} &= \tfrac{g^2}{8M_W^2}(m_{11}^2 - M_A^2) & g_{G^{02}h^2} &= -\tfrac{g^2}{16M_W^2}M_h^2 \\
g_{G^-G^+h^2} &= -\tfrac{g^2}{8M_W^2}M_h^2 & g_{h^4} &= -\tfrac{g^2}{32M_W^2}M_h^2 \\
g_{AG^0hH} &= -\tfrac{g^2}{4M_W^2}(M_A^2 - M_H^2) & g_{A^2H^2} &= -\tfrac{1}{4}\lambda_1 \\
g_{G^{02}H^2} &= \tfrac{g^2}{8M_W^2}(m_{11}^2 - M_A^2) & g_{G^-G^+H^2} &= \tfrac{g^2}{4M_W^2}(m_{11}^2 - M_{H^\pm}^2) \\
g_{h^2H^2} &= \tfrac{g^2}{8M_W^2}(m_{11}^2 - M_H^2) & g_{H^4} &= -\tfrac{1}{8}\lambda_1 \\
g_{AG^0G^+H^-} &= -\tfrac{g^2}{4M_W^2}(M_H^2 - M_{H^\pm}^2) & g_{AG^+hH^-} &= \tfrac{ig^2}{4M_W^2}(M_{H^\pm}^2 - M_A^2) \\
g_{G^0G^+HH^-} &= \tfrac{ig^2}{4M_W^2}(M_{H^\pm}^2 - M_A^2) & g_{G^+hHH^-} &= \tfrac{g^2}{4M_W^2}(M_H^2 - M_{H^\pm}^2) \\
g_{G^{+2}H^{-2}} &= \tfrac{g^2}{8M_W^2}(M_A^2 - M_H^2) & g_{AG^-G^0H^+} &= -\tfrac{g^2}{4M_W^2}(M_H^2 - M_{H^\pm}^2) \\
g_{AG^-hH^+} &= \tfrac{ig^2}{4M_W^2}(M_A^2 - M_{H^\pm}^2) & g_{G^-G^0HH^+} &= \tfrac{ig^2}{4M_W^2}(M_A^2 - M_{H^\pm}^2) \\
g_{G^-hHH^+} &= \tfrac{g^2}{4M_W^2}(M_H^2 - M_{H^\pm}^2) & g_{A^2H^-H^+} &= -\tfrac{1}{2}\lambda_1 \\
g_{G^{02}H^-H^+} &= \tfrac{g^2}{4M_W^2}(m_{11}^2 - M_{H^\pm}^2) & g_{G^-G^+H^-H^+} &= \tfrac{g^2}{4M_W^2}(2m_{11}^2 - M_A^2 - M_H^2) \\
g_{h^2H^-H^+} &= \tfrac{g^2}{4M_W^2}(m_{11}^2 - M_{H^\pm}^2) & g_{H^2H^-H^+} &= -\tfrac{1}{2}\lambda_1 \\
g_{G^{-2}H^{+2}} &= \tfrac{g^2}{8M_W^2}(M_A^2 - M_H^2) & g_{H^{-2}H^{+2}} &= -\tfrac{1}{2}\lambda_1
\end{aligned}
$$

References

[1] A. Djouadi, Phys. Rept. **457**, 1 (2008), arXiv:hep-ph/0503172.

[2] R. Barbieri, L. J. Hall, and V. S. Rychkov, Phys. Rev. **D74**, 015007 (2006), arXiv:hep-ph/0603188.

[3] A. D. Sakharov, Pisma Zh. Eksp. Teor. Fiz. **5**, 32 (1967).

[4] M. Kobayashi and T. Maskawa, Prog. Theor. Phys. **49**, 652 (1973).

[5] E. Accomando *et al.*, Workshop on CP studies and non-standard Higgs physics, (2006), arXiv:hep-ph/0608079.

[6] A. Zee, Phys. Lett. **B93**, 389 (1980).

[7] K. S. Babu, Phys. Lett. **B203**, 132 (1988).

[8] M. Aoki, S. Kanemura, and O. Seto, Phys. Rev. Lett. **102**, 051805 (2009), arXiv:0807.0361.

[9] A. Barroso, L. Brucher, and R. Santos, Phys. Rev. **D60**, 035005 (1999), arXiv:hep-ph/9901293.

[10] A. G. Akeroyd, Phys. Lett. **B368**, 89 (1996), arXiv:hep-ph/9511347.

[11] A. G. Akeroyd, J. Phys. **G24**, 1983 (1998), arXiv:hep-ph/9803324.

[12] L. Brucher and R. Santos, Eur. Phys. J. **C12**, 87 (2000), arXiv:hep-ph/9907434.

[13] M. Aoki, S. Kanemura, K. Tsumura, and K. Yagyu, Models of Yukawa interaction in the two Higgs doublet model, and their collider phenomenology, 2009, arXiv:0902.4665.

[14] J. F. Gunion and H. E. Haber, Phys. Rev. **D72**, 095002 (2005), arXiv:hep-ph/0506227.

[15] J. F. Gunion, H. E. Haber, G. L. Kane, and S. Dawson, *The Higgs Hunter's Guide* (Westview Press, 2000).

[16] A. Arhrib, Phys. Lett. **B612**, 263 (2005), arXiv:hep-ph/0409218.

[17] J. F. Gunion and H. E. Haber, Phys. Rev. **D67**, 075019 (2003), arXiv:hep-ph/0207010.

[18] A. Barroso, P. M. Ferreira, and R. Santos, Phys. Lett. **B652**, 181 (2007), arXiv:hep-ph/0702098.

[19] M. E. Peskin and D. V. Schroeder, *An introduction to quantum field theory* (Addison-Wesley, 1995).

[20] G. Passarino and M. J. G. Veltman, Nucl. Phys. **B160**, 151 (1979).

[21] V. D. Barger, J. L. Hewett, and R. J. N. Phillips, Phys. Rev. **D41**, 3421 (1990).

[22] Y. Grossman, Nucl. Phys. **B426**, 355 (1994), arXiv:hep-ph/9401311.

[23] A. Arhrib, R. Benbrik, R. B. Guedes, and R. Santos, Phys. Rev. **D78**, 075002 (2008), arXiv:0805.1603.

[24] Particle Data Group, C. Amsler *et al.*, Phys. Lett. **B667**, 1 (2008).

[25] A. Denner, Fortschr. Phys. **41**, 307 (1993), arXiv:0709.1075.

[26] A. Sirlin, Phys. Rev. **D22**, 971 (1980).

[27] W. F. L. Hollik, Fortschr. Phys. **38**, 165 (1990).

[28] T. Appelquist and J. Carazzone, Phys. Rev. **D11**, 2856 (1975).

[29] W. Hollik, J. Phys. **G29**, 131 (2003).

[30] K. G. Chetyrkin, M. Faisst, J. H. Kuhn, P. Maierhofer, and C. Sturm, Phys. Rev. Lett. **97**, 102003 (2006), arXiv:hep-ph/0605201.

[31] K. G. Chetyrkin, J. H. Kuhn, and M. Steinhauser, Phys. Lett. **B351**, 331 (1995), arXiv:hep-ph/9502291.

[32] M. Awramik, M. Czakon, A. Freitas, and G. Weiglein, Phys. Rev. **D69**, 053006 (2004), arXiv:hep-ph/0311148.

[33] F. Halzen and B. A. Kniehl, Nucl. Phys. **B353**, 567 (1991).

[34] G. Burgers and F. Jegerlehner, Delta r or the relation between the electroweak couplings and the weak vector boson masses, in *Workshop on Z Physics at LEP*, edited by G. Altarelli, R. H. P. Kleiss, and C. Verzegnassi, CERN, Geneva, 1989.

[35] LEP Higgs Working Group for Higgs boson searches, Search for charged Higgs bosons: Preliminary combined results using LEP data collected at energies up to 209 GeV, 2001, arXiv:hep-ex/0107031.

[36] LEP collaborations, A combination of preliminary electroweak measurements and constraints on the standard model, 2004, arXiv:hep-ex/0412015.

[37] K. Abe *et al.*, Phys. Rev. Lett. **94**, 091801 (2005), arXiv:hep-ex/0410042.

[38] H. E. Haber and H. E. Logan, Phys. Rev. **D62**, 015011 (2000), arXiv:hep-ph/9909335.

[39] J. H. Field, Mod. Phys. Lett. **A13**, 1937 (1998), arXiv:hep-ph/9801355.

[40] P. Gambino and M. Misiak, Nucl. Phys. **B611**, 338 (2001), arXiv:hep-ph/0104034.

[41] Heavy Flavor Averaging Group (HFAG), E. Barberio *et al.*, (2007), arXiv:0704.3575.

[42] M. Misiak *et al.*, Phys. Rev. Lett. **98**, 022002 (2007), arXiv:hep-ph/0609232.

[43] F. Borzumati and C. Greub, Phys. Rev. **D58**, 074004 (1998), arXiv:hep-ph/9802391.

[44] M. Ciuchini, G. Degrassi, P. Gambino, and G. F. Giudice, Nucl. Phys. **B527**, 21 (1998), arXiv:hep-ph/9710335.

[45] A. J. Buras, Weak Hamiltonian, CP violation and rare decays, in *Probing the Standard Model of Particle Interactions*, 1998, arXiv:hep-ph/9806471.

[46] A. G. Grozin, Introduction to the heavy quark effective theory part I, 1992, arXiv:hep-ph/9908366.

[47] F. Borzumati and C. Greub, Phys. Rev. **D59**, 057501 (1999), arXiv:hep-ph/9809438.

[48] B. W. Lee, C. Quigg, and H. B. Thacker, Phys. Rev. **D16**, 1519 (1977).

[49] H. Huffel and G. Pocsik, Zeit. Phys. **C8**, 13 (1981).

[50] S. Kanemura, T. Kubota, and E. Takasugi, Phys. Lett. **B313**, 155 (1993), arXiv:hep-ph/9303263.

[51] S. Kanemura, T. Kasai, and Y. Okada, Phys. Lett. **B471**, 182 (1999), arXiv:hep-ph/9903289.

[52] A. G. Akeroyd, A. Arhrib, and E.-M. Naimi, Phys. Lett. **B490**, 119 (2000), arXiv:hep-ph/0006035.

[53] A. Arhrib, W. Hollik, S. Penaranda, and M. Capdequi Peyranere, Phys. Lett. **B579**, 361 (2004), arXiv:hep-ph/0307391.

[54] I. F. Ginzburg, M. Krawczyk, and P. Osland, Nucl. Instrum. Meth. **A472**, 149 (2001), arXiv:hep-ph/0101229.

[55] A. G. Akeroyd, M. A. Diaz, and M. A. Rivera, Phys. Rev. **D76**, 115012 (2007), arXiv:0708.1939.

[56] T. Hahn, Comput. Phys. Commun. **140**, 418 (2001), arXiv:hep-ph/0012260.

[57] T. Hahn and M. Perez-Victoria, Comput. Phys. Commun. **118**, 153 (1999), arXiv:hep-ph/9807565.

[58] A. Djouadi, Phys. Rept. **459**, 1 (2008), arXiv:hep-ph/0503173.

[59] D. Zeppenfeld, R. Kinnunen, A. Nikitenko, and E. Richter-Was, Phys. Rev. **D62**, 013009 (2000), arXiv:hep-ph/0002036.

[60] S. Ganjour, AIP Conf. Proc. **1078**, 186 (2009), arXiv:0809.5163.

[61] K. Monig and A. Rosca, Eur. Phys. J. **C57**, 535 (2008), arXiv:0705.1259.

[62] R. Unterdorfer and G. Ecker, JHEP **10**, 017 (2005), arXiv:hep-ph/0507173.

Lebenslauf

Persönliche Daten:

Name:	Paul Posch
Geburtsdatum:	17. Februar 1982
Geburtsort:	Wien

Bildungsweg:

10. 2002 - 08. 2009	Studium der Physik an der Universität Wien
03. 2003 -	Studium der Mathematik an der Universität Wien
10. 2003 -	Studium der Japanologie an der Universität Wien
09. 1996 - 09. 2001	HTL für EDV und Organisation

Zivildienst:

02. 2002 - 01. 2003	Zivildienst bei Jugend am Werk (Wohnbetreuung geistig Behinderter)

Berufliche Tätigkeit:

03. 2008 - 06. 2009	Tutor für Theoretische Physik 4 (Thermodynamik und Statistische Mechanik) an der Uni Wien
10. 2008 - 02. 2009	Tutor für Theoretische Physik 3 (Elektrodynamik) an der Uni Wien
03. 2008 - 06. 2008	Studienassistent in der Teilchenphysik Gruppe an der Uni Wien
10. 2007 - 02. 2008	Tutor für Theoretische Physik 1 (klassische Mechanik)
05. 2005 - 08. 2007	Führungen in der Wiener Staatsoper (in Japanisch, Deutsch, Englisch)
10. 2001 - 02. 2002	Programmierung von Webseiten in PHP/MySQL, bei der Telekurier AG

Sprachkenntnisse:	Deutsch (Muttersprache), Englisch (fließend in Wort & Schrift), Japanisch (sehr gut)
Programmiersprachen:	Python, Mathematica, C++, PHP,...

Teilnahme an Schulen (für Physik):

12 - 16. Mai 2008	Frascati Spring School “Bruno Touschek”: Entering the LHC era
19 - 24. August 2008	Summer School of the Young Nuclear and Particle Physicist Group of Japan
14 - 21. September 2008	High Energy Physics Summer School, Svit, Slovakia, Physics at One Loop
28 - 30. November 2009	5th Vienna Central European Seminar on Particle Physics and Quantum Field Theory – Highlights in Computational Quantum Field Theory
1 - 7. März 2009	Schladming Winter School 2009, Fundamental Challenges of QCD